

## Chapter 8

# Fouling in Nanofiltration

Andrea I. Schäfer<sup>1</sup>, Nikolaos Andritsos<sup>2</sup>, Anastasios J. Karabelas<sup>2</sup>, Eric M.V. Hoek<sup>3</sup>, René Schneider<sup>4</sup>, Marianne Nyström<sup>5</sup>

<sup>1</sup>Environmental Engineering, University of Wollongong, Wollongong, NSW 2522, Australia  
ph +61 2 4221 3385, fax +61 2 4221 4738, [A.Schaefer@uow.edu.au](mailto:A.Schaefer@uow.edu.au)

<sup>2</sup>Chemical Process Engineering Research Institute, P.O. Box 361, 57001, Thessaloniki, Greece  
ph ++302310498181, fax ++302310498189  
[andritso@cperi.certh.gr](mailto:andritso@cperi.certh.gr) [karabaj@cperi.certh.gr](mailto:karabaj@cperi.certh.gr)

<sup>3</sup>Chemical & Environmental Engineering, University of California, Riverside, CA 92521, USA, ph: +011-909-787-7345, fax: +011-909-787-5696, email: [hoek@engr.ucr.edu](mailto:hoek@engr.ucr.edu)

<sup>4</sup>Departamento de Microbiologia, Instituto de Ciências Biomédicas, Universidade de São Paulo, Brazil  
ph +55 11 3091 7745, fax +55 11 3091 7354, [schneide@icb.usp.br](mailto:schneide@icb.usp.br)

<sup>5</sup>Lappeenranta University of Technology, Laboratory of Membrane Technology and Technical Polymer Chemistry, P.O.Box 20, FIN-53851 Lappeenranta, Finland  
ph. +358-5-621 2160, fax +358-5-621 2199, [marianne.nystrom@lut.fi](mailto:marianne.nystrom@lut.fi)

## 1 INTRODUCTION

According to Koros *et al.* [1] fouling is “the process resulting in loss of performance of a membrane due to deposition of suspended or dissolved substances on its external surfaces, at its pore openings, or within its pores”. Fouling is also described as flux decline which is irreversible and can only be removed by, for example, chemical cleaning [2]. This is different to flux decline due to solution chemistry effects or concentration polarisation which is described in more detail later in this chapter. Those flux declines can be reversed with clean water and are hence not considered as fouling.

Fouling of membranes is important as it limits the competitiveness of the process due to an increase in costs due to an increased energy demand, additional labour for maintenance and chemical costs for cleaning as well as a shorter lifetime of the membranes. Essential for effective fouling control is a proactive operation of a nanofiltration (NF) or reverse osmosis (RO) plant where an early indication of fouling is acted upon and a good identification of the type of fouling is carried out. Staudé [3] summarised the possible origins of fouling as follows

- Precipitation of substances that have exceeded their solubility product (scaling)
- Deposition of dispersed fines or colloidal matter
- Chemical reaction of solutes at the membrane boundary layer (e.g. formation of ferric hydroxides from soluble forms of iron)
- Chemical reaction of solutes with the membrane polymer
- Adsorption of low molecular mass compounds at the membrane polymer
- Irreversible gel formation of macromolecular substances
- Colonisation by bacteria (mostly hydrophobic interactions).

This gives an indication of the complexity of fouling and an example of such complexity is illustrated in **Figure 1** with electron micrographs of a membrane fouled with surface water without pretreatment. The pictures show colloids and organic matter embedded in a gel like cake layer on top of the membrane. In **Figure 2** another surface water deposit on a NF membrane is shown, except that in this case the surface water is pretreated with ultrafiltration and fouling is dominated by inorganic precipitates.

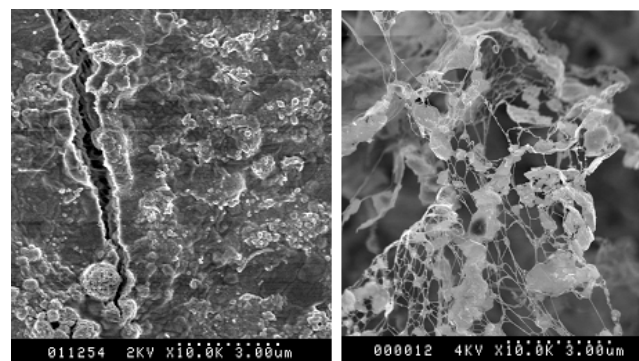


**Figure 1** Complex deposit of surface water on a membrane (adapted from Schäfer [4]).

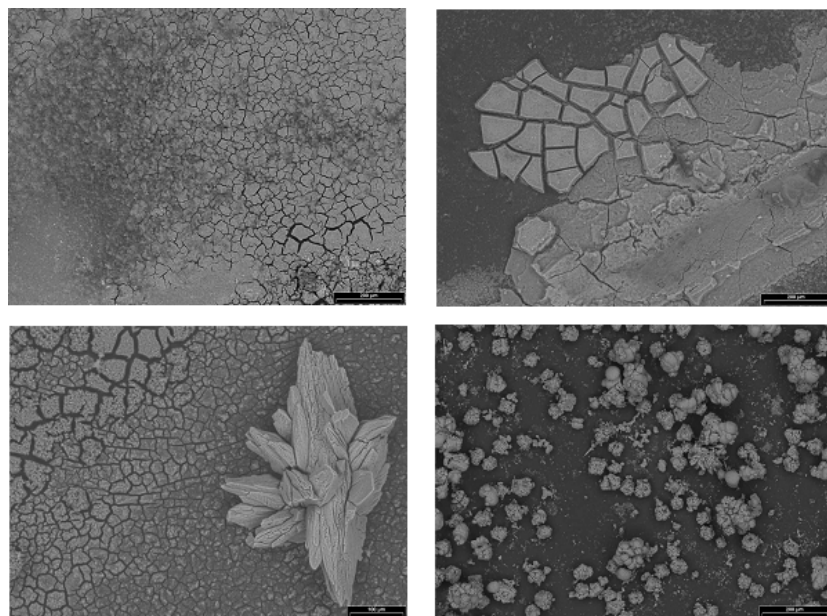


**Figure 2** Scanning electron micrographs (SEM) of membranes fouled during the filtration of ultrafiltration pretreated surface water and examined in an autopsy (bar length 200 µm for all pictures; photos courtesy of Paul Buijs, GEBetz, Belgium)

A number of factors contribute to fouling and are strongly interlinked. The main fouling categories are organic, inorganic, particulate and biological fouling. Metal complexes (for example Fe, Al, Si) are also important. While research traditionally focuses on one category or fouling mechanism at a time, it is well accepted that in most cases it is not one single category that can be identified. In most real life applications all four types of fouling go hand in hand. The types of foulants and where they usually occur in NF/RO systems is summarised in Table 1.

Scaling and silica fouling originates in general from the concentration of inorganics exceeding the solubility limit (see Section 5 Scaling). This most often occurs in the latter membrane stages. Metal oxides and colloids deposit early in the process as drag forces are relatively high (see Section 6 Particulate and Colloidal Fouling). Organic fouling remains poorly understood and very specific to the characteristics of the foulant molecules (see Section 4 Organic Fouling). Organic fouling may occur at the beginning as well as the end stages of the modules depending on the dominating mechanism. Biofouling also can be found throughout all filtration stages (see Section 7 Biofouling). Rapid biofouling can be related to particle attachment which is found mostly in the first stage, whereas the slow biofouling can occur throughout all stages [5]. While in the past bacterial deposition and fouling have often been studied by using latex particles, the adhesive nature of extra-cellular polymeric substances (EPS) makes bacteria more adhesive and their deposition mechanism more complex [6].

**Table 1** Fouling - Where does it occur first (adapted from Hydraulics Technical Service Bulletin TSB107 in Huiting et al. [5])

Type of Foulant	Most susceptible stage of NF/RO
Scaling/silica	Last membranes in last stage
Metal oxides	First membranes of first stage
Colloids	First membranes of first stage
Organic	First membranes of first stage
Biofouling (rapid)	First membranes of first stage
Biofouling (slow)	Throughout the whole installation

In order to reduce or eliminate fouling it is necessary to identify the foulants. This can be achieved by a characterisation of the fouled membrane (membrane autopsy in Section 2.4) or by fouling studies in the laboratory. Once the foulants are identified suitable control strategies can be adapted. An overview of foulants and appropriate control strategies are summarised in Table 2. The strategies encompass a number of categories [6] namely

- Feed pre-treatment
- Membrane selection (non-fouling materials/coatings, suitable surface charge, chlorine compatibility, porosity, hydrophilicity, surface roughness etc.)
- Module design & operation mode
- Cleaning.

Feed pre-treatment is addressed in Chapter 9, Membrane materials in Chapter 3, module design and operation in Chapter 4 and cleaning at the end of this chapter.

**Table 2** Foulants and their control strategies in nanofiltration and reverse osmosis processes (adapted and modified from Fane et al. [6])

Foulant	Fouling Control
General	Hydrodynamics/shear, operation below critical flux, chemical cleaning
Inorganic (Scaling)	Operate below solubility limit, pre-treatment, reduce pH to 4-6 (acid addition), low recovery, additives (antiscalants) Some metals can be oxidised with oxygen
Organics	Pretreatment using biological processes, activated carbon, ion exchange (e.g. MIEX), ozone, enhanced coagulation
Colloids (<0.5 µm)	Pre-treatment using coagulation & filtration, microfiltration, ultrafiltration
Biological solids	Pretreatment using disinfection (e.g. chlorination/dechlorination), filtration, coagulation, microfiltration, ultrafiltration

Membrane fouling is the worst enemy of membrane process applications and yet fouling goes hand in hand with successful filtration. The search to understand fouling has dominated membrane research for some time, yet models fail to predict and adequately describe this complex process. Fouling often requires frequent cleaning of membranes and consequently reduces the membrane life span. In some cases fouling causes membrane biodegradation and a loss of integrity [7]. Cleaning also requires chemicals, possibly an increased cleaning temperature and hence renders membrane processes less

sustainable. Further, it decreases process efficiency due to the reduced flux, requiring either higher transmembrane pressures (and hence more energy) or larger membrane areas. Therefore, fouling is a critical parameter to be considered in NF process design.

This chapter will offer a summary of the components of fouling, most common fouling mechanisms and some control strategies.

## 2 FOULING CHARACTERISATION

### 2.1 Flux Measurement and Fouling Protocols

An important parameter when estimating fouling is to determine clean water flux ( $J_0$ ) which serves as the basis for comparison with the unfouled membrane.  $J_0$  is defined as

$$J_0 = \frac{\eta_T}{\eta_{20^{\circ}C}} \frac{Q}{A \cdot \Delta P} \quad (L/m^2 \cdot h) \quad (1)$$

where  $\eta_T$  is the viscosity of water at temperature T and  $\eta_{20^{\circ}C}$  the viscosity of water at 20°C, Q is the clean water flow at temperature T, A the membrane surface area and  $\Delta P$  the transmembrane pressure difference [8]. This equation is valid for dilute solutions. The relationship between viscosity and temperature is described, for example, by Roorda and van der Graaf [9] and is strictly speaking feed dependent, although dilute feeds can be described by water.

A number of parameters impact on this  $J_0$  as the filtration commences (see compaction below) and is maintained (reversible & irreversible flux decline). Cleaning then aims to restore as much as possible of this initial (or post-compaction)  $J_0$ .

Flux reduction (FR) with regards to clean water flux can be determined as a percentage of  $J_0$  by comparing the  $J_0$  before and after membrane operation as described by Mänttari and Nyström [10]

$$FR_{CWF} = \frac{J_{Ob} - J_{Oa}}{J_{Ob}} \cdot 100 \quad (\%) \quad (2)$$

where the indices a and b reflect before and after filtration of feed, respectively. Alternatively flux reduction can also be described as the difference between permeate and clean water fluxes as follows

$$FR_{PF} = \frac{J_{Ob} - J}{J_{Ob}} \cdot 100 \quad (\%) \quad (3)$$

where PF is subscript for permeate flux. To use this equation a set pressure for clean water flux and permeate flux has to be selected and filtration should have reached steady state.

#### 2.1.1 Membrane Compaction

It should be noted here that membrane compaction, which is commonly observed with NF and RO membranes is not classified as fouling. Compaction is caused by the applied pressure and can be both reversible and irreversible. The compaction may change both the active layer and the support [3]. To overcome the impact of compaction in fouling studies, membranes are often compacted at a higher pressure than the operation pressure to ensure flux stability during experiments (see Figure 3) before pure water flux is determined.

### 2.1.2 Variation of Membrane Permeability with Solution Chemistry

Braghetta *et al.* [11] have investigated the impact of variation in solution chemistry, namely pH and ionic strength on membrane permeability. At low pH and high ionic strength this permeability decreased which was linked to a compaction of the membrane matrix due to charge neutralisation and double layer compression. The authors used the parameter of Debye length to quantify such changes in membrane structure or more precisely the double layer thickness. A reduced Debye length effectively increases the cross-sectional area available for solvent transport.

### 2.1.3 Fouling Study Protocols

Figure 3 shows a typical fouling study protocol where a new membrane is firstly compacted and clean water flux is measured. Subsequently the feed solution (in the case of this figure a natural organic matter (NOM) solution) and flux measured. Depending on the feed water a more or less significant flux decline is observed. This flux decline has a number of components (i) concentration polarisation or the loose accumulation of solutes, (ii) fouling that can be reversed chemically, and (iii) irreversible fouling. Concentration polarisation or loose accumulation can be reversed by a water flush, reversible fouling can be removed with an appropriate chemical cleaning protocol and irreversible fouling, which can be due to the irreversible binding of foulants to the membrane or a membrane compaction cannot be reversed and will ultimately determine the lifetime of a membrane. It should be noted here that some researchers classify all fouling that cannot be reversed with a water flush as irreversible.

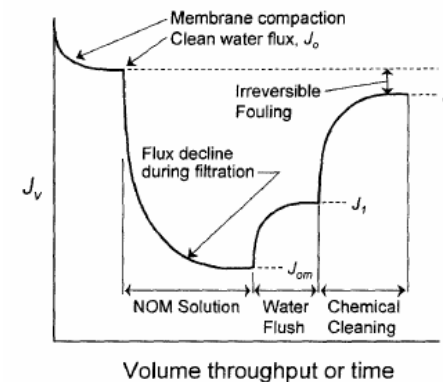


Figure 3 Typical protocol used in fouling studies (adapted from Kilduff *et al.* [12]).

For constant flux operation a protocol would measure the variation of transmembrane pressure in a similar protocol, where transmembrane pressure increases with fouling.

DiGiano *et al.* [13, 14] have developed a range of useful filtration tests that correspond to flux decline and recovery patterns of full scale plants. Such tests are bench scale crossflow filtration tests that can be used for fouling evaluation. As the authors emphasise- such tests should not be used to replace pilot testing.

## 2.2 Normalisation of Membrane Performance

According to Huiting *et al.* [5] variable system parameters need to be normalised in order to compare system performance and correctly evaluate fouling. Those varying parameters are pressure, temperature and feed water quality. The normalised parameters are

- Normalized Water Flow or productivity (expressed as Mass Transfer Coefficient (MTC));
- Normalized Pressure Drop (NPD)
- Normalized Salt Passage (NSP) [5].

Changes in those normalized parameters may indicate a problem. Fouling related changes are in the order of magnitude of 10-15% decrease in MTC, 10-15% increase in NPD, and a “significant” increase of NSP over time [5]. To use this methodology additional monitoring measures are required. Those are, for example, conductivity, flow and pressure indicators in the different membrane stages.

## 2.3 Feed Water Fouling Potential

Feed water analysis can give some indication of likelihood of fouling. While chemical analysis gives very detailed information that then needs to be analysed, indices have also been widely used to determine fouling potential of feedwaters. As described by Huiting *et al.* [5] fouling indices give an indication of particulate fouling. The most commonly used indices (especially in industry) are the silt density index (SDI) and the modified fouling index (MFI) and these are described below.

### 2.3.1 Feed Water Analysis

Feed water analysis plays an important role in the determination of fouling potential. For example, turbidity is a commonly used parameter for the determination of fouling potential in RO [3]. However, as the pre-treatment with membrane processes such as MF and UF becomes more common, this value will not be very meaningful due to the very high removal of turbidity and hence very low turbidity values. The method is not necessarily sensitive enough to determine problems related to small colloids such as silica.

Membrane design software usually requires entering a feed analysis to predict fouling potential, although this is usually limited to scaling. Sparingly soluble salts that are prone to precipitation and scale formation are important to be quantified. The section on scaling in this book gives a detailed overview of common scalants. Metals such as magnesium and iron are also very important. Magnesium has been reported to play an important role in the precipitation of silica [15].

Organics are known to play a substantial part in NF fouling. Dissolved organic carbon (DOC) contributes to fouling by adsorption, gel formations, pore plugging and as a nutrient for microorganisms. Research investigating the fouling of NF by DOC, its fractions natural organic matter (NOM), humic acids (HA), fulvic acids (FA), and hydrophilic acids is very active and will be summarised in the organic fouling section of this chapter. NOM, as most of the above fractions, consists of biodegradable and refractory organics with varying characteristics such as aromaticity, molecular mass, charge, functional groups and affinity towards membrane materials. As a parameter to investigate the characteristics of such bulk organics and their fractions as a means to predict fouling the specific UV absorbance (SUVA) has been introduced.

$$SUVA = \frac{UVA_{254\text{ nm}}}{DOC} \quad (4)$$

where  $UVA_{254\text{ nm}}$  is the UV absorbance of a water sample at 254 nm. SUVA describes the relative aromatic content of organic carbon and is used predominantly in water and wastewater treatment.

Nutrients such as nitrogen and phosphate are also an important measure for fouling potential. The presence of bacterial cells indicates biofouling potential in combination with such nutrients [16]. To link water characteristics and biological growth potential Escobar and Randall [17] have compared two commonly used indicators of bacterial regrowth potential: assimilable organic carbon (AOC) and biodegradable organic carbon (BDOC). It was found that measuring AOC, although only representing 0.1-9% of influent DOC in NF underestimated regrowth potential, while BDOC which represents about 10-30% of DOC overestimates it. AOC was found to be composed of compounds like acetate that are poorly retained by NF and hence can act as a nutrient on the feed and permeate side. In consequence, Escobar and Randall suggested measuring both parameters for a more realistic indication of fouling potential. In terms of methodology, AOC determines the availability of organic matter to increase biomass concentration using a bioassay, counting colonies in water samples to monitor bacterial growth, which is relatively time consuming and complex. BDOC measures the degradation of organic carbon by suspended or fixed bacteria over a certain amount of time.

In response to the need to be able to predict fouling potential Shaalan [18] has attempted to develop a fouling and retention prediction model based on feed water analysis for surface water applications. The model is empirical and based on the performance of a number of treatment plants, but as expected for such complex phenomena the deviation between model and test data is significant. The temptation to develop such models is large and advanced in fouling research may help in the development of adequate relationships.

### 2.3.2 Silt Density Index (SDI)

The silt density index (SDI) is also referred to as colloid index or fouling index. The motivation of this index is to describe a linear relationship between feed particle content and flux decline. The linear relationship however is usually not achievable. The SDI is determined by the repeated filtering of a certain volume of feed through a 0.45µm filter in dead-end and constant pressure mode [3, 19].

$$SDI = \frac{1 - t_1/t_2}{T} \quad (\text{min}^{-1}) \quad (5)$$

where  $t_1$  is the time required to filter volume V at time zero,  $t_2$  is the time required to filter volume V at time T (in min). The SDI is commonly used to estimate the interval length between membrane cleaning and if the module can be used without additional pre-treatment [3]. However, the use of SDI has been criticized and its use as an important monitoring parameter described as a ‘dangerous mistake’ [15].

### 2.3.3 Modified fouling index (MFI<sub>0.45</sub>)

The modified fouling index (MFI) can achieve the linear relationship between concentration and flux decline, but still cannot accurately predict flux decline [3, 8]. Boerlage *et al.* [8] confirmed that this is due to the fact that in RO fouling is caused by smaller colloids that are not retained by the microfiltration membranes used in the MFI. Seeing the above complexities of fouling mechanisms, this is not unexpected. To determine the MFI, the same equipment as for the SDI is used. The protocol suggests the measurement of the filtrate volume at a pressure of 210 kPa every 20 mins for a duration of 20s. The data is presented as  $t/V$  over V and the  $\tan \alpha$  is determined from the slope [3]. MFI can then be calculated as

$$MFI = \frac{\eta_{20^{\circ}C}}{\eta_T} \frac{\Delta P}{210} \tan \alpha \quad (s/L^2) \quad (6)$$

where  $\eta_T$  is the viscosity of water at temperature T and  $\eta_{20^{\circ}C}$  the viscosity of water at 20°C. The equation is based on the Karman-Kozeny relationship and the assumption of an incompressible cake [19]. This value is also referred to as  $MFI_{0.45}$  seeing that the same membrane is used as for the SDI. Some applications also describe the use of a  $MFI_{0.05}$ , hence using a membrane with a 0.05  $\mu m$  pore size. Both MFI and SDI underestimate the fouling observed in practice [19].

### 2.3.4 Modified fouling index UF (MFI-UF)

As the SDI and the MFI do not include smaller colloid sizes, a new index using an ultrafiltration (UF) membrane has been developed [5]. Boerlage *et al.* [8] tested this MFI-UF as a function of molecular weight cut-off (MWCO, 1-100 kDa) of the UF membranes and obtained values ranging from 2000-13000  $s/L^2$  (as compared to MFI values of 1-5  $s/L^2$ ). Higher values were linked to the retention of smaller colloids as well as cake filtration of the retained particles, although a correlation with the MWCO was not apparent. While other membrane characteristics may be partly responsible for those varied results, it is also important to note that fouling at such MWCOs is complex and cannot be solely attributed to particulates. A 13 kDa membrane was established to be the best membrane for such tests.

Boerlage *et al.* [19] used a 13 kDa UF membrane (estimated pore dimension 9 nm) to measure fouling potential and effectiveness of pre-treatment and compare the results with the SDI and the  $MFI_{0.45}$ . MFI-UF can be operated in constant flow or pressure mode. The MFI-UF values were in fact 400-1400 times higher than the  $MFI_{0.45}$  due to the smaller particles captured. The MFI-UF can also be used to determine the effectiveness of pre-treatment with regard to reduction of fouling potential. Roorda and van der Graaf [9] used the MFI-UF to determine the fouling potential of UF membranes and confirmed the dependence on membrane type.

As a general evaluation Reiss and Taylor [20] compared three parameters used to investigate fouling – the silt density index (SDI), the modified fouling index (MFI), and the linear correlation of the water mass transfer coefficient (MTC). Three different NF pilot systems were used with different pretreatments including activated carbon and MF. No correlation between the different parameters was obtained, indicating that the filtration laws on which the models are based might not be valid for NF. Hence, these parameters need to be used with caution.

It is clear that the possibility of a rapid fouling prevention is tempting. How well such indices work in determining fouling in a holistic sense is not clear- it would certainly be useful to establish a method that can combine particulate fouling with other types such as organic, inorganic and biofouling. To do this one would require the membrane to be used and an option to perform such tests are stirred cell experiments combined with BFR under filtration conditions. A suitable test protocol is yet to be developed and may depend on the foreseen operating conditions as in general it is difficult to simulate realistic fouling under laboratory conditions.

### 2.3.5 Biofilm Formation Rate (BFR)

Biofilm formation depends on favourable conditions for microorganisms in the system. Details on Biofouling are presented in Section 7. A number of methods to assess such growth have been summarised by van der Kooij *et al.* [21] as follows

- Determination of the concentration of assimilable organic carbon (AOC) using growth measurements
- Quantification of the biodegradable dissolved organic carbon (BDOC) using suspended or immobilised bacteria
- Measurement of bacterial growth curves using turbidity as an indicator [22]
- Biofilm formation rate (BFR) measurement by exposing a surface to the water in question.

The biofilm formation rate is the most direct measure of biofilm formation as it accounts for all chemicals contributing to the biofilm formation and also accounts for concentration fluctuations [21]. BFR can be measured using an online operated biofilm monitor where the accumulation of active biomass (by means of ATP measurement) is determined as a function of time on glass rings [21]. The BFR value allows the prediction of cleaning intervals and a value of < 1  $\mu g$  ATP/cm<sup>2</sup>.d allows long term stable operation, but such values generally require extensive pretreatment [16]. Temporary BFR values of > 120  $\mu g$  ATP/cm<sup>2</sup>.d indicate severe biofouling potential [23], while for values in between those extremes biofouling is dependent on many other parameters as well and to date not well understood. It is interesting to note that van der Kooij *et al.* [21] found that the material type (in their investigation glass & Teflon) had only minor effects on biofilm formation. This is an important investigation to be repeated for different membrane materials. BFR was enhanced by low concentrations of easily degradable substrates which confirms that the measurement of the chemical composition of feed waters, including low concentration organic compounds, is important. Sadr Ghayeni *et al.* [24] in fact investigated the adhesion of bacteria to RO membranes as a function of solution chemistry and obtained differences in attachment with varying membrane types, ionic strength (increased attachment at higher ionic strength) but not pH. The important issue of conditioning films was also investigated and attachment may vary due to such films. Conditioning films are most likely formed by adsorption of organic compounds as covered in Sections 3.3 and 4.3. This sorption continues with sorption of organic compounds into biofilms as studied by Carlson and Silverstein, where the sorption depends strongly on the characteristics of the organic molecules [25].

### 2.4 Membrane Autopsy

Membrane autopsy is the destructive method to characterise the nature and location of foulants using predominantly surface characterisation techniques. To perform membrane autopsy, the membranes need to be sealed by covering the end caps after the elements are removed from the installation, stored and transported in a cool environment and preferably all analysis performed within 24 hours [23]. Gwon *et al.* [26] used membrane autopsy to investigate the difference of fouling along the length of a membrane by dividing the module into five length sections.

As an example, Vrouwenfelder and van der Kooij [16] used membrane autopsy for the investigation of biofouling. The autopsy comprised the following steps

- Visual inspection of the elements (colour, odour, particle deposits, faults, etc) & lengthways opening of elements
- Selection of samples (adequate special distribution)
- Analysis (adenosinetriphosphate (ATP) concentration to determine active biomass, total direct cell count (TDC), heterotropic plate counts (HPC) to determine colony

forming units (CFU), inductively coupled mass spectrometry (ICP-MS) for quantification of inorganic compounds.

Foulant deposits can be removed from the surface if the fouling layer is sufficiently thick. Such deposits can then be analysed and their composition determined as mass fractions using various analytical techniques. For example, Sayed Razavi *et al.* [27] scraped membrane deposits composed of proteins, lipids and carbohydrates off for rheological measurements to determine which compounds deposited preferentially. The deposits can also be removed by chemical means, for example Cho and Fane [28] dissolved EPS deposits using a phenol solution for further analysis and Lee *et al.* [29] used NaOH to remove NOM deposits for further fractionation onto hydrophobic, transphilic, and hydrophilic fractions. Luo and Wang [15] used FTIR-GC/MS following desorption with NaOH and fractionation with XAD resins to characterise the organic deposits. Organics originating from a desalination system were identified to be fatty acids, carbonyl esters, as well as aromatic species and silicates. Nghiem and Schäfer [30] used acetone to desorb organic trace contaminants for subsequent quantification. Belfer *et al.* [31] used nitric acid (HNO<sub>3</sub>) assisted with sonication to dissolve deposits that were subsequently analysed for inorganic constituents and identified as calcium phosphate scale due to the abundance of substantial amounts of calcium and phosphate, besides silica. Such analysis is usually combined with surface characterisation techniques.

Surface characterisation techniques used for membrane autopsies are energy dispersion of X-Ray spectroscopy (EDX) mapping or scanning electron microscopy (SEM) [6]. Using EDX, Farooque *et al.* [32] have determined that the main foulants on a NF pre-treatment membrane used in seawater desalination by RO were O, Fe, Cl, Na, S and Cr. SEM also revealed the presence of diatoms (confirmed by the presence of an SI peak). Butt *et al.* [33] used also X-ray diffractometry (XRD) to determine the type of species or phases in which scales are present. This method also allows to establish relative amounts. This study determined that most scales were of amorphous nature which was attributed to the presence of anti-scalants and that the bulk of the deposits was biomass. Kim *et al.* [34, 35] have developed well adapted protocols for SEM and transmission electron microscopy (TEM) for membranes. A drawback of such methods is the requirement of high vacuums and hence the limitation to dry samples which may not always give a true picture of the fouling layer. EDX and SEM are used to determine the atomic composition of a membrane deposit [36] and an example of a typical result is shown in Figure 4 for a TFC membrane used in the treatment of tertiary municipal effluent. The fouling in this case was established to be a combination of biofouling and calcium phosphate precipitate as described above [31]. The problem of restrictions to dry samples has recently been overcome by new techniques such as atomic force microscopy (AFM) where wet samples can be analysed or samples can even be immersed in water. The resolution of this technique is extremely high with the possibility of individual NF pores being identified (see cover page of this Book) and surface roughness calculations or force measurements including the interactive forces between foulants and membranes allowing conclusions about mechanisms [37-39]. Such characterisation techniques are described in more detail in Chapter 5.

Attenuated total reflectance Fourier transform infrared (ATR-FTIR) spectroscopy can be used to show the functional groups of foulants and the modification of membrane functional groups due to fouling [36]. Jarusutthirak *et al.* [40] used FTIR to identify fractions of effluent organic matter (EfOM) with deposits found on membranes by comparing FTIR spectra of clean and fouled membranes. Infrared internal reflection spectroscopy (IR-IRS) is a similar technique that can be used to characterise the nature of the deposited layer on the membrane [41].

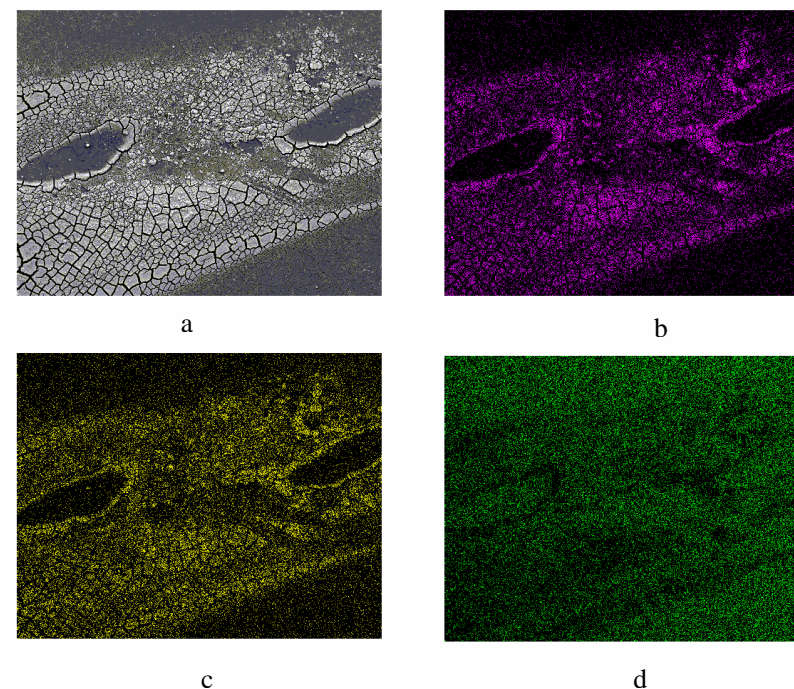


**Figure 4 SEM and EDX scans of a NF270 membrane fouled by tertiary municipal effluent a) SEM micrograph, b) calcium, c) phosphorous, and d) sulphur element scans (pictures reprinted from Belfer *et al.* [31]).**

### 3 FOULING MECHANISMS

Nanofiltration membranes have individual fouling characteristics and in general tighter membranes are known to foul to a lesser extent [42]. If a foulant is able to permeate through a membrane the fouling potential is higher as the penetration into pores is possible [42]. Hence, membrane and foulant characteristics play an important role in fouling (see Chapter 3 and 5). For example, membrane surface charge plays an important role in fouling. It is desirable that the solute and the membrane surface are of identical charge to enhance repulsion, and hence, reduce the likelihood of deposition. However,

hydrophobic interactions between foulants and membranes may overcome electrostatic repulsion [43]. Besides membrane material properties, the operation mode and module design are important, modules are described in Chapter 4.

Fouling has been described in literature using the osmotic pressure and resistance in series models. While the equations are given here, the quantitative description of the contributing mechanisms is given in the subsequent sections. Pure water flux under laminar conditions through a tortuous porous barrier may be described, according to Carman [44] and Bowen and Jenner [45], by equation (7).

$$J = \frac{\Delta P}{\eta R_M} \quad (7)$$

where  $\Delta P$  is the transmembrane pressure difference,  $\eta$  the dynamic solvent viscosity, and  $R_M$  the clean membrane resistance (i.e. the porous barrier).

The Resistance in Series Model describes the flux of a fouled membrane. This is given in equation (8). The resistances  $R_{CP}$ ,  $R_A$ ,  $R_G$ ,  $R_P$  and  $R_C$  denote the additional resistances which result from the exposure of the membrane to a solution containing foulants.  $R_{CP}$  is the resistance due to concentration polarisation,  $R_A$  the resistance due to adsorption,  $R_G$  the resistance due to gel formation,  $R_P$  the internal pore fouling resistance, and  $R_C$  the resistance due to external deposition or cake formation. It should be noted here that the selection of resistances varies in literature and is somewhat ambiguous.

$$J = \frac{\Delta P}{\eta(R_M + R_{CP} + R_A + R_G + R_P + R_C)} \quad (8)$$

The Osmotic Pressure Model, as shown in Eqn (9), is an equivalent description for macromolecules according to Wijmans *et al.* [46]. This equation includes reversible fouling also.  $\Delta \Pi$  is the osmotic pressure difference across the membrane. The osmotic pressure difference can usually be neglected in MF and UF, since the rejected solutes are large and their osmotic pressure small. However, even polymeric solutes (macromolecules) can develop a significant osmotic pressure at boundary layer concentrations [47]. The osmotic pressure can also be incorporated into  $R_{CP}$ .

$$J = \frac{\Delta P - \Delta \Pi}{\eta R_M} \quad (9)$$

Reversible flux decline can be reversed by a change in operation conditions, and is referred to as concentration polarisation. Irreversible fouling can only be removed by cleaning, or not at all. Irreversible fouling is caused by chemical or physical adsorption, pore plugging, or solute gelation on the membrane.

### 3.1 Concentration Polarisation (CP)

Concentration polarisation (CP) is the process of accumulation of retained solutes in the membrane boundary layer and was first documented by Sherwood [48]. Concentration polarisation creates a high solute concentration at the membrane surface compared to the bulk solution. The retained solutes are brought into the boundary layer by convection and removed by a generally slower back diffusion. This back diffusion of solute from the membrane is assumed to be in equilibrium with the convective transport. The concentration in the boundary layer is critical for both, fouling and retention [49]. The schematic of CP is shown in Figure 5 and with regard to scaling in Figure 19. CP is normally assumed

to form rapidly at the beginning of filtration [10]. CP in NF causes a reduction in flux predominantly due to the increased osmotic pressure of retained ions and the formation of gels by retained organic molecules. Colloidal deposits can further increase CP by forming an unstirred layer that increases the boundary layer concentration.

At the membrane, a laminar boundary layer exists (Nernst type layer), with mass conservation through this layer described by the Film Theory Model in equation (10) [3].

$$-Jc_F + Jc_F + D_s \frac{dc_{BL}}{dx} = 0 \quad (10)$$

where  $c_F$  is the feed concentration,  $D_s$  the solute diffusivity,  $c_{BL}$  the solute concentration in the boundary layer and  $x$  the distance from the membrane.

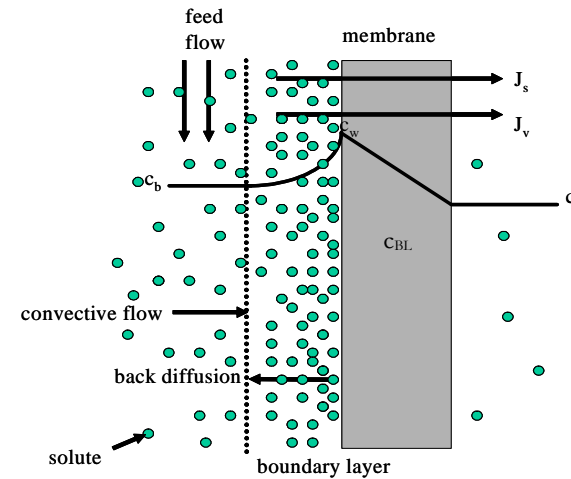


Figure 5 Concentration polarisation (adapted from Sablani *et al.* [49]).

After integrating with the boundary conditions  $c = c_w$  for  $x = 0$  and  $c = c_b$  for  $x = \delta$  (where  $\delta$  is the boundary layer thickness) for similar solute and solvent densities, constant diffusion coefficient, and constant concentration along the membrane, equation (10) can be derived.  $c_w$  is the wall concentration which determines adsorption, gel formation or precipitation, and  $k_s$  the solute mass transfer coefficient.

$$J = k_s \ln \left( \frac{c_w - c_p}{c_b - c_p} \right) \quad \text{with} \quad k_s = \frac{D_s}{\delta} \quad (11)$$

Concentration polarisation can be minimised with turbulence promoters on the feed side of the membrane, such as spacers or introduction of crossflow.

A typical flux versus time diagram for a cyclic operation of a UF system is shown in Figure 6, where cyclic operation means the alternating cycle of filtration or permeate production followed by cleaning. The diagram shows flux for cycles  $i=1$  to  $i=n$  and a very rapid flux decline due to concentration polarisation followed by operation at average flux until cleaning. From cycle to cycle the pure water

permeability as well as the average steady state flux decrease indicating a loss in productivity that cannot be recovered by cleaning until the membrane lifetime is reached. Nikolova and Islam [50] consider concentration polarisation as a more gradual process.

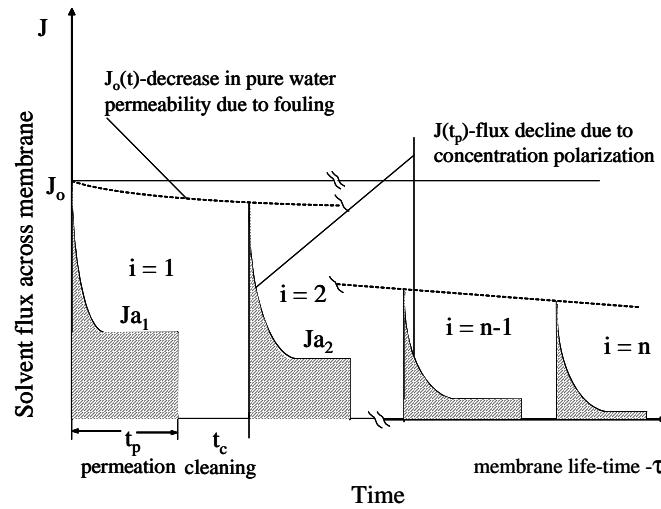


Figure 6 Illustration of flux decline over time due to fouling and concentration polarisation (adapted from Sablani *et al.* [49]).

The effect of concentration polarisation introduces complexity and confusion into the core membrane performance parameter retention. It should be distinguished here between the terms observed ( $R_{OBS}$ ) and real retention ( $R_0$ ). The observed retention is usually measured in membrane applications and calculated as

$$R_{OBS} = \left(1 - \frac{c_p}{c_b}\right) \cdot 100\% \quad (12)$$

where  $c_p$  and  $c_b$  are the permeate and bulk solute concentration as illustrated in Figure 5, respectively. The bulk concentration is often approximated with either the feed concentration or the average of feed and retentate concentration. Considering concentration polarisation, this observed retention does not reflect membrane characteristics, as the retention by the membrane is higher due to the increased wall concentration  $c_w$  at the membrane surface. Hence the real retention is

$$R_0 = \left(1 - \frac{c_p}{c_w}\right) \cdot 100\% \quad (13)$$

To determine the real retention requires knowledge of the solute concentration at the membrane surface which cannot be directly measured. To estimate this wall concentration one requires the velocity dependent mass transfer coefficient which can be determined using mass transfer correlations [51]. The relationship between real and observed retention was published by Koyuncu and Topacik [51] as follows

$$\ln\left(\frac{1-R_{OBS}}{R_{OBS}}\right) = \ln\left(\frac{1-R_0}{R_0}\right) + \frac{J}{k} \quad (14)$$

where  $J$  is the water flux. Hence an increased concentration polarisation at constant intrinsic membrane retention will lead to an increased permeate concentration, and hence, a decreased observed retention.

CP is generally considered as a reversible process that can be controlled by increasing crossflow velocity, permeate pulsing, ultrasound, or an electric field [49]. All those processes aim at the reduction of the solute concentration at the membrane wall ( $c_w$ ), which can only be calculated if the mass transfer coefficient is known. Despite the reversible nature of CP, it contributes to the more problematic fouling mechanisms listed below [49].

- Adsorption of solute
- Precipitation of solute
- Gel layer formation

To reduce CP and fouling, operation below a so-called critical flux [49] is important, which is discussed conceptually in section 3.6.

### 3.2 Osmotic Pressure

Osmotic pressure is closely linked to concentration polarisation. Increased concentration of inorganic or organic solutes causes an increase in osmotic pressure. This osmotic pressure reduces the effective transmembrane pressure and the solvent flux. The osmotic pressure of an inorganic solute can be calculated as

$$\Delta\Pi_{INORG} = \sum j_i \frac{n_i}{V_i} RT \quad (15)$$

where  $j$  is the factor for mole increase due to dissociation for solute  $i$ ,  $n$  the number of moles,  $R$  the ideal gas constant and  $T$  the absolute temperature. For high salt concentrations this equation is inadequate and the Pfitzer equation can be applied. This approach has been used for a nanofiltration application by van der Bruggen *et al.* [52].

The osmotic pressure of an organic solute can be calculated as

$$\Delta\Pi_{ORG} = A_1 c + A_2 c^2 + A_3 c^3 \quad \text{with} \quad A_1 = \frac{R \cdot T}{M} \quad (16)$$

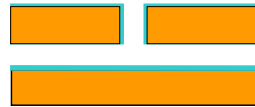
where  $A_i$  are the virial coefficients with  $A_2$  and  $A_3$  considered as negligible for concentrations up to 100 g/L.  $R$  is the universal gas constant,  $M$  the average molecular mass of the organic/polymer and  $T$  the absolute temperature of the solution [50].

### 3.3 Adsorption

Adsorption can be defined as the specific interaction between the membrane and a solute even in the absence of a convective flow through the membrane [50]. The static adsorption (in the absence of flux) is generally lower than in dynamic adsorption due to the increased hydraulic resistance [30].

Adsorption may occur on the membrane surface or in pores, essentially at any point of contact between the solute and the membrane. This is shown in simplified terms in Figure 7.





**Solute < Pore size:** Pore penetration is possible and adsorption of a solute occurs on the membrane surface, in the pores and the back of the membrane

**Solute > Pore size:** Pore penetration is not possible and adsorption sites are only available on the membrane surface

Figure 7 Simplified diagram of adsorption for different solute to pore size proportions.

Adsorption can be measured using the partitioning coefficient between membrane and bulk phase which is defined in Eq (17).

$$K = \frac{\Gamma}{M \cdot C} \quad [\text{L} \cdot \text{m}^{-2}] \quad (17)$$

where  $\Gamma$ : adsorbed quantity of organic ( $\mu\text{g m}^{-2}$ )  
 $M$ : molar mass of the adsorbing compound ( $\text{g/mol}$ )  
 $C$ : equilibrium concentration of the solute in the solution ( $\text{mmol L}^{-1}$ )

Van der Bruggen *et al.* [2] observed flux declines of up to 59% with organics in solutions with concentrations of about 1 g/L. Combe *et al.* [53] also determined foulant – membrane partitioning coefficients and those researchers also considered the solution volume.

Van der Bruggen and Vandecasteele [54] have used an adapted Freundlich equation for the direct description of adsorption from flux decline measurements.

$$J = K_f \cdot C^n \quad (18)$$

where  $J$ : water flux ( $\text{L m}^{-2} \text{h}^{-1}$ )  
 $K_f, n$ : parameters

In filtration the adsorbed amount can determined by mass balance using the following equation

$$C_F V_F = A\Gamma + V_p \sum_1^n C_{pi} + C_c V_c \quad (19)$$

where  $A$  is the membrane area ( $\text{cm}^2$ );  $\Gamma$  is the amount of solute adsorbed per surface area ( $\text{ng cm}^{-2}$ ) and  $n$  is the number of permeate samples;  $C_F, C_p, C_c$  and  $V_F, V_p, V_c$  are concentration and volume of feed, permeate and concentrate respectively. Using this equation for the determination of adsorption assumes that all solute is adsorbed. For higher concentrations this is more correctly expressed as the amount of deposit.

### 3.4 Gel Layer Formation

Gel formation is considered as the precipitation of organic solutes on the membrane surface. This process usually occurs when the wall concentration due to concentration polarisation exceeds the solubility of the organic. Gel formation does not necessarily mean irreversible flux decline.

The Gel Polarisation Model is based on the fact that at steady state flux reaches a limiting value, where an increase in pressure no longer increases the flux. According to the Gel Polarisation model, at this limiting value, the solubility limit of the solute in the boundary layer is reached and a gel formed. For 100% retention, the expression for this limiting flux ( $J_{lim}$ ) is described by Eq (20).  $c_G$  is the gel concentration, beyond which the concentration in the boundary layer cannot increase.

$$J_{lim} = k_s \ln \frac{c_G}{c_B} \quad (20)$$

The model does not include membrane characteristics, and tends to predict a lower flux than observed. An improvement can be achieved in using  $D_s$  for the gel layer rather than the bulk solution [45].



**Solute < Pore size:** Pore penetration is possible and gel formation of a solute occurs on the membrane surface and in the pores

**Solute > Pore size:** Pore penetration is not possible and gel formation occurs only on the membrane surface

Figure 8 Simplified diagram of gel layer formation following adsorption.

### 3.5 Cake Formation and Pore Blocking



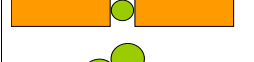






Belfort *et al.* [55] proposed five stages of fouling in microfiltration of macromolecules that are somewhat applicable to NF. These are,

- (1) fast internal sorption of macromolecules,
- (2) build-up of a first sublayer,
- (3) build-up of multisublayers,
- (4) densification of sublayers, and
- (5) increase in bulk viscosity.

The fifth stage can be neglected for dilute suspensions like surface water. The dependence on particle size can be described as

$d_{solute} < d_{pore}$ :	deposit on pore walls, restricting pore size
$d_{solute} \approx d_{pore}$ :	pore plugging or blockage
$d_{solute} > d_{pore}$ :	cake deposition, compaction over time.

Those principles are illustrated in Figure 9. For solutes much smaller than the membrane pores, internal deposition eventually leads to the loss of pores. Solutes of similar size to the membrane pore will cause immediate pore blockage. Particles larger than the pores will deposit as a cake, with the porosity depending on a variety of factors including particle size distribution, aggregate structure and compaction effects. The process of small particles adsorbing in the pores may be a slow process compared to pore plugging, where a single particle can completely block a pore and therefore flux decline should be more severe for the latter case. If the membrane is non porous then the deposition of solutes takes place on the membrane surface with smaller solutes generally forming less permeable deposits.

A	Pore versus Surface Fouling
	<p><b>Pore Adsorption</b> (<math>d_{\text{solute}} \ll d_{\text{pore}}</math>): Colloids or solutes adsorb on the membrane walls, effective pore size is restricted and flux declines</p>
	<p><b>Pore Plugging</b> (<math>d_{\text{solute}} \approx d_{\text{pore}}</math>): Colloid or solutes of a similar size to pore diameter block pores completely, reduction in membrane porosity and severe flux decline</p>
	<p><b>Cake Formation</b> (<math>d_{\text{solute}} \gg d_{\text{pore}}</math>): Colloid or solutes larger than the pores are retained due to sieving effects and form a cake on the membrane surface, depending on pore to particle size ratio flux decline occurs (permeability of the cake layer as well as the cake thickness are important)</p>
B	Impact of Colloid or Solute Stability
	<p><b>Stable Colloids</b> smaller than the pore size are not retained by membrane, unless adsorbed by the membrane material</p>
	<p><b>Tight Aggregates</b> are formed by slow coagulation, are retained and form a cake on the membrane. The aggregate structure may collapse depending on forces on the aggregate and the aggregate stability. Flux through the tight aggregates is usually low unless the aggregates deposit as a porous cake of large particles.</p>
	<p><b>Loose Aggregates</b> are formed by rapid coagulation and are also retained. Such aggregates form a cake on the membrane. The aggregate structure may collapse depending on forces on the aggregate and the stability of the aggregate. Flux through the open aggregates is high if the structure is maintained during filtration.</p>
C	Solute-Solute Interaction
	<p><b>Colloids &lt; pores and stabilised with organics (for example)</b> are not retained by the membrane, unless adsorbed by the membrane material or destabilised with high salt concentrations.</p>
	<p><b>Aggregates with organics adsorbed after aggregation (for example)</b> are fully retained by the membrane, but may penetrate into the upper layer of the membrane. This could also be organics destabilised with multivalent cations.</p>
	<p><b>Colloids which are partially aggregated and destabilised</b> such as a variety of solutes that interact with each other in heterogeneous ways in the presence of salts, colloids and dissolved organics, form small and diverse aggregates which may block pores.</p>

**Figure 9 Colloid – organic fouling mechanisms**

Chang and Benjamin [56] pointed out that the mechanisms of organic colloid deposition and gel layer formation require the application of different models, although many authors fail to differentiate between gel and cake formation. Some authors refer to those mechanisms as deposit formation to simplify the issue. The differentiation is not always simple, especially when considering that aggregation of the gel composites may in fact form a more particulate or colloidal deposit.

**3.6 Critical Flux and Operating Conditions**

Critical flux stems from the concept that the higher the flux the stronger is the drag force towards the membrane (and hence deposition of colloids), the stronger concentration polarisation (and hence the boundary layer thickness and solute concentration) and the higher the compaction of a deposit. The stronger the flux the less dispersible the deposit will be.

Critical flux is defined as the limiting flux value below which a flux decline over time does not occur [57]. Traditionally critical flux derives from the filtration of particulate matter using porous membranes. Mänttari and Nyström [10] describe a strong and weak form of critical flux where the strong form describes the flux where the actual flux starts deviating from the clean water flux, whereas the weak critical flux is the point where flux increase with pressure is no longer linear. This is illustrated in Figure 10 where the solid line is the linear dependence of CWF of pressure, while the dashed line the linear dependence of permeate flux of pressure. The hollow and solid circles show the permeate flux after a stepwise increase and decrease of pressure, respectively. The squares are flux values after filtration at the highest pressure (and hence with significant irreversible fouling).

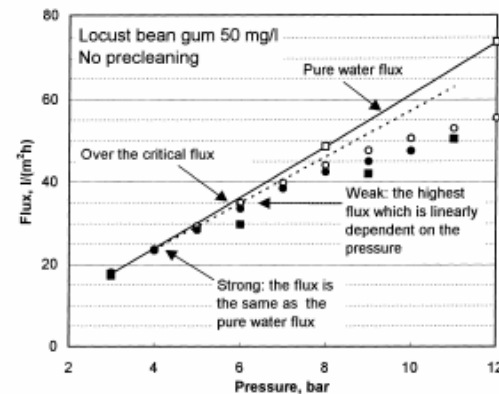


**Figure 10 Critical flux in nanofiltration (reproduced from Mänttari and Nyström [10]). Note that lines represent different experiments.**

A number of parameters influence this critical flux. Crossflow velocity increases the critical flux while solute concentration decreases it. Repulsion between solute and membrane also increase critical flux in the case of high molar mass polysaccharides, while in paper industry effluents only weak forms of critical flux were found [10]. Some authors have noted that the thickness of the fouling layer is primarily dependent on the initial flux [27]. Gwon *et al.* [26] compared NF and RO fouling and found that the fouling layer in NF was mostly organic and could be fully recovered while in RO the fouling was inorganic and organic and could not be recovered. The fouling at the end of the RO modules was

most severe which indicates the importance of reduced crossflow and increased concentration. However the flux at the end of modules would normally be lower than at the module entrance.

### 3.7 Additional Fouling Mechanisms

In nanofiltration processes, the retention of ionic species results in a concentrated layer of ions at the membrane surface (known as *salt concentration polarisation*), which creates an osmotic pressure drop across the membrane. Sub-micrometer colloids are highly Brownian, which means that they are influenced by diffusive, as well as convective transport mechanisms. Also, aggregation and deposition of small colloids are strongly influenced by colloidal forces [58]. The polarized layer of rejected ionic solutes exacerbates colloidal fouling of NF membranes by greatly reducing repulsive electrostatic interactions. Moreover, aggregation of organic macromolecules and precipitated salts may occur in the bulk solution near the membrane surface where rejected ionic solute concentration is higher than in the bulk. These aggregates may act as like very small colloids (typ. < 500 nm) and cause severe fouling because they are not removed in dissolved form by pre-treatment. Therefore, the feed solution chemistry and membrane ion retention are critical to the formation of colloidal-cake layers.

Accumulation of rejected dissolved and (organic, inorganic, or biological) colloidal matter at the membrane surface presents the opportunity for additional fouling mechanisms. These mechanisms arise from interactions between rejected ions and colloids passing through the concentration polarisation layer and at the membrane surface. The classic picture of this situation is presented in Figure 11 where it is assumed that a stagnant cake layer develops with a salt and colloid polarisation layer flowing above the cake layer. In addition, analysis of the factors affecting dissolved solute mass transfer reveals one potential interaction between a colloidal cake layer and the salt CP layer. Increasing the bulk flow rate increases the shear rate, which enhances mass transfer. However, the most influential variable on mass transfer is the solute diffusivity ( $k_s \propto D^{2/3}$ ).

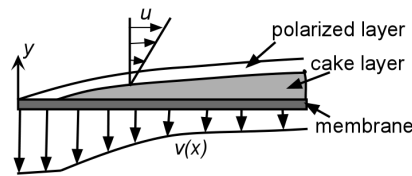


Figure 11 A schematic of a crossflow nanofiltration process showing the development of the cake and concentration polarisation layers, and the corresponding permeate flux decline along the axial direction.

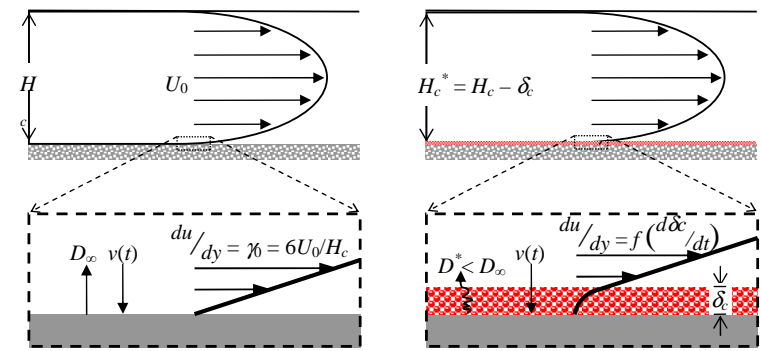


Figure 12 Conceptual illustration of hindered mass transfer in crossflow membrane filtration. The tangential flow velocity,  $U_0$  and the salt ion diffusion coefficient are critical parameters in determining mass transfer in the salt concentration polarisation layer. Tangential flow and salt ion back-diffusion may be locally hindered in the presence of a colloid deposit layer, thus enhancing the membrane surface salt concentration and the resulting trans-membrane osmotic pressure.

It was recently proposed that the mutual diffusion coefficient of rejected salt ions may be hindered within the colloid deposit layers [59-61]. A hindered salt diffusion coefficient was recently used to describe colloid cake-CP layer interactions in crossflow RO/NF membrane filtration [60-62]. The result was elucidation of a single mechanism – “cake-enhanced concentration polarisation” – capable of describing the majority of observed flux decline, as well as the observed decline in salt retention due to colloidal fouling of NF (and RO) membranes. The overall mass transfer coefficient was considered the sum of two mass transfer coefficients, one describing salt back-diffusion from the membrane surface through the cake layer, and one through the remainder of the salt CP layer.

Incorporating the hindered mass transfer coefficient into Eq (11) and solving for the transmembrane osmotic pressure yields

$$\Delta\pi_m^* = f_{os} C_b R_o \exp \left[ \frac{J}{k_s} + v\delta_c \left( \frac{1 - \ln(\varepsilon^2)}{D_s \varepsilon} - \frac{1}{D_s} \right) \right], \quad (21)$$

where  $\Delta\pi_m^*$  is termed the “cake-enhanced osmotic pressure.” The term in brackets in Eq (21) comes from considering a thin cake layer, in which the tangential flow field is assumed unchanged by the presence of the cake, and hindered diffusion alone reduces mass transfer [59, 61]. The reduced salt diffusivity in the cake layer is expressed as  $\varepsilon D_s / \tau$ , with the tortuosity,  $\tau$ , being approximated as  $1 - \ln(\varepsilon^2)$  [59-61, 63]. The only term on the right hand side of Eq (21) that is not a known constant or experimentally measurable parameter is  $\varepsilon$ , the cake layer porosity.

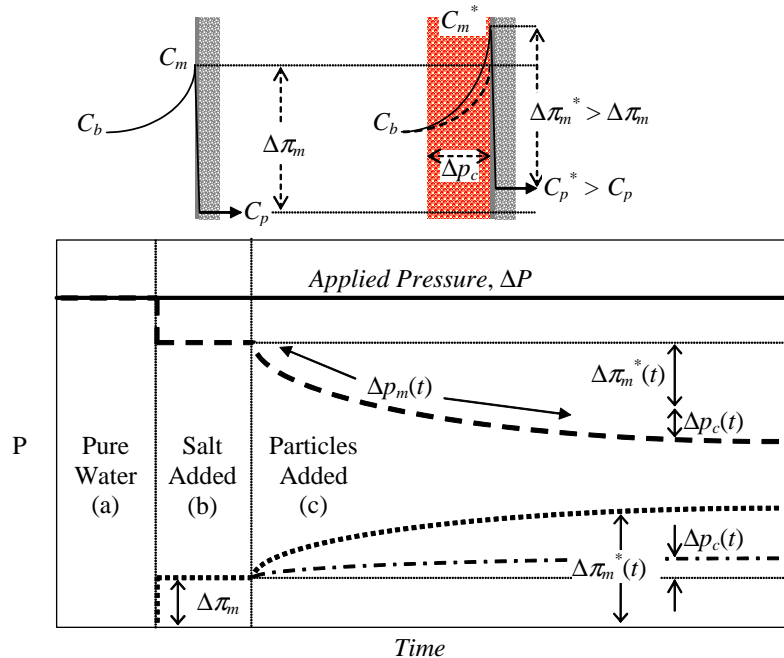


Figure 13 Conceptual illustration of the effect of cake-enhanced concentration polarisation on flux when operating at constant pressure based on laboratory experiments of Hoek *et al.* [61, 64]. Initially, the applied pressure and membrane (hydraulic) resistance control pure water flux (a). For a simple electrolyte feed solution (b), an osmotic pressure drop ( $\Delta\pi_m$ ) across the membrane develops nearly instantaneously due to the accumulation of rejected salt ions at the membrane surface. Trans-membrane pressure is the difference between applied pressure and the trans-membrane osmotic pressure. Immediately after colloidal particles are added to the feed (c) they begin to accumulate on the surface of the membrane and form a “cake” layer. A hydraulic pressure drop forms across the stationary colloid cake layer, which increases as the cake layer thickness increases. More importantly, the concentration of rejected salt ions builds up within in the cake layer because mass transfer (back-transport of salt ions) through the cake layer is hindered. The resulting “cake-enhanced osmotic pressure” ( $\Delta\pi_m^*$ ) can be an order of magnitude greater than the trans-cake hydraulic pressure when membrane salt retention is high.

The greater implication of this finding is that any accumulated mass on the surface of a salt rejecting (NF/RO) membrane may entrap ions, enhancing the trans-membrane osmotic pressure. Therefore, cake-enhanced osmotic pressure may play a role in fouling due to the most ubiquitous and recalcitrant foulants in NF processes, namely biofilms, scale, and organic matter, but this has yet to be proven. Further, the mechanism of salt entrapment within foulant deposit layers helps to explain the commonly

observed decline in salt retention associated with NF membrane fouling. The entrapment of salt ions within the cake layer enhances the membrane surface salt concentration, and therefore, the chemical potential gradient responsible for solute transport through nanofiltration membranes. It is possible that fouling by macromolecules with high charge density (e.g., proteins, humic and fulvic acids, etc.) may actually reject salt ions and other dissolved species if they form densely packed cake or gel layer. In such cases enhanced concentration polarisation phenomena may be suppressed. These interactions are discussed in more detail in the following sections.

## 4 ORGANIC FOULING

Organics interact with membranes in a number of ways. It is difficult to single out individual interaction mechanisms. The mechanism is strongly dependent on the organic type and the chemical characteristics of the molecules as well as their affinity towards the membrane material. Some of those solute-membrane interaction mechanisms are described in Chapter 20.

### 4.1 Introduction and Definition of Organic Fouling

Organic fouling is the irreversible flux decline due to the adsorption or deposition of dissolved or colloidal organic material. This can be the adsorption at a molecular level or as a monolayer, the formation of a gel on the membrane surface, the deposition or cake formation by organic colloids or the pore restriction and blocking by molecules that can penetrate into the membrane. Such organic fouling can be severe and persistent, for example Roudman and DiGiano [65] reported that even rigorous chemical cleaning failed to remove NOM from nanofiltration membranes.

### 4.2 Common Organic Foulants

Organics play an important role in fouling and act in a number of ways. Firstly, organics may adsorb to or deposit on membranes resulting in a variation of the surface characteristics and hence flux and fouling behaviour. Secondly, organics may act as a nutrient source for microorganisms and hence facilitate biofouling. Thirdly, organics may adsorb onto colloids, stabilise small colloids and hence make it more difficult for those colloids to be removed in pre-treatment. In fact, in the natural environment colloids commonly have a negative surface charge due to an adsorbed layer of NOM, which can lead to stabilisation of the colloids [66, 67]. The degree of stability depends on the amount of organics adsorbed. Lastly, some also describe the organics themselves as “colloids” and hence organic and colloidal fouling overlap.

In the water and wastewater industry, natural and effluent organic matter are well known and well studied foulants. The natural organic matter (NOM) is predominantly composed of so-called humic substances [4]. Effluent organic matter (EfOM) is the wastewater equivalent of NOM and contributes to membrane fouling by adsorption, surface accumulation or pore blocking, mostly by the humic fractions and polysaccharides [68]. Wiesner *et al.* [69] identified four NOM categories which are strong foulants - proteins, aminosugars, polysaccharides, and polyhydroxyaromatics. Polysaccharides were also confirmed compounds of relevance to fouling in the field of wastewater treatment [43]. Jarusutthirak *et al.* [40] further fractionated and characterised EfOM. The following fractions were separated

- Colloidal EfOM with hydrophilic character composed of polysaccharides, proteins, aminosugars

- Hydrophobic EfOM with humic substance characteristics (high aromaticity and carboxylic functional groups)
- Transphilic EfOM also with humic substance characteristics
- Hydrophilic EfOM containing low molecular mass acids.

Lee *et al.* [29] determined that both the hydrophilic as well as the hydrophobic fractions adsorbed significantly to UF membranes, whereas transphilic NOM, mostly composed of hydrophilic acids, adsorbed very little.

The humification diagram for a number of NOM samples from surface waters is presented in Figure 14. The relationship to effluent organic matter is visible in the bottom left corner where the approximate location of fulvic acids from sewage treatment plants is indicated. The different characteristics of EfOM and NOM as well as their fractions reflect in different fouling characteristics.

Nyström *et al.* [42] have investigated a number of organic molecules towards their fouling characteristics. A type of starch that had a higher protein content fouled the membranes very strongly. Fouling of polysaccharides and humic substances showed that when the organics were charged fouling was pH dependent with the highest amount of fouling occurring when the charge repulsion was lowest [43]. Further, solute-solute interactions also influence fouling [43]. However, those interactions are to date very poorly understood.

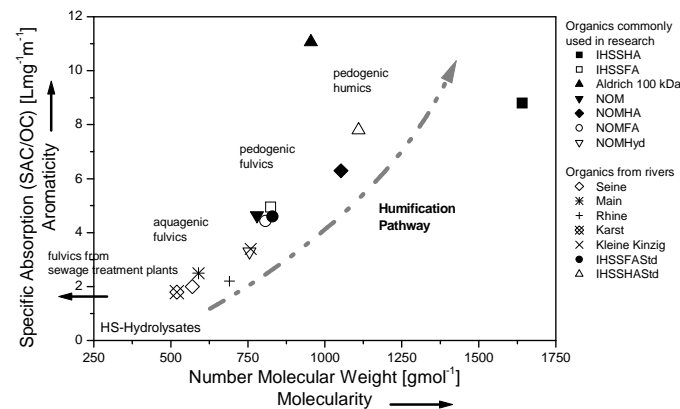


Figure 14 Humification diagram showing the molecular mass and aromaticity for a number of surface waters as reported by Huber [70] and organic compounds used in water research (adapted from Schäfer *et al.* [71]).

Extracellular polymeric substances (EPS) which surround microorganisms and may be produced by a biofilm tend to attach well to surfaces and may also cause pore blockage when removed from the bacterial cells as is described in the biofouling section of this chapter. Chang and Lee [72] have linked fouling and EPS content in a membrane bioreactor (MBR) application and suggested EPS content as a

possible feedwater fouling index for wastewater applications. The importance of EPS in MBR fouling was confirmed by Cho and Fane who determined that fouling occurred in two stages; a gradual deposition of EPS on the (MF) membranes followed by a rapid and sudden stage of biomass growth that required membrane cleaning [28]. Amy and Cho [73] identified polysaccharides as dominant foulants in UF and NF of surface water, although polysaccharide concentration in surface waters would be comparatively low.

The behaviour of foulants in mixtures is a further issue - Mackey [74] for example studied the fouling of UF and NF membranes (cellulose ester and TFC-SR) by various model compounds, such as polysaccharides, polyhydroxyaromatics, and proteins. The larger compounds (polysaccharides and proteins) caused more fouling, and in mixtures the fouling increased.

### 4.3 Adsorption

Adsorption plays an important role in the fouling of NF membranes by organic compounds. In fact, adsorption is often regarded as the first step in membrane fouling. Adsorption of organic compounds can be considered as the formation of a conditioning film which allows the attachment of bacteria and hence biofouling, as an example. Adsorption can also cause pore narrowing and may hence be a precursor to pore plugging. Adsorption of humics has, for example, been shown to occur in pores and on the membrane surface [53]. Adsorption of organic molecules into the membrane matrix changes the free volume in the membrane. Depending on the molecule the interaction can either increase or decrease this free volume and hence flux [42]. Nyström *et al.* [42] showed for example that small vanillin molecules caused an increase in flux, if charged. Longer chained molecules with a charge did not cause fouling due to the lack of interaction with the membrane due to charge repulsion, while proteins cause very strong fouling. The adsorption of NOM renders membranes more hydrophilic and hence facilitates water permeation [65].

Nikolova and Islam [50] showed that in UF of dextran the adsorbed layer is causing most of the flux decline as opposed to osmotic pressure effects, although the adsorption was, in this case, reversible. Adsorption is an equilibrium process between the wall concentration determined by concentration polarisation and the adsorbed organics. According to Nikolova and Islam [50] this relationship between adsorption and concentration is linear. Other authors describe the adhesion more mechanistically in that adhesion occurs due to double layer interactions or hydration forces when adsorbing molecules and the membrane reach close enough contact to interact [27].

Carlsson *et al.* [41] performed a study using pulp mill effluent and UF and found that hydrated lignin sulfonates adsorbed to the membrane surface followed by later deposits of cellulosic oligomers.

Champlin [75] investigated the impact of NOM adsorption on NF membranes in the presence of particulate matter. NOM adsorption was as high as 12.6% of the available NOM, but interestingly this adsorption is reduced in the presence of particulate matter. The postulated mechanisms were particles acting as abrasive scouring or an adsorbent that competes with the membrane surface for NOM.

Adsorption itself can either be the precursor to a more severe fouling layer or cause significant fouling by itself [2]. Adsorption of organic compounds can also alter the membrane surface characteristics (such as increasing hydrophobicity or membrane charge) and hence lead to flux variations. The effect of humic acid on membrane surface charge has been investigated by a number of researchers [76-78] and showed that humic substances influence the surface charge (in general a more negative charge) is

observed) and the adsorbed organics in fact dominate the surface charge with their functional groups. The uptake of organics by hydrophobic membranes is stronger [53]. The deposition of the more aromatic compounds appears stronger and can also be facilitated by the presence of calcium [79]. The multivalent ions act in various ways [80]. Firstly the charge repulsion can be reduced in the presence of the electrolyte, secondly the cations may form bridges between identically charged foulants and membranes and thirdly it may vary the configuration of the foulant molecules. The adsorption of humic substances has also been shown to alter the hydrophobicity of the membrane [81]. The authors anticipated that fouling is more severe when non-polar bonds are formed between the foulant and the membranes as opposed to polar bonds.

A number of compound and membrane characteristics are important in adsorption; those are water solubility, dipole moment, octanol water partitioning coefficient, surface charge, hydrophobicity, molecular size/mass and membrane cut off or pore size [2]. Methods to characterise membranes were described in detail in Chapter 5. Adsorptive fouling of organics not always decreases as the negative charge and hydrophilicity of a membrane increases. In fact, oxidation of the membrane increases negative charge, hydrophilicity and humic acid adsorption [53]. Jarusutthirak and Amy [68] found that negatively charged membranes adsorbed the hydrophobic fraction of EfOM.

Freundlich isotherms were in fact confirmed by other authors for the adsorption of NOM [75].

Nghiem and Schäfer [30] have determined a breakthrough phenomenon for some NF membranes that can be attributed to the adsorption of contaminants at very low (ng/L) concentrations. The amount adsorbed was dependent if a penetration into the active layer by the contaminants was possible. Adsorption was dependent on the pKa of the contaminants with higher adsorption when the compounds are undissociated. Similar trends were observed by Jones and O'Melia [82] when hydrophobic interaction of bovine serum albumin (BSA) with membranes decreased as the isoelectric point (IEP) was exceeded. A summary of adsorbed quantities of trace contaminants in membrane modules is given in Chapter 20.

The actual interaction mechanisms that govern adsorption are not well understood. Roudman and DiGiano [65] suggested the predominance of acid-base interactions and hydrogen bond formation between NOM and membranes. Hydrogen bond formation was also suggested as a predominant mechanism in the adsorption of trace organic contaminants by thin film composite membranes in Chapter 20. To date it is not easily possible to distinguish between hydrogen bond formation and hydrophobic interactions.

The stronger a compound adsorbs to the membrane, the higher the flux decline [2]. Partitioning coefficient appears to increase with dipole moment indicating a possible charge interaction. The partitioning coefficient also increases with the octanol water partitioning coefficient ( $K_{ow}$ ; Log P) and hence hydrophobicity. In other words hydrophobic interactions between membranes and organics cause flux decline. Water solubility describes the polar character of a molecule, but was not identified to have a correlation with adsorption. Seeing the importance of hydrophobic interactions it is not surprising that it is repeatedly reported that hydrophobic membranes foul more [41].

Adsorption can occur on the membrane surface and in the pores [53]. This depends on the pore size, the molecular size and shape as well as the solution chemistry which can change the structure and shape of organics [83]. Chang and Benjamin have estimated the thickness of an adsorbed monolayer of

NOM to have a thickness of about 1.6nm, which is larger than the typical NF pore dimensions. Hence, if pores exist, such adsorption leads to pore restriction or blockage.

#### 4.4 Gel Layer Formation

Gel formation occurs when the solubility of a non-crystalline solute is exceeded. This is often the case when organic molecules flocculate in the presence of salts and at neutral charge conditions [42] such as when the surface concentration increases due to concentration polarisation [84]. More details on coagulation are given below (Section 4.7). Deposits formed on the membrane surface by materials that are too large to penetrate into or through the membrane eventually reach a steady state thickness. Given the importance of concentration polarisation, crossflow velocity can be expected to reduce such phenomena [84]. Chang and Benjamin [56] estimated that such a film could grow at a rate of about 0.3  $\mu\text{m}$  a day in full scale systems that remove NOM in water treatment. Those authors assumed a density of a NOM gel layer to be 1  $\text{g}/\text{cm}^3$ , a water content of 50% and NOM of 50% carbon by mass to calculate such a 0.3  $\mu\text{m}$  thick layer to require 75 mg of DOC per  $\text{m}^2$ , which was estimated to be about 1% of the organic carbon a typical water treatment system would be exposed to.

Gel formation was observed by Jarusutthirak *et al.* [40] in the filtration of EfOM due to the large molecular mass of the colloidal EfOM fraction and the small MWCO of NF. The hydrophobic and transphilic fractions were assumed to cause a gel layer also, initiated by hydrophobic interactions, while charge repulsion reduced fouling by charged molecules.

#### 4.5 Cake Formation

Seidel and Elimelech [84] described fouling of NOM as a combination of permeation drag and calcium binding, hence a coupled process between hydrodynamics and chemical interactions. Very importantly those authors have pointed out that permeation drag can overcome repulsive forces of double layers and cause foulant deposition at typical operating conditions. This observation strongly supports the critical flux phenomena from Section 3.6. At low flux, below such a critical flux, the repulsion between foulant and membrane may be strong enough to prevent deposition. Calcium can adversely affect some fouling prevention strategies such as crossflow velocity. Hong and Elimelech [80] related solution chemistry with the formation of a membrane deposit with varying characteristics (see Figure 15). This illustrates also the change in foulant conformation due to solution chemistry. When the charge of the foulants is low, which for NOM is at high ionic strength, low pH and in the presence of multivalent ions, the NOM is coiled and deposits as a firm cake. If the repulsive forces between the NOM functional groups are enhanced then the cake layer is less sticky and more porous. It should be noted here that the 'solution chemistry' refers not only to the feed characteristics, but also to the conditions in the boundary layer.

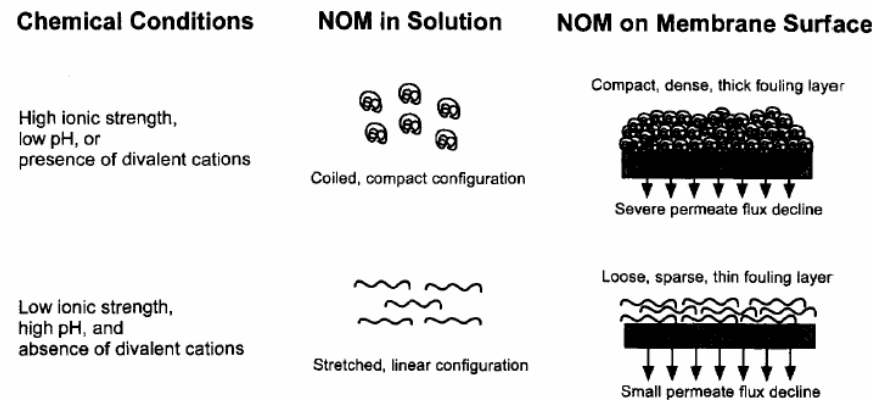


Figure 15 Effect of solution chemistry on the deposit of NOM on a membrane surface (reprinted from Hong and Elimelech [80]).

Such cake deposits will form where space is available- if pores are large enough then this process is accompanied by pore penetration, restriction and plugging.

#### 4.6 Pore Blocking/Plugging

Pore blocking is determined mostly by the size of the organic molecules and the pore size of the membranes. Adsorption can play an important role in pore blocking, where pores are initially restricted due to adsorption of molecules which penetrate into the pores. This is also referred to as pore narrowing [85]. Naturally, pore plugging may occur when the retention of solutes is incomplete [50]. Chang and Benjamin [56] stipulated that pore constriction by trapped molecules is the predominant mechanism with nanofiltration and tight ultrafiltration membranes, while surface gel is a more important process for looser membranes. This was confirmed by Cho *et al.* [86] who described a process of quick flux decline due to pore blockage followed by a gradual narrowing and closing of the remaining pores in UF. Hong and Elimelech [80] observed strong adsorption and pore blocking at low pH for NOM.

Jarusutthirak *et al.* [40] found that the colloidal EfOM fraction was primarily responsible for pore blocking and this mechanism dominated fouling.

Pore blocking would be expected to occur for compounds which are small enough to penetrate into the membrane structure and yet large enough to experience hindrance within this structure [2]. This effect can be achieved due to the size of the molecule itself or due to solute-solute interactions.

#### 4.7 Impact of Solute-Solute Interactions and Salts

Salts in feed solutions or cations in particular can have various effects on fouling. Firstly, such cations may cause intermolecular bridging between the organic foulants and the membranes [84]. Secondly, the cations may form complexes with the organics and at higher salt concentrations cause coagulation or precipitation and gel formation. Such interactions are complex and are to date not well understood. Organics can also act as ligands for multivalent cations (for more details see Chapter 7), form

complexes with specific interactions and affect the retention and scaling of inorganics. This is shown at the example of humic acid and calcium (calcite scale) in Figure 16.

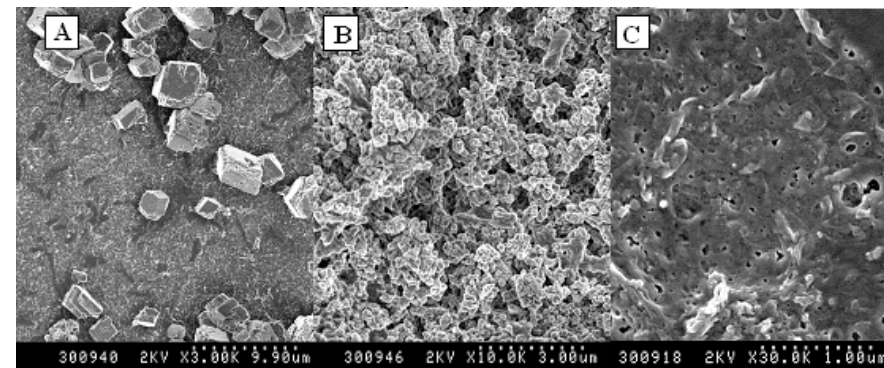


Figure 16 Interaction of calcium and humic substances in fouling A: Calcium Carbonate (pH 10), B: Calcium Carbonate and NOM (pH 10), C: Calcium and NOM (pH 8) (adapted from Schäfer [4]).

Calcium and other multivalent cations are well known to increase organic fouling. Li and Elimelech [87] confirmed the previously suggested mechanism of intermolecular bridge formation of calcium between organic foulants and membrane functional group using atomic force microscopy (AFM). Seidel and Elimelech [84] stated that NOM- calcium complexation and aggregation also causes fouling. Salts also influence solute-solute interactions and may enhance coagulation or aggregation of organics.

Wall and Choppin [88] carried out a comprehensive study of humic acids coagulation due to  $\text{Ca}^{2+}$  and  $\text{Mg}^{2+}$  and established that the Derjaguin-Landau-Verwey-Overbeek (DLVO) theory applies to such organics, in fact even their size distribution changes with time following fractionation. Such a humic colloidal system destabilises when double layer of individual colloids interact and hence precipitation or coagulation occurs. The critical coagulation concentration (CCC) for HA was 0.1-1 M (NaCl), 1-5 mM ( $\text{Ca}^{2+}$ ), 10-50 mM ( $\text{Mg}^{2+}$ ) which is a realistic range for the boundary layer conditions of some membranes. At very high ionic strength (NaCl) the molecular colloids are restabilised and coagulation is prevented. Coagulation also decreased with pH in the range 4-8 rendering the CCC pH dependent (pH 2.5, 4, 7 resulting in CCCs of 1 mM, 100mM and 3M, respectively).  $\text{Mg}^{2+}$  was significantly less efficient in coagulating HA than  $\text{Ca}^{2+}$ . Such studies on solute-solute interactions shed light on the possible mechanisms observed in nanofiltration. Hong and Elimelech [80] confirmed this for NOM fouling in the presence of calcium- where the interaction of those compounds caused the formation of small and coiled macromolecules that deposited at a higher rate.

For example, in the filtration of dye, Koyuncu and Topacik [51] have found that an increase in ionic strength (NaCl) the aggregation of dye reduced flux decline. Similar results were reported by Schäfer *et al.* [89] who use ferric chloride ( $\text{FeCl}_3$ ) as direct pre-treatment to NF and fouling of calcium and HA was reduced. This was attributed to the binding of the foulant HA to  $\text{FeCl}_3$  flocs as well as iron

hydroxides and hence the formation of more porous deposits, unavailability of the HA to form a gel layer and the removal of larger particulates due to shear forces.

#### 4.8 Impact of Fouling on Retention

Fouling can affect the retention of a membrane. For example, Nyström *et al.* [42] have demonstrated that the retention of humic acid decreased in the presence of FeCl<sub>3</sub>. This was explained with the deposition of a gel layer on the membrane. Seidel and Elimelech [84] confirmed a decreased retention of TDS due to fouling, in particular at increased calcium concentrations. This was explained with a reduced Donnan charge exclusion. The Donnan effect was described in detail in Chapter 6. The apparent pore plugging of NF membranes by NOM at low pH was reported to cause a decrease in retention [80]. Schäfer *et al.* [89] established a strong impact of ferric chloride flocs on the retention behaviour of NF membranes. The variations were attributed to the charge of the deposits.

Koyuncu and Topacik [51] studied the effect of reactive black dye (991 g/mol) on the retention of inorganic ions by NF. There the dye deposit was also regarded as a porous gel layer that increased the concentration polarisation effect and acted like a dynamic membrane. Salt retention decreased with increasing dye concentration, reaching negative retention in some cases. This effect of gel layer on retention can potentially be explained via the enhanced concentration polarisation model described in section 3.7 above, especially because these authors reported real rather than observed retention values.

Figure 17 Schematic of the formation of an idealised fouling layer which increased retention of compounds smaller than the membrane pore (above) and that decreases retention (below).

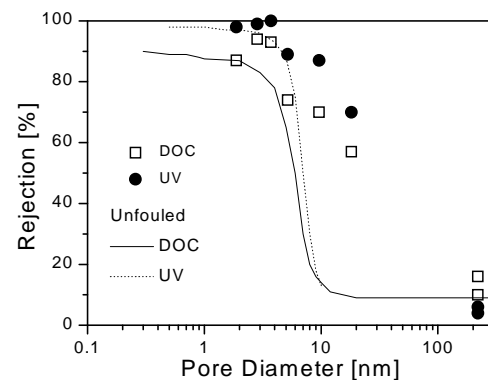
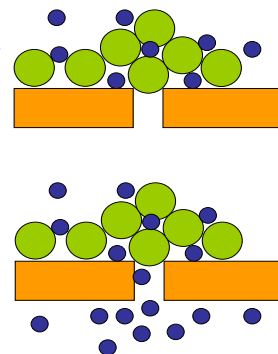


Figure 18 Reduction of the effective pore diameter of membranes and retention of organic compounds due to a fouling layer (calcium and humic substances) [4].

Membrane fouling can modify membrane characteristics and subsequently vary retention behaviour in both directions. For example, Jarusutthirak and Amy [68] observed an increase in retention in consequence of adsorption of EfOM to membranes.

## 5 SCALING

### 5.1 Introduction and Definition of Scaling

A serious problem in NF (and RO) systems and a limiting factor for its proper operation is membrane scaling, resulting from the increased concentration of one or more species beyond their solubility limits and their precipitation onto the membranes [69]. Thus, it is essential to operate NF systems at recoveries lower than a “critical value” in order to avoid scaling, unless the water chemistry is adjusted to prevent precipitation. At present, it is not possible to predict with sufficient reliability the limiting concentration level at which there is a risk of scale formation with a given membrane system and a specific antiscalant treatment [90].

Scaling, also *scale formation* or *precipitation fouling*, occurs in a membrane process whenever the ionic product of a sparingly soluble salt in the concentrate stream exceeds its equilibrium solubility product. The term “membrane scaling” is commonly used when the precipitate formed is a hard scale. Scaling usually refers to the formation of deposits of inverse-solubility salts (CaCO<sub>3</sub>, CaSO<sub>4</sub>·xH<sub>2</sub>O, calcium phosphate etc.), although this term in general denotes hard, adherent deposits of inorganic constituents of water that formed *in situ* [91]. As with the other types of fouling, precipitation fouling reduces the quality and the flux of NF permeate and shortens the life of the membrane system. The problem is usually aggravated in attempts to increase the water (permeate) recovery; then the increasing retentate salt concentration leads to supersaturation, in particular very close to the membrane surface. Inorganic scale formation on the membrane may also lead to physical damage of the membranes due to the difficulty of scale removal and to irreversible membrane pore plugging.

Inorganic foulants found in NF applications include carbonate, sulphate and phosphate salts of divalent ions, metal hydroxides, sulphides and silica. More specifically, the most common constituents of scale are CaCO<sub>3</sub>, CaSO<sub>4</sub>·2H<sub>2</sub>O, and silica, while other potential scaling species are BaSO<sub>4</sub>, SrSO<sub>4</sub>, Ca<sub>3</sub>(PO<sub>4</sub>)<sub>2</sub> and ferric and aluminium hydroxides [69, 92, 93]. Reliable prediction of the scaling propensity of a feed is essential in NF systems in order to maximise recovery and to determine the most efficient scale control method. The main parameters affecting scaling are salt concentration in the concentrate, temperature, fluid velocity, pH and time. These parameters may also include the type and the material of the membrane.

The precipitation or crystallization of a salt onto a membrane surface involves the nucleation and growth from a supersaturated solution. Supersaturation is the thermodynamic driving force for precipitation (or more specifically for the two basic stages of precipitation, nucleation and growth) and it is subsequently discussed in more detail. However, for the sparingly soluble salts precipitation seems to be controlled by the kinetics of the process. It is widely accepted that precipitation kinetics is comprised of two main steps [94] either of which may control the process:

(1) *Nucleation stage*: nuclei (or tiny particles or embryos) are formed at specific sites in pores and at the surface of the membrane. This type of nucleation can be characterised as heterogeneous nucleation, as opposed to homogeneous nucleation, which occurs in the absence of a solid interface. A third form of nucleation is the secondary or surface nucleation, resulting from the presence of a crystallisation phase



in solution (e.g. introduction of seed crystals). The critical value of the supersaturation ratio for the different nucleation processes can be expressed as  $S_{c,homog.} > S_{c,heterog.} > S_{c,surface} > 1$  [95]. In general, nucleation is the most poorly understood step. The rate of nucleation plays an important role in the final scale formation and antiscalants are usually employed to suppress it.

(2) *Crystal growth*: in the case of surface nucleation, the initial nuclei grow in time to form a thin, sometimes porous, layer. In a simplistic way, “growth units” or scale-forming ions diffuse to the crystal surface and attach themselves to that surface. Often, a delay or induction period exists before detectable deposits are formed. The crystal growth process proceeds also in various steps, any of which may control the whole growth process. In the case where nucleation in the bulk dominates, crystal growth takes place in the bulk and the crystalline particles can be deposited onto the membrane surfaces.

In an NF process, the highest risk of scaling exists in the concentrate stream at the last section of the membrane system. The withdrawal of the permeate results in an increase of the concentration level of all dissolved species in the concentrate stream and in the establishment of supersaturation of one or more sparingly soluble salts, which subsequently may precipitate. Therefore, it is necessary to estimate the saturation conditions of the concentrate stream throughout a membrane element. These calculations are based on the knowledge of the feed water composition and of the concentration (or recovery) factor or ratio, CF. For each species *i*, the latter is defined as

$$CF_i = \frac{1 - (1 - R_i)}{1 - y} \quad (22)$$

where *y* is the permeate recovery fraction and *R<sub>i</sub>* the ion retention factor. For most divalent species in NF systems *R<sub>i</sub>* ranges between 0.9 and 1.0, but for monovalent species a significant fraction passes the membrane. The concentration of most ions (Ca<sup>2+</sup>, Sr<sup>2+</sup>, SO<sub>4</sub><sup>2-</sup>, Cl<sup>-</sup> etc.) may be estimated as the CF times the feed water concentration. This cannot be applied to all species present in water (e.g. HCO<sub>3</sub><sup>-</sup>, CO<sub>2</sub>), while for SiO<sub>2</sub> a correction for the pH change is required.

In fact, Eq (22) underestimates the concentrations next to the membrane, since it does not account for the *concentration polarisation effect* [93, 96]. As water permeates through the membrane, the rejected ions accumulate in a boundary layer near the membrane at concentrations higher than those prevailing in the bulk, as illustrated schematically in Figure 19. This means that the supersaturation ratio, and consequently the scaling risk, is higher at the membrane boundary layer. This effect increases with higher permeate fluxes and is higher at low flow velocities.

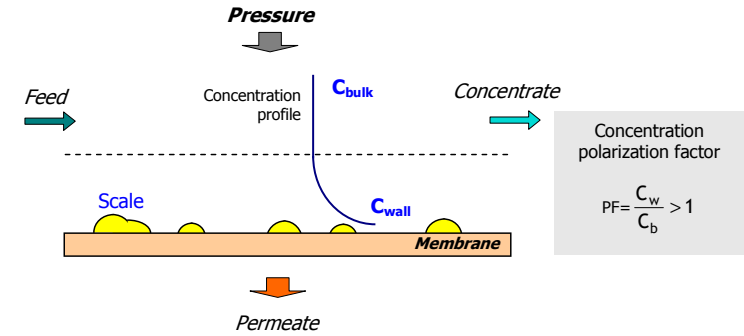


Figure 19 Schematic of concentration polarisation layer at the membrane surface.

The ratio of concentration at the boundary layer to that in the bulk of the concentrate is called the concentration polarisation factor, PF. Typically, PF is estimated as an exponential function of the recovery

$$PF = \exp(K \cdot y) \quad (23)$$

where *K* is a semi-empirical constant, which depends upon permeate flux and ion diffusivity. Discussion on the subject can be found in a following chapter, while a simple technique for determining the concentration polarisation level in a membrane system is described by Sutzkover *et al.* [96]. Because of the pivotal importance of the supersaturation concept, a more detailed description is presented.

## 5.2 Solubility and supersaturation of salts

The phase change associated with precipitation processes can be explained by thermodynamic principles. When a substance is transformed from one phase to another, the change of the Gibbs free energy of the transformation is given by

$$\Delta G = (\mu_2 - \mu_1) \quad (24)$$

where  $\mu_1$  and  $\mu_2$  are the chemical potentials of phase 1 and phase 2, respectively. For  $\Delta G < 0$ , the transition is spontaneous. The molar Gibbs free energy can be also expressed in terms of activity as

$$\Delta G = RT \ln(\alpha / \alpha_0) \quad (25)$$

where *R* is the gas constant, *T* is the absolute temperature,  $\alpha$  is the activity of the solute and  $\alpha_0$  is the activity of the solute in equilibrium with a macroscopic crystal. More specifically, for an ionic substance  $M_nX_m$ , which crystallizes according to the reaction



the thermodynamic driving force for the crystallization either in the bulk or at the membrane surface is defined as the change of the Gibbs free energy of transfer from the supersaturated state to equilibrium:

$$\Delta G = RT \ln \left[ \frac{(M^{a+})^n (X^{b-})^m}{K_{sp}} \right]^{1/(n+m)} = RT \ln \left[ \frac{IAP}{K_{sp}} \right]^{1/(n+m)} \quad (27)$$

In the above equation,  $K_{sp}$  is the thermodynamic solubility product of the phase forming compound and (IAP) is the ion activity product. Quantities in parentheses denote activities of the corresponding ions. The quantity

$$S = \left[ \frac{(M^{a+})^n (X^{b-})^m}{K_{sp}} \right]^{1/(n+m)} = \left[ \frac{IAP}{K_{sp}} \right]^{1/(n+m)} \quad (28)$$

is defined as the supersaturation ratio of the crystalline precipitate. Often in the literature  $S$  is written without the exponent. The activity coefficients can be estimated using various equations applicable to low or high ionic strength. The development of supersaturation is the driving force for both nucleation and crystal growth. Provided that there is sufficient contact time with a foreign substrate, scale formation may take place. Supersaturation in a membrane system is mainly caused by permeate withdrawal and concentration polarisation and, to a lesser extent, by temperature and pH changes.

Nowadays, the solution speciation and the supersaturation ratios of various salts in water are readily computed by various computer codes taking into account all possible ion-pairs and the most reliable values for the solubility products and the dissociation constants. This is covered in more detail in Chapter 7 on solute speciation.

In Figure 20 a typical solubility diagram for a sparingly soluble salt of inverse solubility (such as calcium carbonate, sulphate and phosphate) is shown. The solid line corresponds to the equilibrium. At a point A the solute is in equilibrium with the corresponding solid phase. Any deviation from this equilibrium position may occur with the increase of solute concentration (isothermally, line AB), with the increase of solution temperature due to solubility reduction (at constant solute concentration, line AC), or with varying both concentration and temperature (line AD). A solution departing from equilibrium is bound to return to this state through precipitation of the excess solute. For most of the scale forming sparingly soluble salts, supersaturated solutions may be stable for practically infinite time periods. These solutions are referred to as *metastable*.

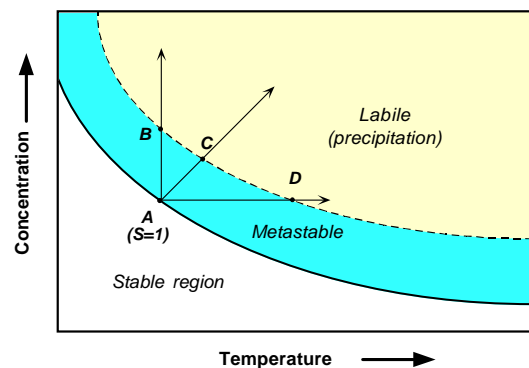


Figure 20 Solubility-supersaturation diagram of a sparingly soluble salt of inverse solubility.

There is, however, a threshold in the extent of deviation from equilibrium marked by the dashed line in Figure 21, which if reached, wall crystallization (scaling) usually occurs first. Spontaneous bulk precipitation may also occur with or without a preceding induction period. This range of supersaturations defines the labile region and the dashed line is known as the supersolubility curve. It should be noted that the supersolubility curve is not well defined and depends on several factors such as concentration level of the scale-forming ions, presence of other ions and ionic strength, presence of suspended matter, wall material and roughness, temperature, pH etc. The formation and subsequent deposition of solids occurs only if the solution conditions correspond to the metastable or to the labile region. Below the solubility curve scaling cannot take place.

Most membrane suppliers and literature sources set  $S > 1$  as criterion for the onset of scaling. Often this criterion is modified, a little below or a little above unity. The argument that for  $S > 1$  precipitation is expected is true for the readily soluble salts, where even a small deviation from equilibrium can induce crystallization. However, for most of the sparingly soluble salts responsible for the scaling problems in the NF/RO systems, a significantly higher value of supersaturation ratio (“critical” supersaturation ratio) in the bulk must be exceeded to result in scaling. This effect is observed in membrane as well as in non-membrane scaling systems. For example, it has been reported that an RO system exceeded 14 times the  $BaSO_4$  equilibrium conditions without scaling problems [97]. A major concern about this “critical” supersaturation ratio is that it is not the same for all scale-forming compounds and that it increases as the solubility of the salts decreases. Consequently, one may expect that this value is higher for the  $CaCO_3$  and  $BaSO_4$  scaling systems than for the  $CaSO_4$  system.

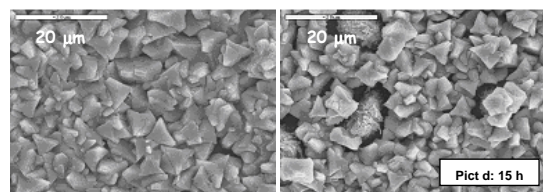
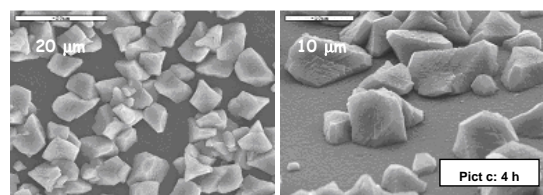
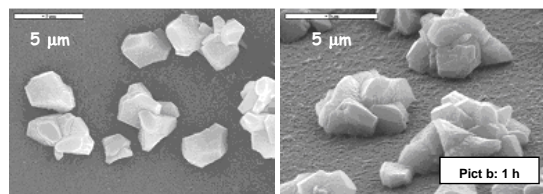
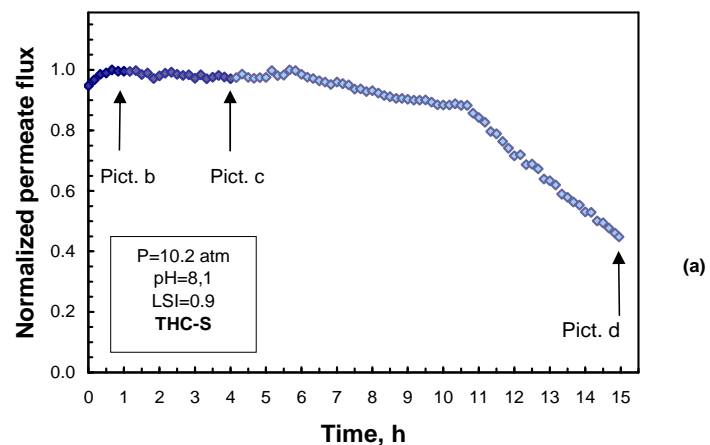


Figure 21 Flux decline curve (a) and SEM images at various times of scaled TCF-S membranes at pH=8.1.

### 5.3 Common Scalants

The following is a brief discussion of the common types of scale found in membrane processes. It is stressed, however, that deposits forming in membrane modules, as well as in other scaling systems, are rarely homogeneous, and in most cases, as seen also in membrane autopsy studies, they consist of a mixture of various sparingly soluble salts and of other foulants (e.g. organics, colloids, biofoulants). In brackish and hard waters,  $\text{CaCO}_3$  and gypsum are the most common scalants for which pre-treatment is required.

#### Calcium Sulphate ( $\text{CaSO}_4$ ) Scale

The most common form of calcium sulphate scales and the polymorph that precipitates at room temperature is gypsum ( $\text{CaSO}_4 \cdot 2\text{H}_2\text{O}$ ). Gypsum is approximately 50 times more soluble than  $\text{CaCO}_3$  at 30°C. Calcium sulphate also exists in two other crystalline forms: hemihydrate ( $\text{CaSO}_4 \cdot \frac{1}{2}\text{H}_2\text{O}$ ) and anhydrite ( $\text{CaSO}_4$ ). The effect of temperature (in the range of 10-40°C) and of pH on gypsum solubility is marginal.

One source of sulphate ions in some treated waters is the addition of sulphuric acid to the feed in order to control  $\text{CaCO}_3$  precipitation. This method of scale control can lead to calcium (or barium and strontium) sulphate deposition, if excessive amounts of sulphuric acid are used for pH control. For this reason, calculations for assessing the potential for sulphate scaling must be carried out using the analysis of feed water after acid addition or other pretreatment methods.

#### Calcium Carbonate ( $\text{CaCO}_3$ ) Scale

Almost all naturally occurring waters contain bicarbonate alkalinity and are rich in calcium, making them prone to scaling problems. The potential for  $\text{CaCO}_3$  scaling exists for almost all well, surface and brackish waters. Calcium carbonate forms a dense, extremely adherent deposit and its precipitation in an NF plant must be avoided. It is by far the most common scale problem in several scaling systems, including cooling water and oil or gas production systems.

Calcium carbonate can exist in three different polymorphs, namely calcite, aragonite and vaterite, in order of increasing solubility. All three polymorphs have been identified in scales, although vaterite is rather rare. Thermodynamics predicts that calcite, the least soluble and more stable polymorph, should be the phase favoured in the precipitation process. Aragonite is also encountered in certain systems. It has been shown that formation of a particular polymorph depends upon water temperature and chemistry (e.g. pH, ionic strength, presence of other ions/impurities/inhibitors). It is also well known that the presence of magnesium ions, in solutions supersaturated with respect to  $\text{CaCO}_3$ , favours the precipitation of aragonite and appears to hinder the formation of vaterite. The tendency to form calcium carbonate can be predicted qualitatively by a plethora of indices derived theoretically or empirically over the past 70 years. The most common indices are the Langelier Index, the Ryznar Index, and the Stiff and Davis Index.

#### Barium Sulphate ( $\text{BaSO}_4$ ) and Strontium Sulphate ( $\text{SrSO}_4$ ) Scale

The solubility of  $\text{BaSO}_4$  is much smaller than that of gypsum ( $K_{sp}=1.05 \times 10^{-10} \text{ mol}^2/\text{L}^2$  at 25°C [98] and can cause a potential scaling problem in the back-end of the NF/RO systems. Its solubility decreases with decreasing temperature.  $\text{BaSO}_4$  scale can only be dissolved by crown ethers and concentrated sulphuric acid, which indicates the severity of the problem. Barium ions are seldom reported in analyses of natural waters, and if found, their concentration does not exceed 200 ppb.  $\text{BaSO}_4$  scale formation is

very rare in membrane scaling systems. Out of 150 elements for which autopsy was performed, no instances of barium sulphate were found [99].

The presence of strontium in many natural waters is more common than that of barium ions. As little as 10-15 mg/L of strontium ions in the concentrate may induce SrSO<sub>4</sub> scale formation. Barium and strontium sulphates are in general more commonly encountered in surface waters.

#### *Silica Scale*

Amorphous silica is one of the major fouling problems in NF/RO systems and in most processes involving water [100]. The silica content in most natural waters can reach 100 mg/L, since silica is one of the primary components of the earth crust. Much has been written about the solubility of amorphous silica in water. Its solubility at room conditions is 100-150 mg/L in the pH range 5-8 and increases significantly with pH at values higher than 9.5. Furthermore, silica solubility increases significantly with temperature. Thus, in usual water treatment operations silica concentration is limited to approx. 120-150 mg/L, the excess precipitates as amorphous silica and silicates. In membrane systems silica scaling has serious consequences: the cleaning of fouled membranes is costly and not without problems.

The solubility of silica minerals generally decreases with increasing ionic strength, in contrast to the solubility of CaCO<sub>3</sub> and sulphate salts. It has been shown [101] that at 25°C and pH 5.0-7.5 the solubility of amorphous silica decreases with the addition of several salts due to the “salting-out” effect of inorganic electrolytes on aqueous silica. This effect is essentially cation dependent and disappears (or better it is reversed) at higher temperatures. Silica scale was found in 66% of about 100 membrane elements investigated recently with membrane autopsy [99]. Iron and aluminium were present in 88% and 75% of the membranes scaled with silica, respectively.

#### *Calcium Phosphate Scale*

In recent years calcium phosphate scale has become more common in membrane systems as autopsies on membrane elements have shown [99, 102]. This can be attributed to the tendency to treat wastewaters, which are rich in phosphates, and to the use of phosphorous containing antiscalants, injected in the form of phosphonates and other organic phosphorous compounds.

The concentrate may become supersaturated with respect to at least four calcium phosphate phases (as in calcium phosphate scale formation in other systems), although no single phase has been identified in autopsy studies. It is often assumed that these phases are amorphous calcium phosphate (ACP, stoichiometry corresponding to Ca<sub>3</sub>(PO<sub>4</sub>)<sub>2</sub>·xH<sub>2</sub>O), dicalcium phosphate dihydrate (DCPD, CaHPO<sub>4</sub>·2H<sub>2</sub>O), octacalcium phosphate OCP, (Ca<sub>8</sub>H<sub>2</sub>(PO<sub>4</sub>)<sub>6</sub>·5H<sub>2</sub>O), and hydroxyapatite (HAP, Ca<sub>5</sub>(PO<sub>4</sub>)<sub>3</sub>OH), the least soluble phase. It is generally agreed that the formation of HAP from a highly supersaturated solution at neutral pH is usually preceded by ACP or other precursor phases, while the presence of ions may affect the polymorph precipitated. Due to the presence of other ions in the feed water, defect apatite can be formed also. The solubility of calcium phosphates strongly depends on solution pH and, consequently, acid addition alleviates the calcium phosphate scaling problem. Other parameters affecting the scaling tendency of calcium phosphates include the supersaturation ratio, temperature and ionic strength.

#### **5.4 Characterisation of Scales**

The techniques for analysis of the crystalline deposits (as in the case with other types of deposits) are

not simple and not standardized. Unfortunately, the interior of membrane elements is not accessible for examination by naked eye or even by an optical microprobe. Direct scale characterisation can only be accomplished by membrane destruction and hence *ex-situ*. Deposit characterization is an important step in the autopsy study of a degraded membrane module. The membrane scales can be characterised by a variety of techniques, the most common of which are briefly mentioned here. Visual and microscopic inspection (SEM) of the scaled surface may comprise the first step of characterisation. Energy dispersive spectroscopy (EDS) is usually employed in conjunction with the SEM system to determine elemental composition, while nuclear magnetic resonance spectroscopy may determine the chemical structure of the scales. The spectroscopic techniques of FT-IR, FT-Raman and XRD can be used to yield quantitative and qualitative results of the scale composition and the dominant crystalline phases. Finally, X-ray photoelectron spectroscopy (XPS) analysis can be used in order to determine the properties of the surface layers of scales. Some of those techniques were described in Chapter 5 and indeed some characterisation techniques for clean and fouled membranes are identical.

An experimental membrane system can also be used to determine how the scales form and the effectiveness of the various antiscalants; several such setups have been employed in recent years (e.g. [103-105]).

#### **5.5 Mechanisms of Scale Formation**

The great complexity of the scale formation process is a direct consequence of the large number of species usually present in a real system and of the plethora of possible physical mechanisms. The latter may include mass, momentum and heat transfer, as well as chemical reactions at the equipment surfaces. Furthermore, the diversity of fluid composition of the various waters treated in membrane systems and the variation of processes taking place along the flow path make difficult the generalization of both the mechanisms responsible for the scale formation and the preventive measures.

There are two main mechanisms to explain flux decline in a membrane system due to the formation of crystalline matter: filter cake formation and surface blockage (e.g. [104, 106]). The former involves crystalline particles formed in the bulk of the solution that are deposited onto the membrane to create usually a porous, not very coherent, soft layer. According to the cake formation model, the deposit layer has a constant porosity, its thickness increases with time and flux decline is due to growth of the layer.

In the mechanism of surface blockage, isolated “islands” of crystals or deposits are initially formed on the exposed membrane surface, which further grow with time, laterally and normally to the surface, to form a continuous and coherent layer. Consequently, the flux would steadily decline as the sections covered by these “islands” would be inaccessible for water permeation. The two main mechanisms of flux decline stem from the different forms of nucleation occurring in the membrane system. As discussed in section 5.2, wall or surface nucleation takes place (for most precipitating species) at lower supersaturation ratios than those needed for nucleation in the bulk (homogeneous, secondary). Consequently, at relatively high supersaturation with respect to a certain salt, bulk nucleation would dominate, resulting in cake formation. On the other hand, at lower supersaturation ratios, membrane fouling would proceed via the growth of crystalline islands. In both mechanisms, an induction period may precede the scale formation process.

The rate of scale formation is determined by several factors, such as the level of supersaturation, the water temperature, the flow conditions and the surface roughness and material of the substrate. A

critical factor in the whole process is the adherence of the deposits to the surface. If the adherence is poor, the deposits might be removed by the fluid flow. If the adherence is strong, the initial crystals grow laterally and perpendicularly to form a coherent scale layer [107]. Sometimes a third step, the stage of recrystallization or aging, is recognized in the scaling process. Gilron and Hasson [106] and Brusilovsky *et al.* [103] demonstrated that the flux decline in an RO unit was due to blockage of the membrane surface by lateral growth of the deposit (surface or heterogeneous crystallization) when investigating the CaSO<sub>4</sub> scaling system. The CaSO<sub>4</sub> scale crystals rested at the edges against the membrane, they were tightly packed with a tendency to grow outwards (“radiate”) from various growth sites. The morphology of these scales strongly supports the assumption of a surface crystallization mechanism. In addition, Hasson and coworkers developed a flux decline model based on the surface blockage and involving the lateral spread of a single crystal layer.

Lee and Lee [104] examined the effect of operating conditions on scale formation in a NF unit. These investigators found that both mechanisms are operative and that the operating conditions (i.e. pressure and crossflow rate) play an important role. Surface crystallization is favoured at a low crossflow velocity and a high operating pressure. Recently, Le Gouellec and Elimelech [105, 108] investigated the presence of several species and of antiscalants to combat gypsum scale formation in a small recirculating unit. No definite conclusions could be drawn on the scaling mechanisms, but the presence of bicarbonate, magnesium ions and humic acid showed a tendency to retard the formation of gypsum nuclei. Moreover, a model was developed for predicting the required antiscalant dosage to control gypsum scale in NF systems.

A similar mechanism as that described for the CaSO<sub>4</sub> by Hasson and coworkers has also been found for the CaCO<sub>3</sub> system in a once-through laboratory NF/RO unit [109]. Figure 21a presents a typical flux decline curve due to calcium carbonate scale formation on a NF membrane. In the same figure, SEM images of scaled membranes are presented (Figure 21cb-d), at different run times, depicting the growth of the scale layer with time. In this particular run (and almost in all runs) the permeate flux was rather constant for an initial period of 4 to 8 hours before declining mainly due to scaling. In the rather limited number of these tests (of maximum duration 15 h), membrane scaling was observed to occur at  $S_c > 3$  (subscript c refers to calcite) or at LSI > 0.9. Comparing these results with scaling experiments in tubes [110] it may be observed that scaling on membranes occurs at lower supersaturation, obviously due to the concentration polarisation effect. SEM micrographs at various run times reveal that even when the CaCO<sub>3</sub> crystals apparently cover about 40% of the membrane (Figure 21c), no detectable flux decline is recorded. This observation somehow contradicts the notion that surface blockage is eventually the main mechanism of membrane flux decline.

## 6 COLLOIDAL AND PARTICULATE FOULING

### 6.1 Introduction and Definition of Colloidal and Particulate Fouling

The term, *colloidal and particulate fouling* refers to loss of both flux and salt retention due to accumulation of retained colloidal and particulate matter on the membrane surface. Colloids are defined as fine suspended particles in the size range of a few nanometers up to a few micrometers [111]. Colloidal matter is ubiquitous in natural waters, as well as many industrial, process, and waste waters [112]. Examples of common colloidal sized foulants include inorganic (clays, silica, salt precipitates, and metal-

oxides), organic (aggregated natural and synthetic organics), and biological (bacteria and other microorganisms, viruses, lipopolysaccharides, and proteins) matter. A review of colloidal and particulate fouling studies reveals the foulants of greatest concern for nanofiltration (NF) separations are colloidal sized substances consisting of silica, organics, metal oxides (specifically iron and manganese), and microorganisms [113-122].

Champlin [75] recommended to remove particles down to 1 µm in size, although this may not be sufficient to avoid fouling. Conventional processes used to pre-treat NF feed waters fail to remove sub-micron colloids, and even MF/UF processes sometimes fail to remove all colloids below a few hundred nm in diameter. Further, the elevated concentration of rejected ionic constituents in the vicinity of the membrane screens electrostatic interactions, which may encourage aggregation of dissolved (organic) matter into colloidal sized particles. The importance of particle-membrane and particle-particle interactions during colloidal fouling are realized when considering the influence of salt retention and concentration polarisation on the solution chemistry in the vicinity of the membrane surface. Electrokinetic properties of colloids and membranes are strongly dependent on pH, ionic strength, and the presence of multi-valent ions [58]. Therefore, distinguishing the fundamental physico-chemical properties of colloids and membranes is critical to understanding colloidal fouling. The summary that follows provides brief descriptions of key colloid and membrane properties, transport and deposition, formation of colloid deposit layers, and mechanisms of colloidal fouling in nanofiltration.

### 6.2 Colloid Properties

*Colloid Properties.* Colloidal matter is typically charged in aqueous electrolyte solutions. The surface charge on colloids arises from a variety of mechanisms including: differential ion solubility (*e.g.*, silver salts), direct ionization of surface groups (*typ.*, -COOH, -NH<sub>3</sub>, or -SO<sub>3</sub>H), isomorphous substitution of surface ions from solution (*e.g.*, clays, minerals, oxides), anisotropic crystal lattice structures (*esp.* in clays), and specific ion adsorption [111, 112, 123, 124]. The surface charges contribute to electrostatic double layer (EDL) interactions, which typically determine colloid aggregation and deposition phenomena [58, 125, 126]. The specific property of colloids used to quantify the relative magnitude of EDL interactions is the surface (zeta) potential,  $\zeta$ , which is commonly determined by measuring the electrophoretic mobility of colloids in a suspension and computing  $\zeta$  from an appropriate theory [127]. It is well known that solution pH and ionic strength directly influence the zeta potential, and thus greatly influence colloidal interactions. It has been shown that the surface charge properties of colloids can dramatically influence colloid-cake layer structure (porosity) and hydraulic resistance [128-134].

Colloid size and shape also contribute to the hydraulic resistance to permeation they impose when accumulated in a cake layer [131, 132, 135]. While colloids are often modeled as spherical, they may be spheroidal (microbes), crystalline (metal salt precipitates), plate-like (clays), or macromolecular (organic aggregates, proteins). In many natural waters the range of polydispersity in colloid and particle size, shape, and electrokinetic character make it quite difficult to accurately describe with any tractable modelling approach. Therefore, an average, “spherical” hydrodynamic diameter is determined from dynamic light scattering or potentiometric methods and used in conjunction with a measured average particle zeta potential to predict the influence of colloidal interactions. A unique size fractionation water quality analysis for a real agricultural drainage water sampled from the Alamo River in Imperial Valley, California is provided in Table 3. Agricultural drainage water is a valuable alternative water

source being considered for reuse if many parts of the world; however, desalination is typically required since it may be brackish [136-138]. Depending on the intended reuse application reverse osmosis or nanofiltration are being considered for performing the desalination process.

**Table 3** Size fractionation water quality determination for agricultural drainage water. Data provided by E.M.V. Hoek, University of California, Riverside are unpublished.

Filter Size	pH	EC mS/cm	TDS mg/L	Turb NTU	TOC mg/L	Solids mg/L	Size $\mu\text{m}$	ZP mV
Raw	8.17	3.322	2256	108.0	21.0	2750	9.89	-11.6
8.0 $\mu\text{m}$	8.48	3.232	2198	7.540	18.4	2326	2.01	-14.4
1.0 $\mu\text{m}$	8.51	3.303	2254	1.380	13.4	2268	1.74	-14.5
0.4 $\mu\text{m}$	8.51	3.158	2148	0.321	12.3	2151	0.29	-11.5
0.1 $\mu\text{m}$	8.59	3.140	2106	0.175	9.11	2107	0.00	-7.47

Notes:  
 DOC (after 0.22 $\mu\text{m}$  filter) = 11.04 ppm  
 Bacteria Count = 160 to 420; Enterococcus = 0 to 30 cfu/ml

The data shown in Table 3 was obtained following standard methods for all analyses. In the table column headings are EC = electrical conductivity, TDS = total dissolved solids, Turb = turbidity, TOC = total organic carbon, Solids = total solids by gravimetric analysis, Size = hydrodynamic diameter, and ZP = zeta potential. The raw water was allowed to settle for 24 hours in a cold room (5°C) and then sequentially filtered under vacuum through 8.0, 1.0, 0.4, and 0.1  $\mu\text{m}$  polycarbonate, track-etched membranes. The size was determined by dynamic light scattering and confirmed with a Coulter Counter (only for raw, 8  $\mu\text{m}$ , and 1  $\mu\text{m}$  fractions). Measured electrophoretic mobilities were converted to zeta potential via the Smoluchoski equation [124]. The results shown are unpublished and are intended only to qualitatively illustrate the physical and chemical properties of natural colloidal matter. In addition, an analysis such as this could be used to justify the selection of a pre-treatment process to remove colloidal foulants prior to desalination by nanofiltration (or reverse osmosis).

### 6.3 NF Membrane Properties

Physical and chemical properties of NF membranes (*i.e.*, permeability, salt retention, “pore” size, etc.) also contribute to the rate and extent of colloidal fouling [60-62, 139]. The high hydraulic resistance of NF membranes enables substantial colloid cake layers to form before fouling is detected, and retention of ionic solutes exacerbates colloidal fouling by screening electrostatic interactions. It has recently been demonstrated that nanofiltration membrane surface properties (*i.e.*, zeta potential, roughness, hydrophobicity) are strongly correlated to the initial rate of colloidal fouling [139-148]. Figure 22 illustrates the range of surface morphologies that may exist for commercially available thin-film composite NF membranes. Nanofiltration membrane properties are discussed in Chapter 3, while their individual contributions to NF colloidal fouling are described below.

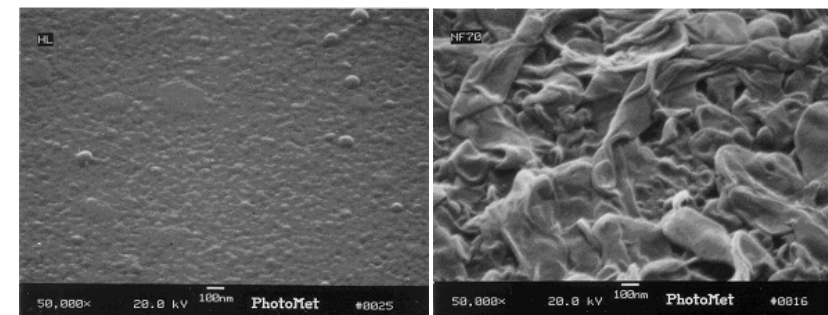


**Figure 22** Field-emission scanning electron microscopy (FESEM) images of two commercially available nanofiltration membranes with RMS roughness values of (HL) 12.8 and (NF70) 56.5 nm (taken from [60]). Additional (HL) and (NF70) membrane properties include zeta potentials of -18 and -25 mV (at 10 mM and pH 7), contact angles of 51.9 and 51.7, hydraulic resistances of  $3.26 \times 10^{10}$  and  $3.13 \times 10^{10}$  Pa.s/m, and salt retentions of 35 and 83% (at 50 L/m<sup>2</sup>.h and 10 mM NaCl), respectively.

Analyses of numerous additional polyamide thin-film composite membranes reveals a consistent set of physical and chemical properties. Table 4 presents atomic force microscope roughness analyses of nine different membranes, along with experimentally determined surface (zeta) potentials and pure water contact angles. The zeta potential was determined from a streaming potential analyzer (EKA, Brookhaven Instruments) following methods described elsewhere [149]. The data indicate a range of surface roughness that varies (on average) between a few nanometers to 50 nm and with some features on the order of half a micron. Surface area difference (SAD) is an indication of the increase in surface area (over a flat plane of equal projected area) due to the roughness of the surface. SAD is a standard AFM roughness analysis statistic and is also known as Wenzel’s roughness ratio [150].

Membrane surface (zeta) potentials range between -20 and -35 mV at neutral pH in a 10 mM NaCl electrolyte. One membrane has a significantly lower zeta potential (LFC1), ostensibly to lower the fouling potential of the membrane as it is often referred to as a “low fouling composite” by the manufacturer (Hydranautics, San Diego, CA). The nine membranes samples exhibit a range of “wettabilities” as depicted by the pure water contact angles. These contact angles were determined by the sessile drop technique at room temperature with low relative humidity.

**Table 4** Surface properties of typical polyamide thin-film composite membranes. Data provided by E.M.V. Hoek, University of California, Riverside are unpublished.

Membrane (name)	Ra (nm)	Rq (nm)	Rm (nm)	SAD (%)	ZP <sup>1</sup> (mV)	θ <sub>w</sub> (°)
NF270	5.2	6.0	63	0.3	-29	69
SG	9.1	13.1	161	2.3	-21	63
HL	10.5	15.9	200	5.3	-10	40
ESPA	31.8	40.0	469	58	-34	41
AK	33.3	42.2	403	40	-23	66
CPA3	33.5	45.8	482	31	-22	69
LFC1	34.7	44.9	368	27	-7	60
NF90	37.9	48.7	415	17	-32	38
XLE	43.4	56.7	560	30	-25	58

<sup>1</sup> at pH 7, 10 mM NaCl

Ra = average roughness, Rq = RMS roughness, Rm = max roughness, SAD = surface area difference, ZP = surface (zeta) potential, θ<sub>w</sub> = pure water contact angle

#### 6.4 Colloid Transport and Deposition

The key to understanding colloidal fouling is to understand the fundamental transport processes by which particles are brought to the surface of the membrane, how they deposit or attach, and why they accumulate in the form of a cake. Particle transport and deposition in fluids can be described by the convective diffusion equation [151], which in its general form is given by

$$\frac{\partial c}{\partial t} + \nabla \cdot \mathbf{J} = Q \quad (29)$$

where  $c$  is the particle concentration,  $t$  is the time,  $\mathbf{J}$  is the particle flux vector, and  $Q$  is a source or sink term. The particle flux vector  $\mathbf{J}$  is given by

$$\mathbf{J} = -\mathbf{D} \cdot \nabla c + \mathbf{u}c + \frac{\mathbf{D} \cdot \mathbf{F}}{kT} c \quad (30)$$

where  $\mathbf{D}$  is the particle diffusion tensor,  $\mathbf{u}$  is the particle velocity induced by the fluid flow,  $k$  is Boltzmann's constant,  $T$  is absolute temperature, and  $\mathbf{F}$  is the external force vector. The terms on the right hand side of Equation (30) describe the transport of particles induced by diffusion, convection, and external forces, respectively.

In colloidal fouling of membranes, the relevant external forces are colloidal and gravitational, that is

$$\mathbf{F} = \mathbf{F}_G + \mathbf{F}_{col} \quad (31)$$

where  $\mathbf{F}_G$  is the gravitational force and  $\mathbf{F}_{col}$  represents the colloidal forces acting between the suspended particles and the collector surface. The gravitational force is usually negligible for the sub-micron colloidal systems encountered in NF operations. The colloidal force can be derived from the gradient of the total interaction potential,  $\phi_T$ , as follows:

$$\mathbf{F}_{col} = -\nabla \phi_T \quad (32)$$

Within the framework of the traditional Derjaguin-Landau-Verwey-Overbeek (DLVO) theory [125, 126],  $\phi_T$  is the sum of van der Waals and electrical double layer (EDL) interactions. A theoretical study by Song and Elimelech [152] utilized the general form of the convection-diffusion equation to investigate colloidal deposition onto permeable (membrane) surfaces. Numerical simulations

demonstrated that the initial rate of particle deposition was mainly controlled by the interplay between permeation drag and EDL repulsion. Subsequent experimental studies have confirmed the role of permeation drag and EDL repulsion on the initial rate of colloid deposition [131, 132].

While the above formulation is fundamentally correct, direct solution of such equations is impractical for all but academic purposes. Cohen and Probstein [153] provided a facile, but approximate, approach towards quantifying the impact of the physicochemical properties of stable colloids (described via the DLVO approach) on colloid cake layer formation. In this classic paper, the authors studied the rate of flux decline of reverse osmosis membranes due to iron oxide nano-particles. They assumed that at least a monolayer of coverage by the positively charged colloidal foulants would coat the negatively charged membrane surface, but the similar charge of subsequently depositing foulants and the foulant-coated membrane surface would result in repulsive (electrostatic) interactions. The authors provided “order-of-magnitude” approximations for the particle fluxes resulting from permeate convection, Brownian diffusion, lateral (inertial) lift, shear induced diffusivity, and repulsive interfacial forces. The conclusion was that the net deposition rate must be determined by a balance between permeate convection and the interfacial flux due to repulsive electrostatic interactions, all other diffusive or convective fluxes being negligible.

Goren [154] performed a detailed theoretical analysis of hydrodynamic interactions between colloidal particles and membrane surfaces occurring as particles are convected towards the membrane under force of permeation drag. The net effect of these hydrodynamic interactions is to increase the effective drag force on a particle as it approaches the membrane surface over that predicted by the Stokes equation. Goren's analysis yields a correction factor that increases dramatically as a particle approaches a membrane surface and is a complex function of the particle size, membrane resistance, and separations distance. So, in addition to bulk convective and diffusive interactions and interfacial physicochemical interactions, it is (theoretically) important to consider the impact of interfacial micro-hydrodynamic interactions on colloidal fouling. Following the approach of Cohen and Probstein [153] described above an order of magnitude analysis can be performed employing the following representative operating conditions and membrane surface properties and water quality data from Table XX: flux of 11 gfd (~5×10<sup>-6</sup> m/s), cross-flow velocity of 0.5 m/s ( $Re = 1000$ ), membrane resistance of 3×10<sup>13</sup> m<sup>-1</sup>, membrane surface zeta potential of -20 mV, foulant zeta potentials and sizes from Table 3.

Figure 23 plots the theoretical foulant fluxes due to permeate convection (bulk value – dashed line with open blue diamonds, and Goren corrected value – solid line with solid blue diamonds) and the various back-transport mechanisms of shear induced diffusion, lateral (inertial) lift, Brownian diffusion, and interfacial (DLVO) forces. The conclusion is that without accounting for the correction to permeation drag, the back-transport of colloidal sized foulants by both shear induced diffusion and interfacial forces is estimated to be orders of magnitude larger than the flux due to permeation and no foulant deposition would be anticipated. By applying the hydrodynamic correction provided by Goren the permeate convection flux is increased by several orders of magnitude and prevails over the back-transport fluxes. Analyses of this nature are at best order of magnitude approximations and have not been systematically tested at any scale, but by considering all known transport mechanisms a better understanding of colloidal fouling may be accessible.

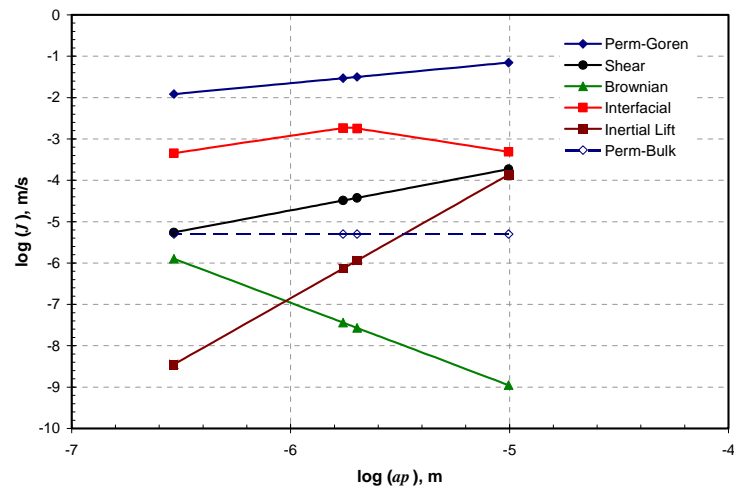


Figure 23 Plot of various colloidal foulant fluxes assuming representative NF membrane properties, operating conditions, and foulant properties (size and zeta potential take from Table 3). The data labels “Perm-Bulk” and “Perm-Goren” indicate fluxes of foulant particles towards the membrane surface due to permeate convection – using Stokes’ drag (bulk) and Goren’s drag (described above), respectively. Back transport mechanisms of Brownian diffusion (“Brownian”), shear induced diffusion (“Shear”), lateral inertial lift (“Inertial Lift”), and DLVO (“Interfacial”) are plotted for comparison.

The extent to which membrane surface properties influence long term fouling (i.e., through cake formation) is unknown because it is unclear how membrane properties might affect subsequent particle deposition once the membrane is covered with a thin layer of particles. Wiesner et al. [155] provided one of the earliest known studies on membrane filtration of coagulated colloidal suspensions. They compared the effect of colloid stability on cake layer structure (porosity) and permeate flux decline for both stable and unstable colloids experimentally and theoretically. Subsequent studies, both theoretical and experimental have confirmed the importance of colloid stability, colloid and membrane surface properties, and colloidal hydrodynamics on cake formation and permeate flux decline in various membrane filtration processes [55, 130, 132, 133, 156, 157].

Although DLVO interactions enable a large amount of experimental aggregation and deposition data to be explained, additional short-range colloidal interactions must also be considered. Such non-DLVO forces include repulsive hydration interactions (due to oriented water molecules adsorbed at each interface), attractive hydrophobic interactions (because of the relatively strong affinity of water to itself compared to that between water and most solid matter), and repulsive steric interactions (from deformation or penetration of adsorbed polymers) [158]. The existence of these non-DLVO forces has

long been recognized, but it has only recently been demonstrated experimentally that non-DLVO interactions significantly colloidal fouling of polymeric membranes [147].

Other experimental studies suggest that surface roughness [130, 133, 148, 159] influences the initial rate of colloid deposition onto membrane surfaces. Figure 24 shows AFM images of the NF membranes from Figure 22 after filtering a colloidal suspension under the same physico-chemical conditions. The membrane on the right had significantly more particles deposit on the surface and the colloids appear to have deposited preferentially in the valleys of the rough surface. Additional, model calculations supported the preferential deposition of colloids in the valleys of rough membranes [60].

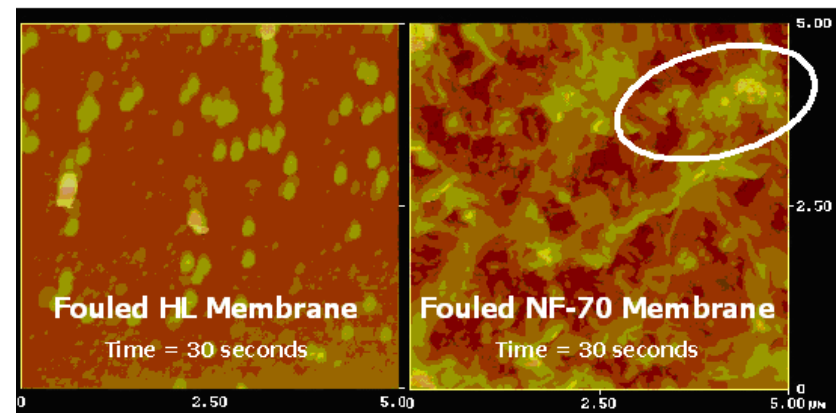


Figure 24 Atomic force microscope images of nanofiltration membranes challenged with a 0.0002% (v/v) suspension of 100 nm spherical silica colloids at 10 mM NaCl,  $1 \times 10^{-5}$  m/s (20 gfd) flux, 19.2 cm/s crossflow velocity, 25°C, and pH 7. The filtration experiment lasted only 30 seconds. After filtration, the membranes were removed, rinsed in a particle free electrolyte and allowed to dry before Tapping Mode™ AFM imaging in air with a silicone nitride cantilever tip [60]. The circled area indicates a large cluster of colloids deposited in the valley of the rough NF membrane.

## 7 BIOFOULING

### 7.1 Introduction and Definition of Biofouling

Biofouling is a term used to describe all instances of fouling where biologically active organisms are involved [160]. Membrane biofouling is caused by bacteria and, to a lesser degree, fungi [161]. The fundamental difference between biofouling and other types of fouling discussed in this chapter is the dynamic nature of the biofouling process. Whilst the different forms of chemical fouling reflect largely passive deposition of organic or inorganic materials on membrane surfaces, biofouling is a dynamic process of microbial colonization and growth, which results in the formation of microbial biofilms.



Biofilms are microbial communities that grow attached to surfaces. Biofilm formation invariably precedes biofouling, which becomes an issue only when biofilms reach thicknesses and surface coverages that reduce permeability. In serious cases, biofilms may cause total blockage of feedwater channels and mechanical collapse of modules by telescoping [162, 163]. Biodegradation of cellulose acetate NF membranes has also been reported [7].

## 7.2 Biofilms

Microorganisms accumulate on membrane surfaces by two processes, attachment and growth. Attachment is preceded by the transport of microbes to the membrane surface either by passive diffusion, gravitational settling or active movement (motility). The rate of microbial deposition depends on the rheological properties of fluid flow. Biofilm formation is initiated by adhesion of primary colonizing organisms to a membrane surface. This membrane surface is usually a conditioned surface, e.g. a surface physicochemically modified by adsorption of organic and inorganic molecular or ionic components of the feedwater [164, 165]. Microbial adhesion is a physicochemical process controlled initially by long-range forces (attractive van der Waals forces and repulsive electrostatic forces, [166, 167]). Once the cell approaches the substratum surface to a distance of 3-5nm, the adhesion process becomes dependent on short-range interaction forces. Adhesion itself ends with the formation of strong adhesive bonds between the adhering cell and the conditioned membrane surface.

Once cells are firmly attached to a membrane, they may begin to grow by conversion of organic matter and other nutrients supplied in the liquid phase (e.g. the feedwater or the permeate) into cell mass and extracellular materials. Microorganisms utilize a wide range of strategies to grow on surfaces, including the production and release of daughter cells [168], the movement of daughter cells away from each other [169] and, most relevant for biofilm buildup, the formation of microcolonies where microorganisms are held together by a cohesive layer of glycocalyx. Eventually the membrane surface becomes covered with a large number of microcolonies. These microcolonies will grow further, incorporating new types of bacteria, which colonize newly formed ecological niches inside the biofilm, including anaerobic pockets at the base of the microcosm. Microcolonies, each one initially a pure culture of a primary colonizer, coalesce and form columns and other types of biofilm structures composed of different microbial species, which may incorporate algae, fungi and protozoa. The coalescence of individual microcolonies or columns does usually not result in the coverage of the substratum surface by a compact gel-like biofilm, since even mature biofilms are crisscrossed by a network of channels, which allow access of nutrients and removal of waste products from within the slime layer [170, 171]. Biofilms therefore produce a self-replicating fouling layer. Biofilms in water channels will grow to a thickness where the shear force of the moving water tears away the upper parts of the biofilm structure. Biofilms will block water channels if shear forces are not strong enough to disrupt them. An example of a fouled spiral wound membrane module is shown in Figure 25 and the fouling of spacers is depicted in Figure 26. More details on modules, spacers and their configurations were given in Chapter 4.

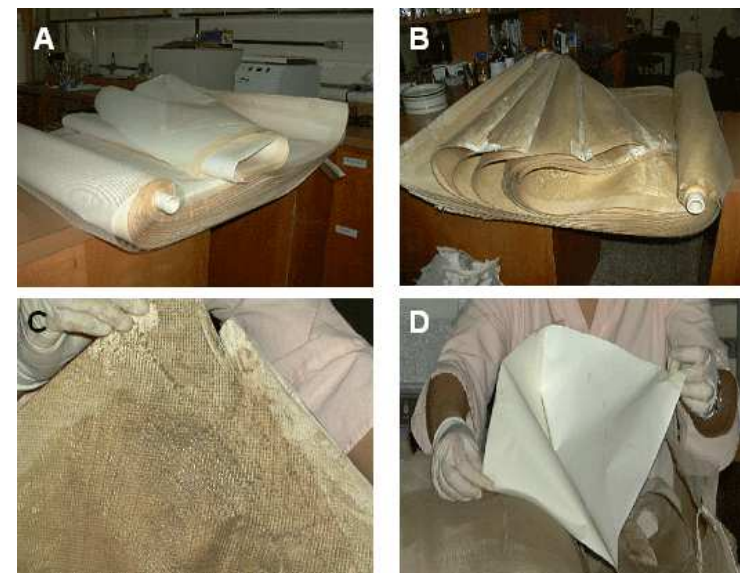


**Figure 25 Membrane biofouling.** *A: relatively clean membrane (opened spiral wound module). B: heavily fouled membrane. C: macroscopically visible fouling layers on heavily fouled membrane. D: clean permeate side appears white, whilst fouled feedwater side has a brownish colour.*

Biofilm bacteria obtain carbon and energy for growth from dissolved feedwater organics. The growth rate of microbes in biofilms depends on the rate of supply of essential nutrients and organic substrates (food sources for microbes within the biofilm). Part of the organic carbon metabolised by the cells is converted into extracellular matrix polymers, growth yields therefore tend to be lower inside biofilms than in the planktonic (suspended) phase. Growth rates of microbes within biofilms are nowhere near the maximum growth rates achievable in well mixed media with balanced nutrient composition, except for growth of initial colonizers directly exposed to liquid. Microbial growth inside the biofilm occurs under diffusion-limited conditions. The pores of the glycocalyx limit the access of large molecules to cells inside the biofilm and create a tortuous diffusion path for small molecules between the biofilm-liquid interface and the cells embedded in the biofilm matrix [172, 173].

Biofilms established on the surfaces of porous supports such as membranes, however, may grow faster than biofilms established on non-porous supports such as piping, because, in a membrane module, a significant proportion of fluid (up to 15% in the case of RO or NF spiral wound elements) flows across the biofilm thus carrying nutrients into the biofilm and washing waste metabolic byproducts out of the structure. This positive effect of higher water fluxes across biofilms is, however, counteracted by a greater compression of biofilms on membrane surfaces, which operate under high pressure differentials. This compression may result in denser, less porous biofilms and hence greater flux decline.

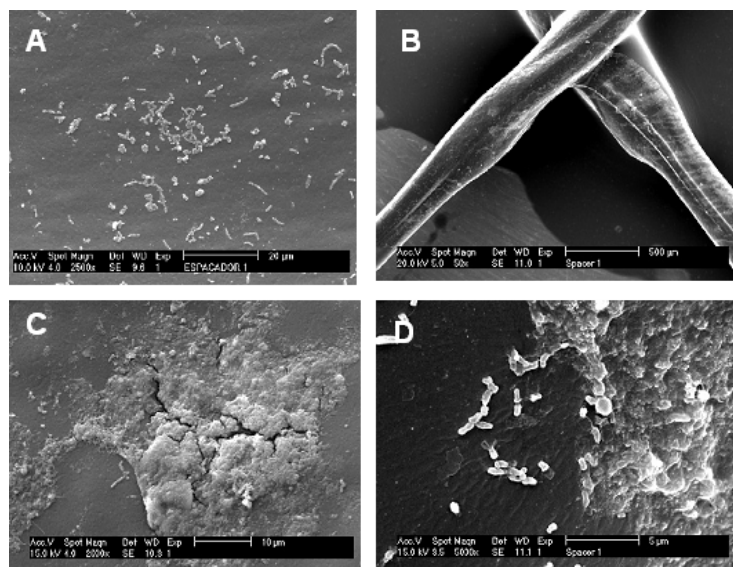


**Figure 26 Biofouling on feedwater spacers. A: lightly fouled spacer. Most bacteria appear as individual organisms, no indication of extracellular matrix. B: macroscopic view of heavily fouled spacer. C: fouling layer on heavily fouled spacer. D: transition zone between relatively clean spacer surface, colonized by a few clusters of microbes, and biofilm embedded in thick glycolalx on fouled spacer surface.**

Microbial populations inside biofilms are often stratified. Aerobes colonize the surfaces of biofilms and of channels inside the microcosms, but high oxygen consumption and diffusion-limited supply of this electron-acceptor usually limits the depth to which aerobes can grow to about 100-200  $\mu\text{m}$  from the biofilm surface [173]. Deeper layers inside biofilms are colonized by anaerobic organisms, including denitrifiers, sulfate-reducers and methanogens [173]. The glycocalyx acts as an immobilisation agent and assures that neighbouring organisms remain locked in their positions for prolonged periods of time. This facilitates the establishment of consortia that degrade complex organic matter by metabolic complementation, whereby each member of the community catalyses one or several steps in the biodegradation pathway of a structurally complex compound. The glycocalyx may function as a sponge and adsorb nutrients present in very small concentrations in the aquatic phase. Microbial biofilms will therefore grow in very low nutrient environments such as ultrapure water systems.

### 7.3 Detection of Biofilms in Membrane Systems

Detecting biofilms in a non-destructive manner inside membrane modules is possible only by indirect methods such as comparison of cell counts at inlets and outlets to detect whether microbial growth occurred inside the module. Direct microscopic comparison of samples of feedwater and of retentate

may reveal the existence of biofilms if one detects clusters of microorganisms sloughed from biofilms in the outlet and not in the inlet stream.

Membrane autopsies permit the direct detection of microbial biofilms by analysis of membrane or spacer surfaces using fluorescence microscopy or scanning electron microscopy (SEM). An example of such a SEM picture is shown in Figure 26. Confocal laser scanning microscopy allows the non-destructive analysis of biofilms on membrane surfaces by producing optical slices through the biofilm structure, which are reconstructed digitally to obtain a three-dimensional image of the biofilm [174].

Bacteria may be removed from membrane surfaces and analysed either by simple direct count methods using dyes that stain DNA (DAPI, acridine orange, [175]), or by more sophisticated gene probing techniques such as fluorescent *in situ* hybridisation [176]. Microbial community structure of membrane surfaces may be analysed after extraction of DNA [177] or phospholipid fatty acids (PLFA, [178]). The physiological activity of cells within biofilms can be assessed with fluorescent dyes such as CTC [179].

### 7.4 Microbial Composition of Membrane Biofilms

A large diversity of fungi and bacteria have been isolated from membrane biofilms [162]. Fungal genera recovered from fouled cellulose acetate membranes include *Acremonium*, *Candida*, *Cladosporium*, *Rhodotorula*, *Trichoderma*, *Penicillium*, *Phialophora*, *Fusarium*, *Geotrichum*, *Mucorales*, and others. Bacterial genera isolated from membrane biofilms include *Acinetobacter*, *Arthrobacter*, *Pseudomonas*, *Bacillus*, *Flavobacterium*, *Micrococcus*, *Micromonospora*, *Staphylococcus*, *Chromobacterium*, *Moraxella*, *Alcaligenes*, *Mycobacterium*, *Lactobacillus*, etc. It is not known whether these organisms colonize membranes in a random sequence, or whether particular microbial species are always involved in primary colonization. Ridgway [180] reported that *Mycobacterium* sp. were the initial colonizers of TFC RO membranes installed at Water Factory 21 in Orange County. The range of organisms identified in biofouling studies of RO and NF membranes differs between studies, suggesting that the species composition on membrane biofilms varies between sites.

There are very few studies about the origin of the organisms that form biofilms on membranes. These cells arrive at their location by transport in the feed water. Most nanofiltration and reverse osmosis systems require some form of pre-treatment of the feed water. Incorrectly operating or planned pre-treatment stages may represent a significant source of biofilm bacteria in membrane installations. Surfaces in pretreatment systems such as ion exchangers, sand filters, granulated activated carbon filters, degasifiers, cartridge filters, holding tanks and piping are all excellent sources of biofilm-forming organisms on the feed side of membranes in RO or NF systems. Biofilms on permeate spacers originate from bacteria introduced into those locations during manufacturing or from microbes which reach the permeate through holes in the membrane.

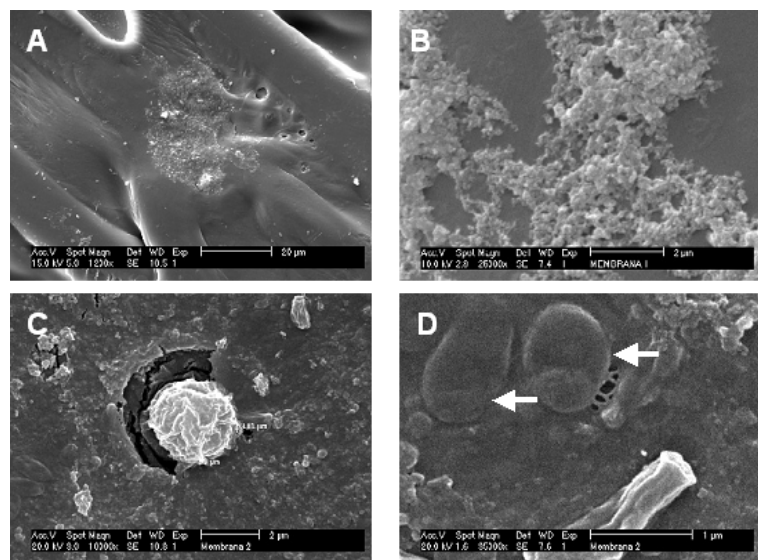


**Figure 27** Electron microscope analysis of fouled membrane surfaces. **A:** lightly fouled membrane, covered with a few microbes (individual particles) and an aggregate consisting of microbes mixed with predominantly colloidal matter. **B:** amplified view of colloidal matter in **A**. **C:** heavily fouled membrane with inclusion body consisting primarily of sulfur. **D:** Bacteria embedded in the biofilm covering the heavily fouled membrane (arrows). Note very thick layer of slime and other organic material covering heavily fouled membrane.

#### Consequences of biofilm formation in membrane systems

Biofilm formation on membrane surfaces leads to the typical symptoms of fouling, flux decline. Flux decline caused by biofouling usually occurs in two stages. Colonization and growth of a microbial biofilm on a clean membrane causes an initial strong flux decline which is followed by a second slower phase, where flux declines in an almost asymptotic manner, probably because of the equilibrium between biofilm growth and removal. The molecular basis of flux decline caused by biofouling is poorly understood. Biofilm growth on a membrane surface leads to the establishment of a second filtration layer. In biofilms established on the surface of filtration media such as membranes, water flux occurs in a direction transversal to the substratum surface, as opposed to biofilms established on solid surfaces, where water may penetrate only in a tangential direction relative to the substratum surface. Although mature biofilms exhibit channel structures which link the biofilm surface to the substratum surface, these channels are probably not sufficiently large and numerous to absorb the bulk of permeate flow. Water that enters the channels leaves the biofilm across the membranes. Any debris or particles carried by this water stream will therefore be retained on the membrane surface and probably block the channels over time. Most permeate probably originates from water that crosses the biofilm through the matrix and matrix porosity is therefore the major controlling element for membrane flux across

biofouled membranes. Leslie *et al* [181] and Hodgson *et al* [182] demonstrated that treatments which enhance glycolyx permeability result in increased fluxes and passages of macromolecules, whilst treatments such as EDTA, which remove the glycolyx from cell surfaces, result in pore blockage by extracellular polymeric substances (EPS) of the glycolyx. Flemming *et al* [183] demonstrated that chemical modifications of the EPS structure can increase its water and solute permeability.

Biofilms form on all surfaces within a membrane system in contact with the water phase, including the surfaces of spacers and tubing. The establishment of a biofilm reduces turbulent mixing on the membrane surface, thus increasing concentration-polarisation. The association of high concentrations of rejected salts with a large diversity of biological organic molecules may lead to enhanced precipitation of salts within the biofilm glycolyx. The increase of fluid frictional resistance due to biofilm development in feed channels may increase module differential pressure to the point where adjacent membrane leaves within the module may shift and cause a telescopic failure of the module. Biofilms in permeate channels or spacers are a potential source of bacterial contamination of the filtrate, an issue of serious concern in industries which require high purity water, such as the electronic industry and the pharmaceutical industry. Filamentous fungi belonging to the genera *Penicillium* and *Aspergillus* often degrade glue lines that separate feed from permeate channels and thus disrupt the integrity of membrane modules. Microbial products produced by biofilm bacteria may deteriorate membrane polymers either by direct attack of biodegradative enzymes (cellulose esters) or indirect attack via metabolic byproducts.

#### 7.5 Biofilm Matrix and Biofilm Control

A characteristic feature which distinguishes microbial biofilms from planktonic organisms (organisms suspended as single cells in the water column) is the capability of self-immobilisation of biofilm cells on surfaces by production of a thick extracellular slime or glycolyx [184]. This glycolyx contains between 50% to 90% of the organic carbon of biofilms and is composed primarily of exopolysaccharides, but it includes other materials of biological origin such as proteins, DNA, RNA, lipids, etc. The glycolyx that surrounds the cells in biofilms has important implications for the treatment of biofouling. The glycolyx is a porous structure, which does not significantly restrict the access of small, uncharged molecules such as oxygen, nitrates, sulfates, etc., to the cells. The glycolyx, however, retains very effectively molecules with affinity for its constituents, which become adsorbed and thus immobilized within the structure and it does exclude any compound whose molecular dimensions are larger than the average pore size. The polysaccharides within the glycolyx are very hygroscopic, e.g. they remain hydrated even in low water activity environments.

The glycolyx remains a major challenge for biofilm control. Effective control of biofilms requires disruption of the glycolyx to allow access of biocides to cells inside the biofilm. Oxidizing agents have a low efficiency in biofilm control, since these substances are largely consumed in the oxidation of glycolyx compounds and do not reach the cells. Biocides have to be used together with compounds such as detergents, chaotropic agents and chelating agents, which effectively disrupt the glycolyx structure and allow the biocides to act upon the cells directly [185]. An increase in transmembrane flux after chemical cleaning may not necessarily reflect good removal of biofilm bacteria from membrane surfaces, it may be due solely to a disruption of biofilm structure [186]. Repeated use of the same cleaning solution against a particular biofilm may result in the selection of resistant strains and thus decrease the biofilm's susceptibility to the cleaning agent. Effective biofilm control therefore depends

on the periodic change of the cleaning and sanitizing solutions. Care must also be applied in the selection of antiscalants used for chemical fouling control. Some organic antiscalants are good substrates for microbial growth, and worsen considerably biofouling problems [187].

Membrane systems should be designed and operated in ways to minimize biofilm buildup on membranes. The most effective means for pre-treatment are filtration systems such as ultra- and microfiltration which remove bacteria effectively from feedwaters. An outline of pre-treatment technologies for nanofiltration was given in Chapter 9. These advanced pre-treatment technologies, however, do not remove or destroy organic carbon sources for microbial growth. Pretreatment systems which combine filtration with bioreactors designed for removal of bioavailable organic carbon in feedwaters to minimal levels are probably the most effective combination for biofouling control since low numbers of organisms and low concentrations of organics will limit the growth of biofilms on membrane surfaces [188, 189]. Continuous dosing of oxidizing biocides such as chlorine at low concentrations has proven effective in many membrane operations, but it is important to stress that such measures need to be adopted from the very start of membrane operation, before a biofilm is formed. Biofilm formation may also be minimized by appropriate choice of membrane polymers. In recent years manufacturers have introduced several types of low-fouling polymers on the membrane market [190, 191]. Once formed, only periodic cleaning with chemical cocktails containing a combination of detergents, chaotropic agents, chelating agents and biocides will be capable of effectively controlling biofilm growth. Further details on cleaning options will be given in the following section.

## 8 FOULING PREVENTION & CLEANING

### 8.1 Pretreatment as Fouling Prevention

In NF normally frequent cleaning is avoided by using different types of pretreatment. For example, particulate matter is aggregated and settled until an almost particle free feed is achieved. As described in the previous sections, MF and UF may be more effective in removing such particulates than conventional treatment, but small colloidal matter may still permeate. Such pre-treatment results in a very low (less than 3) silt density index (SDI). A success story was reported by Gwon et al. [26] who attributed the absence of biofouling to pre-treatment with UF. In pretreatment also biocides and chlorine pretreatment can be used to avoid biofouling. More details on pretreatment in NF can be found in Chapter 9 and in an article of pretreatment for RO included by Shahalam [192].

### 8.2 Membrane Modification for Fouling Prevention

Another option to avoid fouling and subsequent cleaning, beside pretreatment, is to modify the membrane or the membrane surface in particular. Normally the modification aims to produce a more hydrophilic membrane [193], a more resistant membrane or sometimes to a more charged membrane. The problem with modification is that the modification material takes up space in the membrane polymer, and thus the flux decreases. The modification is, therefore, a compromise between fouling and pure water flux. Lee et al. [29] have studied the effects of anionic and cationic surfactants on UF membranes used for NOM filtration. While anionic surfactants had no effect on flux or retention, cationic surfactants decreased flux which was accompanied by an increase in NOM retention. In

contrast, Combe et al. [53] determined that anionic surfactants reduced adsorption of humic acids considerably.

An attempt to make modifications of NF membranes (NF 270) has been performed by Belfer and Gilron [194], see Table 5. The membranes have been modified in situ (also spiral elements) with acrylates or other similar monomers. The crosslinking agent was Ethylene Glycol Dimethacrylate (EGDMA) and the reaction time 15-60 minutes. It can be seen that the flux has decreased somewhat due to the modification, but also the fouling has decreased (measured as the difference of the pure water flux before (PWF<sub>b</sub>) and after the experiment) especially with the HEMA-modified membranes. A similar procedure for RO membranes has been reported by Gilron et al. [195]. Coating membranes with a layer of pre-adsorbed polymer may sterically prevent the foulants from entering into the membrane matrix. The effectiveness of such a treatment depends on the membrane characteristics. Hydrophobic membranes generally are more susceptible to adsorption and fouling and hence making such a membrane more hydrophilic is likely to improve performance [85].

Kilduff et al. [12] have developed a technique to modify the surface of NF membranes using UV irradiation and UV-assisted graft polymerisation. Such treatment resulted in increased hydrophilicity of the membranes possibly due to the formation of surface hydroxyl groups. Less fouling however, came at the cost of decreased retention.

**Table 5 NF270 membranes modified in situ by redox-initiated graft polymerisation with potassium persulfate/potassium metabisulfate as the initiator (0.005-0.03 M). Retention (R) of UV-absorbing compounds (UV) and of Total Organic Carbon (TOC) and fouling in NF of paper machine clear filtrate. Modification agents used: Acrylic acid (AA), Methacrylic Acid (MA), Polyethylene Glycol ester of Methacrylic Acid (PEGMA), Hydroxymethyl ester of Methacrylic Acid (HEMA), (Belfer and Gilron [194]).**

Modification	Pure Water Flux (L./m <sup>2</sup> h)	Permeate flux (L./m <sup>2</sup> h) (0-3 h)	R, UV (%)	R, TOC (%)	Fouling (%)
Original	205	132	51	80	21.6
MA- 1M 30%PEGMA	65	40	92.7	80	-
AA-1M	226- 183	130	97	83	13
MA-0.5M PEGMA-0.002M	232	148	90.2	69	22.5
HEMA-1M	156	123	98	80	4.9
HEMA-0.5M	173	120	96.8	72	1.4
HEMA-0.2M	204	118	96.6	72 74	1.4
HEMA-0.2M (circulated cell)	175	125	97.7	82	0.6

### 8.3 Cleaning Methods

#### 8.3.1 Physical Cleaning Methods

While the main focus in this section is on chemical cleaning, some form of physical cleaning is generally part of a cleaning protocol and hence a brief overview is provided. Physical cleaning generally uses mechanical forces to remove foulants [196] and such methods include

- **Backflush/Forward Flush/Reverse Flush**
- **Scrubbing (e.g. using foam balls for tubular modules)**
- **Air Sparge**
- **CO<sub>2</sub> Back Permeation**
- **Vibrations**
- **Sonication**

While a number of researchers have used permeate backwash for TFC membranes, this is somewhat surprising as the risk of damage to the thin active layer in backwash operation is considerable. However, Chen *et al.* [196] have reported beneficial effects of such backflushes presumably due to the disruption of the foulant layer which was subsequently removed by a forward flush.

Sonication is a relatively novel method for membrane cleaning, although ultrasound is commonly used in membrane autopsies to remove the fouling deposits from the membranes for chemical analysis. Lim and Bai [197] have used sonication in microfiltration (MF) and found that the technique was very efficient in removing cake deposits, but not effective in removing pore blockages. This resulted in a decrease of cleaning efficiency over time as mechanisms like pore plugging became more predominant. Hence it was required to combine sonication with backwashing as well as a chemical cleaning protocol.

#### 8.3.2 Chemical Cleaning Agents and Processes

Chemical cleaning relies on chemical reactions to break bonds and cohesion forces between membranes and foulants [196]. Such chemical reactions include

- **Hydrolysis**
- **Saponification**
- **Solubilisation**
- **Dispersion**
- **Chelation**
- **Peptization [198].**

In many cases NF membrane manufacturers are co-operating with a cleaning agent manufacturer to establish the most suitable cleaning process for the membranes produced by the membrane manufacturer. However, as described above, the cleaning protocol not only is membrane specific, but also foulant dependent. Some typical producers of formulated cleaning agents are Diversey-Lever A/S, Henkel-Ecolab GmbH & CO, Onco Nalco Ltd. and Novadan A/S. [199, 200] and several authors have listed cleaning mixtures or protocols [15, 26, 27, 196, 201, 202]. Li and Elimelech [203] established in a very fundamental study that cleaning can only be effective when calcium ion bridging

could be removed by the chemical cleaning agent. The authors used SDS and EDTA for those studies with organic foulants and multivalent ions.

**Alkaline Cleaning:** The alkaline cleaning is often the most important as many foulants, especially in natural waters or wastewaters are of organic nature or inorganic colloids may be coated by organics. The alkaline cleaning is aiming to remove organic foulants from the surface of the membrane and from the pores of the membrane. The high pH is usually a result of using sodium hydroxide and sodium carbonate containing cleaning solution. In most cases then a surfactant is included in the formulated cleaning agent. This surfactant emulsifies fat containing particles and prevents the foulant from adhering back on the surface. The surfactant is mostly anionic or non-ionic and acts together with the alkaline agent (caustic) to remove the foulant. In many cases some sequestering agent like EDTA is added to the formulation to remove multivalent ions like calcium and magnesium. It appears that alkaline cleaning is often the most effective cleaning step [26].

**Acid Cleaning:** The acid cleaning aims at removing precipitated salts (scaling) from the surface of the membrane and from the “pores”. The acid procedure can be the most important cleaning step in RO as the scaling problem occurs in connection with salt retention. Often the acid used is nitric acid at a pH of 1-2. In many cleaner formulations citric acid has been used as well as phosphonic and phosphoric acid. The large use of nitric acid depends on its fairly mild oxidising ability. In the acid cleaner formulations also detergents, cationic or non-ionic, as well as some sequestering agents can be present.

**Enzymatic cleaning:** Enzymes are used on a larger scale today than earlier. There are enzymes that can take very high temperatures (70-90°C) even though in most cases their optimal temperature is much lower. Enzymes can often be used when a more neutral pH for cleaning is considered, when biofouling is expected or when polysaccharides are the typical foulants. Because, often the extra-cellular substance secreted by the biofouling microbes is polysaccharide in nature enzymatic cleaning is important. The enzymes are mostly very specific in their action and are, therefore, selected for specific foulants or when other cleaning agents do not help. Special caution has to be taken so that the enzyme cannot attack the membrane itself [204].

**Biocides for control of microorganisms and biofouling:** Zeiher and Yu [205] describe three terms of importance in the control of biological fouling, namely *sanitization* which describes a cleaning process with antimicrobial characteristics. In a “3 log” or 1,000 fold reduction in microbial counts is achieved. *Disinfecting* is the process in which microorganisms are destroyed, inactivated or removed in the order of magnitude of a “6 log” or 1,000,000 fold reduction in counts. Lastly, *Sterilizing* means making a system free of all living cells, viable spores, viruses and sub-viral agents capable of replication. According to Zeiher and Yu [205] it is sterilizing that is desired in membrane systems. The use of biocides and their common concentrations are summarised in Table 6. It should be noted here that many NF membranes are not chlorine resistant and application of biocides should be in consultation with the membrane manufacturer to avoid membrane damage. For example, Staude indicates that ozone destroys some polymeric membranes, while the resistance to various disinfectants is membrane dependent [3]. Some of those biocides have been reported to cause membrane swelling which loosens foulants attached to the membranes and hence increases cleaning efficiency [196].

Table 6 Typical Biocide Concentrations for RO Sanitizing (adapted from Zeiher and Yu [205])

Biocide	Dosage	Comments
Chlorine	0.1 - 1.0 ppm	CA membranes and other chlorine resistant only
Peracetic acid	0.02 - 1.0 %	pH of neat product is 3 - 4
Formaldehyde	0.5 - 3.0 %	carcinogen
Glutaraldehyde	0.5 - 5 %	not recommended
Isothiazolone	0.01 - 0.15 %	slow
Quaternary amines	0.01 - 1 %	not recommended
DBNPA	up to 200 ppm	fast, easy disposal
Bisulfite	1.5 % (preservative) or as needed for Cl <sub>2</sub> removal	preservative, biostatic, Cl <sub>2</sub> scavenger

### 8.3.3 Choice of Cleaning Method

According to Chen *et al.* [196] the selection of appropriate cleaning protocols is usually based on a trial and error approach. This means testing various cleaning protocols that have been selected by rule of thumb and experience for presumed foulants. If foulants have not been identified, assumptions based on feedwater characteristics need to be made. The different categories of foulants have been described in detail in previous sections. In terms of their contributions to fouling, van Hoof *et al.* [99] have concluded from extensive membranes autopsy surveys that worldwide about 50% of the foulants are of organic nature. This organic foulant fraction is higher in Europe than it is in the USA. Ferric oxide and silica are the next most common foulants followed by alumina, calcium phosphate, calcium carbonate and calcium sulphate. Silica is apparently more abundant in the USA and calcium phosphate in the UK. The effective selection of a cleaning agent is usually preceded by a determination of the foulant using feed analysis or membrane autopsy. However, this procedure has limitations in that if several foulants are identified cleaning protocols may become extensive. For this reason Luo and Wang [15] have optimised a CIP method and established that it is sufficient to remove selected essential foulants as subsidiary foulants may be removed simultaneously. No doubt the nature and complexity of fouling can make it very difficult to find the ideal cleaning agent. For this reason Chen *et al.* [196] have developed a methodology that applies a statistically designed approach (factorial design) to cleaning optimisation. The impact of this optimisation at the example of a UF membrane is shown in Figure 28 with a significantly increased productivity. Weis *et al.* [206] have trialled various cleaning protocols as a function of membrane characteristics and established that the choice of cleaning agent was instrumental in achieving a steady state flux value.

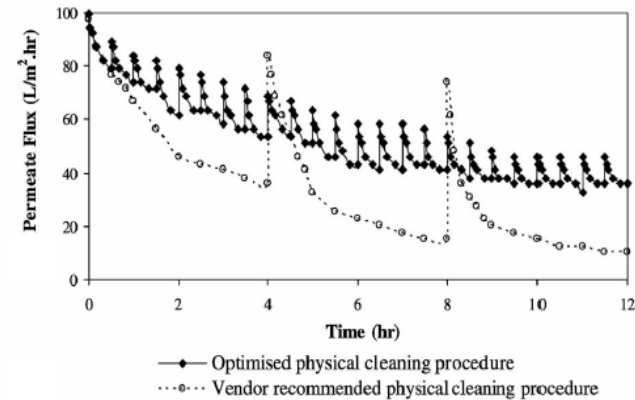


Figure 28 Impact of cleaning procedure optimisation on flux (reprinted from Chen *et al.* [196]).

The cleaning process to be adapted depends on the type of foulant, the tolerance of the membrane towards the suggested cleaning agent and the regulations applying to cleaning agents for a particular application. For instance directives exist dealing with issues such as what formulations are acceptable and those certainly differ from country to country (e.g. EU and the USA have different norms).

Cleaning is in most cases performed using caustic, acid or enzymes solutions, mixtures of those, combinations of additives or proprietary commercial cocktails. For sanitation often chlorine gas is required in some of the treatment steps, although formaldehyde has also been reported.

The effectiveness of such cleaners is usually offset by the damage caused to the membrane materials and hence membrane durability is an important consideration in order not to adversely affect membrane lifetime.

### 8.3.4 Determination of Cleaning Requirement and Frequency

Generally in industry the cleaning interval is designed in such a way that the cleaning is taking place when a certain amount of flux is lost, although there is evidence that cleaning at an early fouling stage is more efficient than when the fouling is well established and the fouling layer compacted [207]. A flux loss of 10-30 % is usually the highest allowable decrease in flux. Another option is to clean on a regular basis for instance once a week or less frequently depending on the fouling situation of the process. In some cases NF can be used almost without cleaning if the operating conditions are such that only sub-critical fluxes are used. An example of that is NF in humic water treatment in Norway at low flux and low temperature [208].

In most cases NF processes need less cleaning than UF and MF processes. The reason for this is that the common and usually detrimental pore plugging in UF and MF is less important in NF. However, on the other hand, cleaning is needed more often than in RO due to the more open structure of NF membranes.

Due to the similarities of RO and NF often the same types of cleaning agents and cleaning processes are used. In most cases the cleaning protocols are dependent on the fluids to be processed by using NF (foulant types).

The cleaning interval depends both on the foulant amounts on the membranes (mostly measured as increased pressure to keep up constant flux) or on the fact that the membranes need to be cleaned and disinfected at regular times (daily in the dairy industry). Very few papers on cleaning of NF membranes have been published up-to-date. In the dairy industry fouling and cleaning of MF and UF membranes and visualisation of fouling and cleaning efficiency have been reported. Most of the principles are thus reviewed.

#### 8.4 Determination of Cleaning Effectiveness

##### 8.4.1 Water Productivity and Membrane Resistance

There are different ways to establish how effective a particular cleaning protocol is. Firstly, the clean water flux can be measured and compared to the CWF before and immediately after filtration to determine if flux has recovered due to cleaning. This can be done in situ in the process. The recovery of the original steady state process flux is, of course, the most natural way to see that cleaning has been successful [201]. Flux recovery can be calculated as

$$FR = \frac{J_c}{J_0} \quad (33)$$

where  $J_c$  is the flux after cleaning and  $J_0$  the flux of the virgin, unfouled membrane [201]. Alternatively the effectiveness can also be represented by clean water flux recovery [196] as

$$J \text{ Recovery} = \frac{J_o}{J_c} \quad (34)$$

The variation of flux has been illustrated in Figure 3 showing the impact of fouling and cleaning on flux and the impact of several successive cleaning steps to fill recovery is shown in Figure 29 at the example of an UF membrane fouled with proteins, lipids and carbohydrates and cleaned with a rinse wash (water), an alkaline clean (NaOH 0.5 w%), followed by a protease detergent (0.75 w%), followed by sodium hypochlorite (150 mg/L). The sodium hypochlorite is used as a sanitising agent and its cleaning effectiveness was attributed to its ability to cause swelling of the membrane [27].

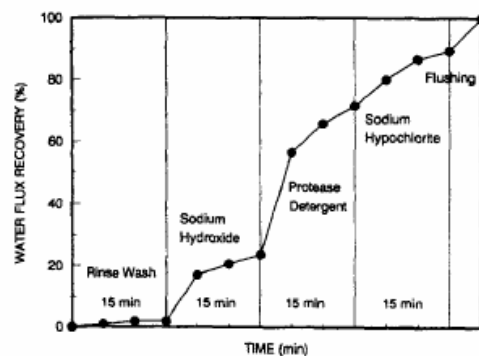


Figure 29 Flux recovery in the case of successive cleaning steps (figure reprinted from Sayed Razavi et al. [27]).

In accordance with the resistance in series model, this can also be depicted as a variation of membrane resistance as shown in Figure 30. From this graph conclusions can be drawn regarding the nature of the foulants and the effectiveness of cleaning. A reduction of resistance by rinsing indicates a loosely

associated deposit such as a concentration polarisation or a loose gel layer or cake. The resistances are; the intrinsic hydraulic membrane resistance ( $R_M$ ), residual resistance after cleaning ( $R_{RES}$ ), resistance after filtration (in this case UF;  $R_{UF}$ ), reversible fouling resistant ( $R_{RF}$ ), irreversible fouling resistance ( $R_{IF}$ ), the total fouling resistance ( $R_F$ ), hydraulic resistance of the cleaned membrane ( $R_{CW}$ ). Cleaning can be assumed to be complete when  $R_{CW} \approx R_M$  allowing for experimental error [202].

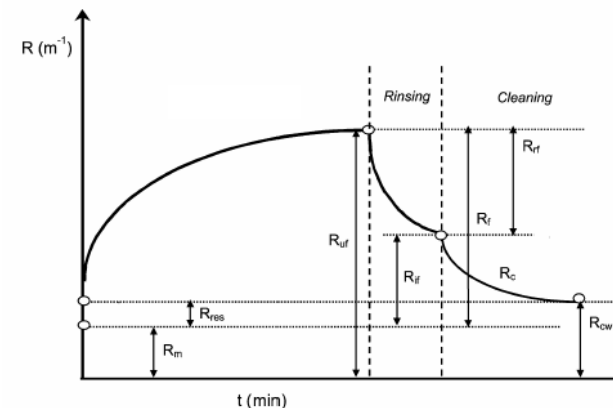


Figure 30 Resistances in filtration, rinsing and cleaning (adapted from Argüllo et al. [202]).

In this case of presentation as resistances, cleaning efficiency can be determined as

$$E_{RW} = \frac{R_{IF} - R_{RES}}{R_{IF}} \cdot 100 \quad (35)$$

##### 8.4.2 Foulant Content of Cleaning Solutions

Secondly, the variation of the composition of the cleaning solution can be investigated. Often changes are visible, such as precipitates when scaling is removed or a dark yellow or brown colour when NOM is removed. Chemical analysis of cleaning solutions can quantify such observations. For example Liikanen et al. [201] measured pH, turbidity, colour, total solids (TS) and cations in the cleaning solutions. Conducting a mass balance and comparing the amounts removed in the cleaning solution to the amount remaining on the membranes gives further information not only on cleaning efficiency but on the reversibility of certain foulants. Gwon et al. [26] found that calcium and iron were found predominantly in acid cleans and silica in alkaline cleans. Further, iron was most resistant to removal and adhered strongly to the membranes throughout the cleaning process. This was established with a sonication technique as described in the autopsy section.

##### 8.4.3 Membrane Surface Investigation

Thirdly, the membrane surface can be examined after cleaning to determine if all contaminants have been removed. It has, however, been observed that despite complete flux recovery, not all foulants are taken off. Available methods are similar to those used for membrane autopsies like streaming potential measurements, contact angle methods, FTIR or SEM. These characterisation methods are mostly

destructive methods. A combination of several methods is the best way to analyse the cleaning efficiency [209, 210].

#### **8.4.4 Membrane Retention**

Retention is affected by fouling as summarised in Section 4.8. As a consequence cleaning results in either a restoration or decrease in retention. For example, Chen *et al.* [196] reported a 10% increase in TDS retention after cleaning.

Other important parameters in membrane cleaning are the wash water usage and loss of production. The wash water usage can be represented as the volume of wash water used per total volume of water produced (taking into account that wash water is often membrane permeate and hence product) [196] and loss of production is calculated by multiplying the time for cleaning with the average water flux during operation. For the calculation of environmental impact both water consumption and the generation of a potentially hazardous waste stream need to be considered.

#### **8.4.5 Influence of Operating Parameters on Cleaning Efficiency**

**Duration:** It appears from the literature that shorter filtration cycles (and hence more frequent but shorter cleaning procedures) are beneficial as the fouling layers compact with time and become more difficult to remove. Further, the degree of fouling is an important parameter in recovery during cleaning which supports the argument for more frequent cleaning (see also Figure 28) [196].

**Temperature:** In general cleaning efficiency increased with temperature but increases are limited by the heat tolerance of the membranes [201]. It is a rule in cleaning processes to clean at the same or higher temperature as the NF process has been operating. If cleaning is undertaken at a lower temperature there is a risk that the foulants will re-adsorb on the membrane once normal processing is continued.

Optimal cleaning results have been obtained repeatedly in literature (for UF) at a temperature of 50°C [211-213], and also in NF this temperature has seemed to be quite good to use if the membranes are tolerant to such elevated temperature. A higher temperature could give even better cleaning results, but membranes that can endure temperatures between 70 and 90°C remain scarce. The importance of a high enough temperature in cleaning has two reasons, firstly the enhanced removal of foulants and secondly the removal of heat sensitive microbes. Another possibility to circumvent this problem is to give the membranes a short heat shock. Inorganic membranes can endure this type of heat treatment, but their applications are to date limited.

**Pressure and Air/Water Backwashing:** In most cases it has been shown that a high pressure is not beneficial when cleaning. Especially with porous membranes the pressure pushes the foulants deeper into the membrane, which is also true with open NF membranes. The applied pressure also causes compaction of the fouling layer [27].

It appears most beneficial to just let the membranes soak in the cleaning solution and then transport it out of the module using as little pressure as possible. However, usually a compromise between pressure and flow velocity has to be made in order to get the best fouling removal efficiency.

In UF and MF, cleaning is often enhanced by back pulsation, but this is not a possibility in NF due to the membrane and module structures used. For example, with TFC membranes the active layer would be damaged during backwash due to the lack of the support layer, and air backwash is not possible as air cannot penetrate through the small pores in NF.

#### **8.4.6 Impact of Cleaning on Permeate Quality**

According to Liiikanen *et al.* [201] who performed permeate analysis for TOC, UV absorbance (254 nm), pH, alkalinity, hardness and conductivity, the permeate conductivity generally increased after cleaning. Acidic cleaning assisted in restoring the ion retention of membranes.

#### **8.4.7 Impact of Cleaning on Membrane Durability**

NF membranes are generally somewhat less durable than other types of membranes used today. UF and MF membranes can be made of PVDF, Teflon, polypropylene, polysulphone and other very strong and resistant materials. In most cases it has not been possible to make NF membranes of these materials. Such materials however are commonly used as supports for the active layer. NF membranes are most often made of aromatic amides, e.g. poly-(piperazine amide) (See Chapter 3). Generally membranes used in NF have different resistance to chemicals, heat and pH. Hence cleaning processes need to be substantially different [214]. Membrane durability can be examined by measuring pure water flux and salt retention. A combined increase in flux and decrease in salt retention after cleaning as compared to the virgin state of the membrane most likely indicates a reduced membrane integrity.

**Acid/Alkali Resistance:** The alkaline resistance of normal NF membranes goes to about pH 11 and the acid resistance to around pH 1 for the best membranes, depending on the material. In many cases the NF membranes can withstand higher or lower pH values for shorter times especially if their temperature limits are not exceeded. In fact, a high pH cleaning can often increase the membrane capacity because the high pH modifies the membrane to give a higher flux without a decrease in retention [215].

Many industries use NF membranes for fractionation of their process or effluent streams. The obstacle has been the high or the low pH that the membranes cannot tolerate. For this reason there is a lot of EU research directed to manufacture NF membranes that can operate in a broader pH range, aiming at an increase in 1-2 units in each direction [216]. The durability of the membranes is checked by characterisation of retention of glucose/sucrose and salts and by inspection of the surfaces for cracks by using SEM.

**Temperature Resistance:** NF membranes are not normally very tolerant to heat – up to a limit. Most NF membranes can endure around 40°C and according to some reports their stability extends to 50-60°C. It is of great importance that the membranes can tolerate at least 50-70°C in processes, which demand elevated temperatures, and also in cleaning which would allow them being sanitised.

Some studies have been carried out on the heat stability of typical NF membranes, as summarised in Figure 31 [217]. Generally, with increasing temperature flux increases while retention decreases (retention not shown in the Figure). In some cases, decreasing temperature causes the membranes to become tighter (even after a short heat treatment at 65°C), hence the flux of such membranes decreases and retention increases (see e.g. membrane XN-40 in Figure 31). Alkaline cleaning then again increases flux.



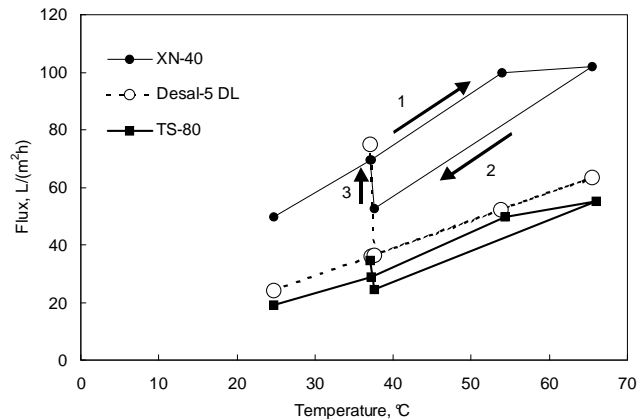


**Figure 31 Influence of temperature on fluxes during the filtration of 250 ppm glucose solution. 1: Temperature was increased from 24 to 65°C, 2: Temperature was decreased from 65 to 37°C, 3: change in flux after alkaline cleaning (adapted from Mänttari *et al.* [217]).**

## 8.5 Examples of Cleaning Applications and Cleaning Process Protocols

It is best to divide the cleaning procedures according to what foulants are to be removed or the types of process streams that are filtered. Hence the cleaning protocols used by a number of example applications is described in the following subsections. In industrial processes cleaning is generally performed as a cleaning in place (CIP) procedure which commences automatically either at set time intervals, when transmembrane pressure in constant flux applications reaches a critical limit or when flux has decreased below the tolerance level in constant pressure filtration.

### 8.5.1 Food Industry

In the food industry, especially in the dairy industry, there are regulations that membranes should be cleaned and sanitised daily. This requirement comes from the fact that these food products are very sensitive to microbial growth. Due to this cleaning requirement, membranes in such applications are operated at higher fluxes as fouling prevention is not a priority. In the dairy industry the foulants are mainly proteins, salts and sugar or their degradation products. For removal foulants an alkaline cleaning cycle is needed and for salt removal (calcium salts) an acid cleaning step. Normally this is carried out in three steps: alkaline, acid and alkaline. The protocol varies from process to process but it is often more or less standardised also including sanitation. An example of such a cleaning procedure in the food industry (soy flour extract) was given in Figure 29 [27]. Most membranes are cleaned according to a Cleaning in Place (CIP) procedure [218-221]. Alternatively enzymatic cleaning has been trialled, but was described as having a low cleaning efficiency and long cleaning times. Some proteins are not removed with enzymes [202].

### 8.5.2 Water and Wastewater Treatment

In most water and wastewater applications cleaning is not carried out on a daily basis and the NF process is aiming at as few cleanings as possible, which means that the processes are run at lower average fluxes.

In cases where the waters contain some organics like NOM or humic acids usually an alkaline cleaning is required. For example, Li and Elimelech [87] have investigated a number of cleaning agents to remove deposits of HA and calcium. It was found that EDTA was most effective and recovered 100% of the flux when applied at pH 11, while NaOH was ineffective. Sodium dodecyl sulphate (SDS) was effective independent of pH when applied above its critical micelle concentration (CMS). In contrast, Lee *et al.* [29] found that SDS was ineffective for NOM foulants whereas 0.1 M NaCl was relatively effective compared to more common cleaning agents such as surfactants. Caustic solutions were effective at removing hydrophobic foulants, while hydrophilic NOM fractions were more difficult to remove. In an extensive study determining the efficiency of 13 cleaning schemes, Liikainen *et al.* [201] determined that Na<sub>4</sub>EDTA was very effective, although it was pointed out that this may be dependent on the membrane type, which implies that every membrane may require a cleaning optimisation for a particular feedwater. Hong and Elimelech [80] who confirmed the effectiveness of EDTA postulated that EDTA removes the calcium from a solution and in this way reduces (or in the specific case reverses) fouling. This makes EDTA an effective agent not only for cleaning but also for pre-treatment. Roudman and DiGiano [65] used a commercial inorganic caustic detergent (MC-3) at pH 10.3 and ultrapure water rinses which could not remove NOM deposits.

### 8.5.3 Desalination and other Industries

In desalination the acid cleaning is the most important. Often the alkaline and the acid cycles are not run directly after each other, but maybe one more often than the other, the frequency usually depends on pretreatment and local demands. The cleaning interval is at least one week and in some cases the process can be run without cleaning for several months [201, 207, 208, 222].

### 8.6 Regeneration of Cleaning Solutions

Regeneration of cleaning solutions is an important issue, not only because of economic concerns, but also for environmental reasons. Unfortunately, Argüllo *et al.* [202] have determined that independent of the initial concentration, about 30% of activity is lost in each cleaning cycle for enzyme cleaners used for whey fractionation in UF.

In fact, NF was trialled to treat the cleaning solutions to recover and reuse the acid or caustic fractions in the process. The concentrate would contain the foulants (which for example could be regenerated in the dairy industry as animal food) and the permeate would contain e.g. the alkali/acid and the other parts of the formulated cleaning agent. This permeate would then be concentrated by using RO [223-225].

## 9 CONCLUSIONS

This chapter has provided a comprehensive overview of fouling characteristics, common foulants, fouling characterisation and membrane autopsy as well as a review of current models. A detailed description of the main fouling categories, namely organic fouling, scaling, colloidal and particulate fouling, and biofouling was followed by a brief description of cleaning methodologies.

While fouling has always been a primary part of membrane research and almost always found in company of effective membrane filtration, it is clearly membrane cleaning where substantial progress will be made in future research.

## 10 ACKNOWLEDGEMENTS

Shyam S. Sablani from the Sultan Qaboos University in Oman is acknowledged for providing Figure 5 and Figure 6. Linda Dudley from Ondeo-Nalco, UK is thanked for supplying extensive materials on membrane fouling, scaling and cleaning. Paul Buijs, GEBetz, Belgium supplied Figure 2 and Jack Gilron, Ben Gurion University, Israel Figure 4 which is much appreciated.

## 11 GLOSSARY & SYMBOLS

### 11.1 Glossary

CWF	Clean Water Flux	DOM	Dissolved Organic Matter
FR	Flux Reduction	EDS	Electron Dispersive Spectra
PF	Permeate Flux	EDTA	Ethylene Diamine Tetra Acetic Acid
NOM	Natural Organic Matter	FA	Fulvic Acid
CA	Cellulose Acetate	FESEM	Field Emission Scanning Electron Microscopy
DOC	Dissolved Organic Carbon		

### 11.2 Greek symbols

$\alpha$	activity of the solute	$\Gamma$	quantity of organic adsorbed onto the membrane surface
$\alpha_O$	activity of the solute in its crystal stage	$\eta_T$	viscosity of water at temperature T
$\delta$	boundary layer thickness	$\mu$	chemical potential of the solute
$\Delta\pi_m^*$	cake enhanced osmotic pressure	$v$	velocity of water (normal to the membrane surface)
$\epsilon$	cake layer porosity	$\tau$	membrane tortuosity
$\phi_T$	total interaction potential		

### 11.3 Alphabetical symbols

A	membrane surface area	$C_w$	solute concentration at the membrane/water interface
C	equilibrium concentration of the solute in the solution	D	particle diffusion tensor
$C_B$	solute concentration in the bulk solution	$\Delta G$	Gibb free energy
$C_{BL}$	solute concentration in the boundary layer	$\Delta\Pi$	osmotic pressure difference across the membrane
$C_F$	solute concentration in the feed	$\Delta P$	transmembrane pressure
$C_F$	concentration factor or ratio	$\Delta\pi_m^*$	cake enhance osmotic pressure
$C_P$	solute concentration in the permeate	$D_s$	solute diffusion coefficient

F	external force vector	$R_{CW}$	resistance of the membrane after cleaning
IAP	ion activity product	$Re$	Reynolds number
J	water flux	$R_F$	total fouling resistance
$J_C$	water flux after cleaning	$R_G$	resistance due to gel formation
$J_O$	initial water flux	$R_{IF}$	irreversible fouling resistance
k	Boltzmann's constant	$R_M$	intrinsic membrane resistance
K	partitioning coefficient between membrane and solution phase	$R_O$	real retention
$k_s$	mass transfer coefficient of the solute	$R_{OBS}$	observed retention
$k_{sp}$	thermodynamic solubility product of the phase forming compound	$R_P$	resistance due to internal pore fouling
M	molecular mass of the solute	$R_{RES}$	residual resistance after cleaning
$P_F$	concentration polarisation factor	$R_{RF}$	reversible fouling resistance
Q	volume flowrate	S	supersaturation ratio
R	gas constant	t	time duration
$R_A$	resistance due to adsorption	u	particle velocity induced by the fluid flow
$R_C$	resistance due to cake formation	V	volume
$R_{CP}$	resistance due to concentration polarisation	x	distance from the membrane surface
		y	permeate recovery fraction

## 12 REFERENCES

- [1] W. J. Koros, Y. H. Ma, T. Shimizu, Terminology for membranes and membrane processes - IUPAC recommendations 1996, Journal of Membrane Science 120 (1996), 149-159.
- [2] B. van der Bruggen, L. Braeken, C. Vandecasteele, Flux decline in nanofiltration due to adsorption of organic compounds, Separation and Purification Technology 29 (2002), 23-31.
- [3] E. Staude, Membranen und Membranprozesse - Grundlagen und Anwendungen VCH: Weinheim, Germany, 1992.
- [4] A. I. Schäfer, Natural Organic Matter Removal using Membranes: Principles, Performance and Cost CRC Press: Boca Raton, USA, 2001.
- [5] H. Huiting, J. W. N. M. Kappelhof, T. G. J. Bosklopper, Operation of NF/RO plants: from reactive to proactive, Desalination 139 (2001), 183-189.
- [6] A. G. Fane, P. Beatson, H. Li, Membrane fouling and its control in environmental applications, Water Sci. Technol. 41 (10-11) (2000), 303-308.
- [7] J.-H. Choi, S. Dockko, K. Fukushi, K. Yamamoto, A novel application of a submerged nanofiltration membrane bioreactor (NF MBR) for wastewater treatment, Desalination 146 (2002), 413-420.
- [8] S. F. E. Boerlage, M. D. Kennedy, M. Dickson, D. E. Y. El-Hodali, J. C. Schippers, The modified fouling index using ultrafiltration membranes (MFI-UF): characterisation, filtration mechanisms and proposed reference membrane, Journal of Membrane Science 197 (2002), 1-21.
- [9] J. H. Roorda, J. H. J. M. van der Graaf, New parameter for monitoring fouling during ultrafiltration of WWTP effluent, Water Sci. Technol. 43 (10) (2001), 241-248.

*Introduction*

- [10] M. Mänttari, M. Nystrom, Critical flux in NF of high molar mass polysaccharides and effluents from the paper industry, *Journal of Membrane Science* 170 (2) (2000), 257-273.
- [11] A. Braghetta, F. A. Digiano, W. P. Ball, Nanofiltration of natural organic matter: pH and ionic strength effects, *Journal of Environmental Engineering* 123 (7) (1997), 628-641.
- [12] J. E. Kilduff, S. Mattaraj, J. P. Pieracci, G. Belford, Photochemical modification of poly(ether sulfone) and sulfonated poly(sulfone) nanofiltration membranes for control of fouling by natural organic matter, *Desalination* 132 (2000), 133-142.
- [13] F. A. DiGiano, S. Arweiler, A. J. J. Riddick, Alternative tests for evaluating NF fouling, *Journal AWWA* 92 (2) (2000), 103-115.
- [14] F. A. DiGiano, in *ICR Workshop on Bench-scale and Pilot-scale Evaluations*; AWWA, Cincinnati, Ohio, 1996.
- [15] M. Luo, Z. Wang, Complex fouling and cleaning-in-place of a reverse osmosis desalination system, *Desalination* 141 (2001), 15-22.
- [16] J. S. Vrouwenvelder, D. van der Kooij, Diagnosis of fouling problems of NF and RO membrane installations by a quick scan, *Desalination* 153 (2002), 121-124.
- [17] I. C. Escobar, A. A. Randall, Assimilable organic carbon (AOC) and biodegradable dissolved organic carbon (BDOC): complementary measurements, *Water Research* 35 (18) (2001), 4444-4454.
- [18] H. F. Shaalan, Development of fouling control strategies pertinent to nanofiltration membranes, *Desalination* 153 (2002), 125-131.
- [19] S. F. E. Boerlage, M. D. Kennedy, M. P. Aniye, E. M. Abogrean, D. E. Y. El-Hodali, Z. S. Tarawneh, J. C. Schippers, Modified fouling index<sub>Ultrafiltration</sub> to compare pretreatment processes of reverse osmosis feedwater, *Desalination* 131 (2000), 201-214.
- [20] C. R. Reiss, J. S. Taylor, in *Membrane Technology Conference*; ed. AWWA) 433-448 AWWA, Reno, Nevada, 1995.
- [21] D. van der Kooij, H. R. Veenendaal, C. Baars-Lorist, D. W. van der Klift, Y. C. Drost, Biofilm formation on surfaces of glass and teflon exposed to treated water, *Water Research* 29 (7) (1995), 1655-1662.
- [22] B. Hamsch, Untersuchungen zu mikrobiellen Abbauprozessen bei der Uferfiltration, Universität Karlsruhe, Karlsruhe, Germany, 1992.
- [23] J. S. Vrouwenvelder, D. van der Kooij, Diagnosis, prediction and prevention of biofouling of NF and RO membranes, *Desalination* 139 (2001), 65-71.
- [24] S. B. Sadr Ghayeni, P. J. Beatson, S. R.P., F. A.G., Adhesion of waste water bacteria to reverse osmosis membranes, *Journal of Membrane Science* 138 (1998), 29-42.
- [25] G. Carlson, J. Silverstein, Effect of Molecular Size and Charge on Biofilm Sorption of Organic Matter, *Water Research* 32 (5) (1998), 1580-1592.
- [26] E.-m. Gwon, M.-j. Yu, H.-k. Oh, Y.-h. Ylee, Fouling characteristics of NF and RO operated for removal of dissolved matter from groundwater, *Water Research* 37 (2003), 2989-2997.
- [27] S. K. Sayed Razavi, J. L. Harris, F. Sherkat, Fouling and cleaning of membranes in the ultrafiltration of the aqueous extract of soy flour, *Journal of Membrane Science* 114 (1) (1996), 93-104.
- [28] B. D. Cho, A. G. Fane, Fouling transients in normally sub-critical flux operation of a membrane bioreactor, *Journal of Membrane Science* 209 (2002), 391-403.
- [29] H. Lee, G. Amy, J. Cho, Y. Yoon, S.-H. Moon, I. S. Kim, Cleaning strategies for flux recovery of an ultrafiltration membrane fouled by natural organic matter, *Water Research* 35 (14) (2001), 3301-3308.
- [30] D. L. Nghiem, A. I. Schäfer, Adsorption and Transport of Trace Contaminant Estrone in NF/RO Membranes, *Environmental Engineering Science* 19 (6) (2002), 441-451.
- [31] S. Belfer, R. Fainstain, Y. Daltrophe, Y. Gelman, A. Toma, M. Priel, J. Gilron, in *Israeli Desalination Society Conference*; ed. IDS) Haifa Israel, 2003.

*Chapter 8 – Fouling in Nanofiltration*

- [32] A. M. Farooque, A. Hassan, M., A. Al-Amoudi, in *IDA World Congress on Desalination and Water Reuse*; 77-87 International Desalination Association, San Diego, California, 1999.
- [33] F. H. Butt, F. Rahmani, U. Badhuruthamal, Hollow fine fibre vs. spiral-wound reverse osmosis desalination membranes Part 2: Membrane autopsy, *Desalination* 109 (1997), 83-94.
- [34] K. J. Kim, V. Chen, A. G. Fane, Characterization of Clean and Fouled Membranes Using Metal Colloids, *J. Membr. Sci.* 88 (1) (1994), 93-101.
- [35] K. J. Kim, M. R. Dickson, V. Chen, A. G. Fane, Applications of Field-Emission Scanning Electron-Microscopy to Polymer Membrane Research, *Micron Microscopia Acta* 23 (3) (1992), 259-271.
- [36] M. Rabiller-Baudry, M. Le Maux, B. Chaufer, L. Begoin, Characterisation of cleaned and fouled membrane by ATR-FTIR and EDX analysis coupled with SEM: application of UF of skimmed milk with a PES membrane, *Desalination* 146 (2002), 123-128.
- [37] W. R. Bowen, N. Hilal, R. W. Lovitt, C. J. Wright, Direct measurement of interactions between adsorbed protein layers using an atomic force microscope, *Journal of Colloid and Interface Science* 197 (2) (1998), 348-352.
- [38] W. R. Bowen, T. A. Doneva, Atomic force microscopy studies of membranes: Effect of surface roughness on double-layer interactions and particle adhesion, *J. Colloid Interface Sci.* 229 (2000), 544-549.
- [39] W. R. Bowen, T. A. Doneva, A. G. Stoton, The use of atomic force microscopy to quantify membrane surface electrical properties, *Colloids Surf. A* 201 (2002), 73-83.
- [40] C. Jarusutthirak, G. Amy, J.-P. Croue, Fouling characteristics of wastewater effluent organic matter (EfOM) isolates on NF and UF membranes, *Desalination* 145 (1-3) (2002), 247-255.
- [41] D. J. Carlsson, M. M. Dal-Chin, P. Black, C. N. Lick, A surface spectroscopic study of membranes fouled by pulp mill effluent, *Journal of Membrane Science* 142 (1998), 1-11.
- [42] M. Nyström, L. Kaipia, S. Luque, Fouling and retention of nanofiltration membranes, *Journal of Membrane Science* 98 (1995), 249-262.
- [43] M. Mänttari, L. Puro, J. Nuortila-Jokinen, M. Nyström, Fouling effects of polysaccharides and humic acid in nanofiltration, *Journal of Membrane Science* 165 (2000), 1-17.
- [44] P. C. Carman, Fundamental principles of industrial filtration - A critical review of present knowledge, *Trans Inst Chem Eng* 16 (1938), 168-188.
- [45] W. R. Bowen, F. Jenner, Theoretical Descriptions of Membrane Filtration of Colloids and Fine Particles - An Assessment and Review, *Adv. Colloid Interf. Sci.* 56 (1995), 141-200.
- [46] J. G. Wijmans, S. Nakao, F. R. van den Berg, F. R. Troelstra, C. A. Smolders, Hydrodynamic resistance of concentration polarization boundary layers in ultrafiltration, *J. Membrane Sci.* 22 (1985), 117-134.
- [47] W. S. W. Ho, K. K. Sirkar, *Membrane Handbook* Chapman & Hall: New York, 1992.
- [48] T. K. Sherwood, P. L. T. Brian, R. E. Fisher, L. Dresner, Salt concentration at phase boundaries in desalination by reverse osmosis, 4 (1965), 113-118.
- [49] S. S. Sablani, M. F. A. Goosen, R. Al-Belushi, M. Wilf, Concentration polarization in ultrafiltration and reverse osmosis: a critical review, *Desalination* 141 (2001), 269-289.
- [50] J. D. Nikolova, M. A. Islam, Contribution of adsorbed layer resistance to the flux decline in an ultrafiltration process, *Journal of Membrane Science* 146 (1998), 105-111.
- [51] I. Koyuncu, D. Topacik, Effect of organic ion on the separation of salts by nanofiltration membranes, *Journal of Membrane Science* 195 (2) (2002), 247-263.
- [52] B. Van der Bruggen, B. Daems, D. Wilms, C. Vandecasteele, Mechanisms of retention and flux decline for the nanofiltration of dye baths from the textile industry, *Separation and Purification Technology* 22-23 (2001), 519-528.
- [53] C. Combe, E. Molis, P. Lucas, R. Riley, M. M. Clark, The effect of CA membrane properties on adsorptive fouling by humic acid, *Journal of Membrane Science* 154 (1999), 73-87.

*Introduction*

- [54] B. van der Bruggen, C. Vandecasteele, Flux decline during nanofiltration of organic components in aqueous solution, *Environmental Science and Technology* 35 (17) (2001), 3535-3540.
- [55] G. Belfort, R. H. Davis, A. L. Zydney, The behavior of suspensions and macromolecular solutions in crossflow microfiltration: review, *J. Membr. Sci.* 96 (1994), 1-58.
- [56] Y.-J. Chang, M. M. Benjamin, Modeling formation of natural organic matter fouling layers on ultrafiltration membranes, *Journal of Environmental Engineering* January (2003), 25-32.
- [57] R. W. Field, D. Wu, J. A. Howell, B. B. Gupta, Critical flux concept for microfiltration fouling, *Journal of Membrane Science* 100 (1995), 259-272.
- [58] M. Elimelech, J. Gregory, X. Jia, R. Williams, Particle deposition and aggregation: measurement, modeling, and simulation Butterworth-Heinemann Ltd.: Jordan Hill, Oxford, 1995.
- [59] E. M. V. Hoek, A. S. Kim, M. Elimelech, Influence of channel height and crossflow hydrodynamics on colloidal fouling of reverse osmosis membranes, *Environmental Engineering Science* (in press) (2002),
- [60] E. M. V. Hoek, Colloidal Fouling Mechanisms in Reverse Osmosis and Nanofiltration, Ph.D., Yale University, New Haven, CT, 2002.
- [61] E. M. V. Hoek, A. S. Kim, M. Elimelech, Influence of Crossflow Membrane Filter Geometry and Shear Rate on Colloidal Fouling in Reverse Osmosis and Nanofiltration Separations, *Environ. Eng. Sci.* 19 (6) (2002), 357-372.
- [62] E. M. V. Hoek, M. Elimelech, Cake-enhanced concentration polarization: A major fouling mechanism for salt rejecting membranes, *Environ. Sci. Technol.* (2002), (submitted).
- [63] B. P. Boudreau, The diffusive tortuosity of fine-grained unlithified sediments, *Geochim. Cosmochim. Ac.* 60 (16) (1996), 3139-3142.
- [64] E. M. V. Hoek, M. Elimelech, Cake-enhanced concentration polarization: A new fouling mechanism for salt rejecting membranes, *Environ. Sci. Technol.* 37 (2003), 5581-5588.
- [65] A. R. Roudman, F. A. Digiano, Surface energy of experimental and commercial nanofiltration membranes: effects of wetting and natural organic matter fouling, *Journal of Membrane Science* 175 (2000), 61-73.
- [66] C. L. Tiller, C. R. O'Melia, Natural organic matter and colloidal stability: Models and measurements, *Colloids and Surfaces A: Physicochemical and Engineering Aspects* 73 (1993), 89-102.
- [67] R. Beckett, N. P. Le, The role of organic matter and ionic composition in determining the surface charge of suspended particles in natural waters, *Colloids and Surfaces* 44 (1990), 35-49.
- [68] C. Jarusutthirak, G. Amy, Membrane filtration of wastewater effluents for reuse: effluent organic matter rejection and fouling, *Water Science and Technology* 43 (10) (2001), 225-232.
- [69] M. R. Wiesner, e. al., Committee Report: membrane processes in potable water treatment, *J. AWWA* Jan (1992), 59-64.
- [70] S. A. Huber, Organics - The value of chromatographic characterisation of TOC in process water plants, *Ultrapure Water* (1998), 16-20.
- [71] A. I. Schäfer, R. Mauch, A. G. Fane, T. D. Waite, Charge effects in the fractionation of natural organics using ultrafiltration, *Environmental Science & Technology* 36 (2002), 2572-2580.
- [72] I.-S. Chang, C.-H. Lee, Membrane filtration characteristics in membrane-coupled activated sludge system - the effect of physiological states of activated sludge on membrane fouling, *Desalination* 120 (1998), 221-233.
- [73] G. Amy, J. Cho, Interactions Between Natural Organic Matter (NOM) and Membranes: Rejection and Fouling, *Water Science and Technology* 40 (9) (1999), 131-139.
- [74] E. D. Mackey, Fouling of ultrafiltration and nanofiltration membranes by dissolved organic matter, Rice University, Houston, 1999.
- [75] T. L. Champlin, Using circulation tests to model natural organic matter adsorption and particle deposition by spiral-wound nanofiltration membrane elements, *Desalination* 131 (2000), 105-115.

*Chapter 8 – Fouling in Nanofiltration*

- [76] M. Elimelech, W. H. Chen, J. J. Waypa, Measuring the zeta (electrokinetic) potential of reverse osmosis membranes by a streaming potential analyzer, *Desalination* 95 (1994), 269-286.
- [77] A. E. Childress, S. S. Deshmukh, Effect of humic substances and anionic surfactants on the surface charge and performance of reverse osmosis membranes, *Desalination* 118 (1998), 167-174.
- [78] A. E. Childress, M. Elimelech, Effect of solution chemistry on the surface charge of polymeric reverse osmosis and nanofiltration membranes, *Journal of Membrane Science* 119 (1996), 253-268.
- [79] A. I. Schäfer, A. G. Fane, T. D. Waite, Nanofiltration of natural organic matter: removal, fouling and the influence of multivalent ions, *Desalination* 118 (1998), 109-122.
- [80] S. Hong, M. Elimelech, Chemical and physical aspects of natural organic matter (NOM) fouling of nanofiltration membranes, *Journal of Membrane Science* 132 (1997), 159-181.
- [81] C. R. Bouchard, J. Jolicoeur, P. Kouadio, M. Britten, Study of humic acid adsorption on nanofiltration membranes by contact angle measurements, *The Canadian Journal of Chemical Engineering* 75 (April) (1997), 339-345.
- [82] K. L. Jones, C. R. O'Melia, Ultrafiltration of protein and humic substances: effect of solution chemistry on fouling and flux decline, *Journal of Membrane Science* 193 (2) (2001), 163-173.
- [83] K. Ghosh, M. Schnitzer, Macromolecular structures of humic substances, *Soil Science* 129 (5) (1980), 266-276.
- [84] A. Seidel, M. Elimelech, Coupling between chemical and physical interactions in natural organic matter (NOM) fouling of nanofiltration membranes: implications for fouling control, *Journal of Membrane Science* 203 (2002), 245-255.
- [85] J. Lindau, A.-S. Jönsson, Adsorptive fouling of modified and unmodified commercial polymeric ultrafiltration membranes, *Journal of Membrane Science* 160 (1999), 65-76.
- [86] J. Cho, G. Amy, J. Pellerino, Membrane Filtration of Natural Organic Matter: Initial Comparison of Rejection and Flux Decline Characteristics with Ultrafiltration and Nanofiltration Membranes, *Water Research* 33 (11) (1999), 2517-2526.
- [87] Q. Li, M. Elimelech, 2004 (15/01/2004) (2003), Yale University, [http://www.yale.edu/env/elimelech/index\\_research.htm](http://www.yale.edu/env/elimelech/index_research.htm).
- [88] N. A. Wall, G. R. Choppin, Humic acids coagulation: influence of divalent cations, *Applied Geochemistry* 18 (2003), 1573-1582.
- [89] A. Schäfer, A. Fane, D. Waite, Direct coagulation pretreatment in nanofiltration of waters rich in organic matter and calcium, *Desalination* 131 (1-3) (2000), 215-224.
- [90] D. Hasson, A. Drak, R. Semiat, Inception of CaSO<sub>4</sub> scaling on RO membranes at various water recovery levels, *Desalination* 139 (2001), 73-81.
- [91] J. C. Cowan, D. J. Weintritt, Water-Formed Scale Deposits Gulf Publ. Co.; Houston, 1976.
- [92] K. A. Faller, AWWA, 1999.
- [93] R. Rautenbach, R. Albrecht, Membrane Processes John Wiley & Sons: New York, 1989.
- [94] J. W. Mullin, Crystallisation Butterworths: London, 1992.
- [95] J. A. Dirksten, T. A. Ring, Fundamentals of crystallization: kinetic effects on particle size distributions and morphology, *Chem. Eng. Sci.* 46 (1991), 2389-2427.
- [96] I. Sutzkover, D. Hasson, R. Semiat, Simple technique for measuring the concentration polarization level in a reverse osmosis system, *Desalination* 131 (2000), 117-127.
- [97] C. A. C. van de Lisdonk, B. M. Rietman, S. G. J. Heijman, G. R. Sterk, J. C. Schippers, Prediction of supersaturation and monitoring of scaling in reverse osmosis and nanofiltration membrane systems, *Desalination* 138 (2001), 259-270.
- [98] R. M. Smith, A. E. Martell, R. J. Motekaites, NIST critically selected stability constants of metal complexes database, Gaithersburg, MD (1996),
- [99] S. C. J. M. van Hoof, J. G. Minnery, B. Mack, Performing a membrane autopsy, *Desalination & Water Reuse* 11 (4) (2001), 40-46.

*Introduction*

- [100] T. Koo, Y. J. Lee, R. Sheikholeslami, Silica fouling and cleaning of reverse osmosis membranes, *Desalination* 139 (2001), 43-56.
- [101] W. L. Marshall, J. M. Warakowski, Amorphous silica solubilities II: Effects on aqueous salt solutions at 25°C, *Geochimica Cosmochimica Acta* 44 (1980), 915-924.
- [102] F. H. Butt, F. Rahman, U. Baduruthamal, Characterization of foulants by autopsy of RO desalination membranes, *Desalination* 114 (1997), 51-64.
- [103] M. Brusilovsky, J. Borden, D. Hasson, Flux decline due to gypsum precipitation on RO membranes, *Desalination* 86 (1992), 187-222.
- [104] S. Lee, C. H. Lee, Effect of operating conditions on CaSO<sub>4</sub> scale formation mechanism in nanofiltration for water softening, *Water Res.* 34 (2000), 3854-3866.
- [105] Y. A. Le Gouellec, M. Elimelech, Calcium sulfate (gypsum) scaling in nanofiltration of agricultural drainage water, *Journal of Membrane Science* 205 (1-2) (2002), 279-291.
- [106] J. Gilron, D. Hasson, Calcium sulphate fouling of reverse osmosis membranes: Flux decline mechanism, *Chemical Engineering Science* 42 (1987), 2351-2360.
- [107] O. Söhnel, J. Garside, *Precipitation. Basic Principles and Industrial Applications* Butterworth-Heinemann: Oxford, 1992.
- [108] Y. A. Le Gouellec, M. Elimelech, Control of calcium sulfate (gypsum) scale in nanofiltration of saline agricultural drainage water, *Environ Eng Sci* 19 (2002), 387-397.
- [109] T. Pahiadaki, N. Andritsos, S. G. Yiantsios, A. J. Karabelas, Calcium carbonate fouling of RO and NF membranes, (in preparation),
- [110] N. Andritsos, A. J. Karabelas, P. G. Koutsoukos, Morphology and structure of CaCO<sub>3</sub> scale layers formed under isothermal flow conditions, *Langmuir* 13 (1997), 2873-2879.
- [111] D. Myers, *Surfaces, Interfaces, and Colloids* John Wiley & Sons: New York, 1999.
- [112] P. C. Hiemenz, R. Rajagopalan, *Principles of Colloid and Surface Chemistry* Marcel Dekker: Monticello, NY, 1997.
- [113] M. K. H. Liew, A. G. Fane, P. L. Rogers, Fouling of microfiltration membranes by broth-free antifoam agents, *Biotechnology and Bioengineering* 56 (1) (1997), 89-98.
- [114] S. T. Kelley, A. L. Zydney, Protein fouling during microfiltration: comparative behavior of different model proteins, *Biotechnology and Bioengineering* 55 (1, July 5) (1997), 91-100.
- [115] K. Hagen, Removal of particles, bacteria and parasites with ultrafiltration for drinking water treatment, *Desalination* 119 (1-3) (1998), 85-91.
- [116] L. T. Fu, B. A. Dempsey, Optimizing membrane operations with enhanced coagulation of TOC for drinking water treatment, *Abstracts of Papers of the American Chemical Society* 212 (1996), 13-ENVR.
- [117] J. J. Porter, Recovery of polyvinyl alcohol and hot water from the textile wastewater using thermally stable membranes, *Journal of Membrane Science* 151 (1) (1998), 45-53.
- [118] D. E. Potts, R. C. Ahlert, S. S. Wang, A critical review of fouling of reverse osmosis membranes, *Desalination* 35 (1981), 235-264.
- [119] G. Tchobanoglous, J. Darby, K. Bourgeois, J. McArdle, P. Genest, M. Tylla, Ultrafiltration as an advanced tertiary treatment process for municipal wastewater, *Desalination* 119 (1-3) (1998), 315-321.
- [120] E. Van Houtte, J. Verbauwheide, F. Vanlerberghe, S. Demunter, J. Cabooter, Treating different types of raw water with micro- and ultrafiltration for further desalination using reverse osmosis, *Desalination* 117 (1998), 49-60.
- [121] L. Vera, R. Villarroel-Lopez, S. Delgado, S. Elmaleh, Cross-flow microfiltration of biologically treated wastewater, *Desalination* 114 (1) (1997), 65-75.
- [122] S. K. Hong, M. Elimelech, Chemical and physical aspects of natural organic matter (nom) fouling of nanofiltration membranes, *J. Membrane Science* 132 (1997), 159-181.
- [123] W. Stumm, J. J. Morgan, *Aquatic Chemistry* Wiley-Interscience: New York, NY, 1996.

*Chapter 8 – Fouling in Nanofiltration*

- [124] M. Elimelech, J. Gregory, X. Jia, R. A. Williams, *Particle Deposition & Aggregation: Measurement, Modeling and Simulation* ed. R. A. Williams) Butterworth-Heinemann: Woburn, MA, 1995.
- [125] B. V. Derjaguin, L. D. Landau, Theory of the stability of strongly charged lyophobic sols and of the adhesion of strongly charged particles in solutions of electrolytes, *Acta Physicochim. URSS* 14 (1941), 733.
- [126] E. J. W. Verwey, J. T. G. Overbeek, *Theory of the Stability of Lyophobic Colloids* Elsevier: Amsterdam, NL, 1948.
- [127] R. H. Ottewill, J. N. Shaw, *Electrophoretic Studies On Polystyrene Latices*, *J. Electroanal. Chem.* 37 (JUN) (1972), 133-142.
- [128] P. Bacchin, P. Aimar, V. Sanchez, Model for Colloidal Fouling of Membranes, *Aiche Journal* 41 (2) (1995), 368-376.
- [129] D. T. Waite, A. I. Schafer, A. G. Fane, A. Heuer, Colloidal fouling of ultrafiltration membranes: Impact of aggregate structure and size, *Journal of Colloid and Interface Science* 212 (1999), 264-274.
- [130] X. H. Zhu, M. Elimelech, Colloidal Fouling of reverse osmosis membranes - measurements and fouling mechanisms, *Environ. Sci. Technol.* 31 (1997), 3654-3662.
- [131] S. Hong, R. S. Faibish, M. Elimelech, Kinetics of permeate flux decline in crossflow membrane filtration of colloidal suspensions, *Journal of Colloid and Interface Science* 196 (2) (1997), 267-277.
- [132] R. S. Faibish, M. Elimelech, Y. Cohen, Effect of interparticle electrostatic double layer interactions on permeate flux decline in crossflow membrane filtration of colloidal suspensions: An experimental investigation, *J. Colloid Interface Sci.* 204 (1) (1998), 77-86.
- [133] X. H. Zhu, M. Elimelech, Fouling of Reverse-Osmosis Membranes by Aluminum-Oxide Colloids, *Journal of Environmental Engineering-Asce* 121 (12) (1995), 884-892.
- [134] S. G. Yiantsios, A. J. Karabelas, The effect of colloid stability on membrane fouling, *Desalination* 118 (1-3) (1998), 143-152.
- [135] D. Y. Kwon, S. Vigneswaran, H. H. Ngo, H. S. Shin, An enhancement of critical flux in crossflow microfiltration with a pretreatment of floating medium flocculator/prefilter, *Water Science and Technology* 36 (12) (1997), 267-274.
- [136] A. G. Abulnour, M. H. Sorour, H. A. Talaat, Comparative economics for desalting of agricultural drainage water (ADW), *Desalination* 152 (1-3) (2003), 353-357.
- [137] W. Reimann, Treatment of agricultural wastewater and reuse, *Water Science and Technology* 46 (11-12) (2002), 177-182.
- [138] H. A. Talaat, M. H. Sorour, N. A. Rahman, H. F. Shaalan, Pretreatment of agricultural drainage water (ADW) for large-scale desalination, *Desalination* 152 (1-3) (2003), 299-305.
- [139] C. Combe, E. Molis, P. Lucas, R. Riley, M. M. Clark, The effect of CA membrane properties on adsorptive fouling by humic acid, *J. Membrane Sci.* 154 (1) (1999), 73-87.
- [140] K. Riedl, B. Girard, R. W. Lencki, Influence of membrane structure on fouling layer morphology during apple juice clarification, *J. Membrane Sci.* 139 (2) (1998), 155-166.
- [141] W. R. Bowen, T. A. Doneva, Atomic force microscopy studies of membranes: Effect of surface roughness on double-layer interactions and particle adhesion, *J. Colloid Inter. Sci.* 229 (2000), 544-549.
- [142] J. W. Carter, G. Hoyland, A. P. M. Hasting, Concentration polarisation in reverse osmosis flow systems under laminar conditions. Effect of surface roughness and fouling, *Chem. Eng. Sci.* 29 (1974), 1651-1658.
- [143] M. Hirose, H. Ito, Y. Kamiyama, Effect of skin layer surface structures on the flux behaviour of RO membranes, *J. Membrane Sci.* 121 (2) (1996), 209-215.
- [144] J. Y. Kim, H. K. Lee, S. C. Kim, Surface structure and phase separation mechanism of polysulfone membranes by atomic force microscopy, *J. Membrane Sci.* 163 (2) (1999), 159-166.
- [145] T. Knoell, J. Safarik, T. Cormack, R. Riley, S. W. Lin, H. Ridgway, Biofouling potentials of microporous polysulfone membranes containing a sulfonated polyether-ethersulfone/polyethersulfone

*Introduction*

- block copolymer: correlation of membrane surface properties with bacterial attachment, *J. Membrane Sci.* 157 (1) (1999), 117-138.
- [146] M. D. Louey, P. Mulvaney, P. J. Stewart, Characterisation of adhesional properties of lactose carriers using atomic force microscopy, *Journal of Pharmaceutical and Biomedical Analysis* 25 (3-4) (2001), 559-567.
- [147] J. A. Brant, A. E. Childress, Assessing short-range membrane-colloid interactions using surface energetics, *J. Membr. Sci.* 203 (1-2) (2002), 257-273.
- [148] E. M. V. Hoek, S. Hong, M. Elimelech, Influence of membrane surface properties on initial rate of colloidal fouling of reverse osmosis and nanofiltration membranes, *Journal of Membrane Science* 188 (1) (2001), 115-128.
- [149] S. L. Walker, S. Bhattacharjee, E. M. V. Hoek, M. Elimelech, A novel asymmetric clamping cell for measuring streaming potential of flat surfaces, *Langmuir* 18 (2002), 2193-2198.
- [150] C. J. van Oss, *Interfacial Forces in Aqueous Media* Marcel Dekker, Inc.: New York, NY, 1994.
- [151] L. F. Song, M. Elimelech, Particle Deposition Onto a Permeable Surface in Laminar-Flow, *Journal of Colloid and Interface Science* 173 (1) (1995), 165-180.
- [152] L. Song, M. Elimelech, Theory of concentration polarization in crossflow filtration, *J. Chem. Soc. Faraday Trans.* 91 (19) (1995), 3389-3398.
- [153] R. D. Cohen, R. F. Probst, Colloidal Fouling of Reverse-Osmosis Membranes, *Journal of Colloid and Interface Science* 114 (1) (1986), 194-207.
- [154] S. L. Goren, The hydrodynamic force resisting the approach of a sphere to a plane permeable wall, *Journal of Colloid and Interface Science* 69 (1) (1973), 78-85.
- [155] M. R. Wiesner, M. M. Clark, J. Mallevialle, Membrane Filtration of Coagulated Suspensions, *Journal of Environmental Engineering-Asce* 115 (1) (1989), 20-40.
- [156] W. R. Bowen, A. Mongruel, P. M. Williams, Prediction of the rate of cross-flow membrane ultrafiltration: A colloidal interaction approach, *Chemical Engineering Science* 51 (18) (1996), 4321-4333.
- [157] W. R. Bowen, A. O. Sharif, Hydrodynamic and colloidal interactions effects on the rejection of a particle larger than a pore in microfiltration and ultrafiltration membranes, *Chemical Engineering Science* 53 (5) (1998), 879-890.
- [158] J. N. Israelachvili, *Intermolecular and Surface Forces* Academic Press: London, 1992.
- [159] M. Elimelech, X. Zhu, A. E. Childress, S. Hong, Role of membrane surface morphology in colloidal fouling of cellulose acetate and composite aromatic polyamide reverse osmosis membranes, *J. Membrane Sci.* 127 (1997), 101-109.
- [160] H. M. Lappin-Scott, J. W. Costerton, Bacterial biofilms and surface fouling, *Biofouling* 1 (1989), 323-342.
- [161] H. C. Flemming, G. Schaule, T. Griebe, J. Schmitt, A. Tamachkiarowa, Biofouling - the Achilles heel of membrane processes, *Desalination* 113 (1997), 215-225.
- [162] H. F. Ridgway, H.-C. Flemming, Membrane biofouling, in *Water Treatment Membrane Processes* (eds. J. Mallevialle, P. E. Odendaal, M. R. Wiesner) McGraw Hill, New York, 1996, 6.1-6.62.
- [163] H.-C. Flemming, *Biofouling bei Membranprozessen* Springer: Berlin, 1995.
- [164] S. B. Sadr Ghayeni, P. J. Beatson, R. P. Schneider, A. G. Fane, Adhesion of waste water bacteria to reverse osmosis membranes, *J. Membrane Science and Technology* 138 (1997), 29-42.
- [165] R. P. Schneider, Conditioning film-Induced modification of substratum physicochemistry - analysis by contact angles, *J. Colloid & Interface Science* 182 (1996), 204-213.
- [166] R. Bos, H. C. van der Mei, H. J. Busscher, Physicochemistry of initial microbial adhesive interactions - its mechanisms and methods of study, *FEMS Microbiol. Rev.* 23 (1999), 179-230.
- [167] K. C. Marshall, R. Stout, R. Mitchell, Mechanism of initial events in the sorption of marine bacteria to surfaces, *J. Gen. Microbiol.* 68 (1971), 337-348.

*Chapter 8 – Fouling in Nanofiltration*

- [168] K. C. Marshall, Adsorption and adhesion processes in microbial growth at interfaces, *Adv. Colloid Interface Sci.* 25 (1986), 59-86.
- [169] K. Power, K. C. Marshall, Cellular growth and reproduction of marine bacteria on surface-bound substrate, *Biofouling* 1 (1988), 163-174.
- [170] J. W. Costerton, Z. Lewandowski, D. DeBeer, D. Caldwell, D. Korber, G. James, Biofilms, the customized microniche, *J. Bact.* 176 (1994), 2137-2142.
- [171] J. W. Costerton, P. S. Stewart, E. P. Greenberg, Bacterial biofilms: a common cause of persistent infections, *Science* 284 (1999), 1318-1322.
- [172] J. D. Bryers, F. Drummond, Local macromolecule diffusion coefficients in structurally non-uniform bacterial biofilms using fluorescence recovery after photobleaching (FRAP), *Biotechnol. Bioeng.* 60 (1998), 462-473.
- [173] M. Kühl, B. B. Jorgensen, Microsensor measurements of sulfate reduction and sulfide oxidation in compact microbial communities of aerobic biofilms, *Appl. Env. Microbiol.* 58 (1992), 1164-1174.
- [174] J. D. Bryers, Two photon excitation microscopy for analysis of biofilm processes, *Method Enzymol.* 337 (2001), 259-269.
- [175] G. A. McFethers, F. P. Yu, B. H. Pyle, P. S. Stewart, Physiological assessment of bacteria using fluorochromes, *J. Microbiol. Meth.* 21 (1995), 1-13.
- [176] R. I. Amann, W. Ludwig, K.-H. Schleifer, Phylogenetic Identification and in-situ Detection of Individual Microbial Cells Without Cultivation, *Microbiol. Rev.* 59 (1995), 143-169.
- [177] H. Y. Dang, C. R. Lovell, Bacterial primary colonization and early succession on surfaces in marine waters as determined by amplified rRNA gene restriction analysis and sequence analysis of 16S rRNA genes, *Appl. Env. Microb.* 66 (2000), 467-475.
- [178] D. M. Moll, R. S. Summers, Assessment of drinking water filter microbial communities using taxonomic and metabolic profiles, *Water Sci. Technol.* 39 (1999), 83-89.
- [179] G. G. D. Rodriguez, D. Phipps, K. Ishiguro, H. F. Ridgway, Use of fluorescent probe for direct visualization of respiring bacteria, *Appl. Env. Microbiol.* 58 (1992), 1801-1808.
- [180] H. F. Ridgway, Microbial fouling of reverse osmosis membranes: genesis and control, in *Biological fouling of Industrial Water Systems: A Problem Solving Approach* (eds. M. W. Mittelman, G. G. Geesey) Water Micro Associates, San Diego, California, 1987, 138-193.
- [181] G. L. Leslie, R. P. Schneider, A. G. Fane, K. C. Marshall, C. J. D. Fell, Fouling of a microfiltration membrane by two Gram-negative bacteria, *Colloids and Surfaces, A: Physicochemical and Engineering Aspects* 73 (1993), 165-178.
- [182] P. H. Hodgson, G. L. Leslie, R. P. Schneider, A. G. Fane, C. J. D. Fell, K. C. Marshall, Cake resistance and solute rejection in bacterial microfiltration: the role of the extracellular matrix, *Journal of Membrane Science* 79 (1993), 35-53.
- [183] H.-C. Flemming, G. Schaule, R. McDonough, H. F. Ridgway, Effects and extent of biofilm accumulation on membrane systems, in *Biofouling and Biocorrosion in Industrial Water Systems* (eds. G. G. Geesey, Z. Lewandowski, H.-C. Flemming) CRC Press, Boca Raton, 1992, 63-89.
- [184] J. W. Costerton, R. T. Irvin, The bacterial glycocalyx in nature and disease, *Ann. Rev. Microbiol.* (1981), 299-324.
- [185] L. H. Rowley, Eleven biocides are investigated for microbial efficacy and membrane compatibility to use at the Yuma desalting plant, *Desalination* 97 (1994), 35-43.
- [186] J. S. Vrouwenvelder, D. van der Kooij, in *AWWA Membrane Technol. Conf.; 7 AWWA*, San Diego, California, 2001.
- [187] J. P. van der Hoek, J. A. M. H. Hofman, P. A. C. Bonné, M. M. Nederlof, H. S. Vrouwenvelder, RO treatment: selection of a pretreatment scheme based on fouling characteristics and operating conditions based on environmental impact, *Desalination* 127 (2000), 89-101.
- [188] E. van Houtte, F. Vanlerberghe, in *AWWA Membrane Technol. Conf.; 7 AWWA*, San Diego, California, 2001.

- [189] J. Lozier, S. Kommineni, Z. Chowdhury, F. Miller, M. Pearthree, M. P. Ring, in AWWA Membrane Technol. Conf.; 18 AWWA, San Diego, California, 2001.
- [190] M. Jenkins, M. B. Tanner, Operational experience with a new fouling resistant reverse osmosis membrane, *Desalination* 119 (1998), 243-250.
- [191] J. A. Redondo, Improve RO system performance and reduce operating cost with FIMTEC fouling-resistant (FR) elements, *Desalination* 126 (1999), 249-259.
- [192] A. M. Shahalam, A. Al-Harthy, A. Al-Zawhry, Feed water pretreatment in RO systems: unit processes in the Middle East, *Desalination* 150 (2002), 235-245.
- [193] A. Maartens, E. P. Jacobs, P. Swart, UF of pulp and paper effluent: membrane fouling-prevention and cleaning, *J. Membrane Sci.* 209 (2002), 81-92.
- [194] S. Belfer, J. Gilron, EU-report, 2002.
- [195] J. Gilron, S. Belfer, P. Väisänen, M. Nyström, Effects of surface modification on antifouling and performance properties of reverse osmosis membranes, *Desalination* 140 (2001), 167-179.
- [196] J. P. Chen, S. L. Kim, Y. P. Ting, Optimization of membrane physical and chemical cleaning by a statistically designed approach, *Journal of Membrane Science* 219 (1-2) (2003), 27-45.
- [197] A. L. Lim, R. Bai, Membrane fouling and cleaning in microfiltration of activated sludge wastewater, *Journal of Membrane Science* 216 (2003), 279-290.
- [198] G. Trägårdh, Membrane cleaning, *Desalination* 71 (1989), 325-335.
- [199] J. Wagner, *Membrane Filtration Handbook: Practical Tips and Hints* Osmonics, Inc.2001.
- [200] R. Deqian, Cleaning and regeneration of membranes, *Desalination* 62 (1987), 363-371.
- [201] R. Liikane, J. Yli-Kuivila, R. Laukkanen, Efficiency of various chemical cleanings for nanofiltration membrane fouled by conventionally treated surface water, *J. Membrane Sci.* 195 (2002), 265-276.
- [202] M. A. Argüello, S. Alvarez, F. A. Riera, R. Alvarez, Enzymatic cleaning of inorganic ultrafiltration membranes used for whey protein fractionation, *Journal of Membrane Science* 216 (2003), 121-134.
- [203] Q. Li, M. Elimelech, Organic fouling and chemical cleaning of nanofiltration membranes: measurements and mechanisms, *Environmental Science & Technology* submitted (2003),
- [204] M. J. Munoz-Aguado, D. E. Wiley, A. G. Fane, Enzymatic and detergent cleaning of a polysulphone ultrafiltration membrane fouled with BSA and whey, *J. Membrane Sci.* 117 (1996), 175-187.
- [205] E. H. K. Zeiher, F. P. Yu, Membranes: biocides used for industrial membrane system sanitization, *Ultrapure Water* 17 (3) (2000), 55-64.
- [206] A. Weis, M. R. Bird, M. Nyström, The influence of morphology, hydrophobicity and charge upon the long term performance of ultrafiltration membranes fouled with spent sulphite liquor, *Journal of Membrane Science* (submitted),
- [207] K. Kosutic, B. Kunst, RO and NF membrane fouling and cleaning and pore size distribution variations, *Desalination* 150 (2002), 113-120.
- [208] T. Thorsen, Fundamental studies on membrane filtration of coloured surface water, NTNU, Trondheim, Norway, 2001.
- [209] W. Weis, M. Bird, M. Nyström, The variation of zeta-potential with pH for UF membranes subjected to a range of fouling and cleaning protocols, in *Fouling, Cleaning and Disinfection in Food Processing* (eds. D. I. Wilson, P. J. Fryer, A. P. M. Hastings), Proceedings of a conference held at Jesus College, Cambridge, 2002, 181-188.
- [210] H. Zhu, M. Nyström, Cleaning results characterized with flux, streaming potential and FTIR measurements, *Colloids Surfaces A: Phys. Eng. Asp.* 138 (2-3) (1998), 309-321.
- [211] C.-J. Shorrock, M. R. Bird, J. A. Howell, Membrane cleaning: removal of irreversibly fouled yeast deposits, *Trans. IChemE.* 76 (part C) (1998), 1-8.
- [212] M. Bartlett, M. R. Bird, J. A. Howell, An experimental study for the development of a qualitative membrane cleaning model, *J. Membrane Sci.* 105 (1995), 147-157.

- [213] M. Nyström, H. Zhu, Characterization of cleaning results using combined flux and streaming potential methods, *J. Membrane Sci.* 131 (1997), 195-205.
- [214] P. Fu, H. Ruiz, J. Lozier, K. Thompson, C. Spangenberg, A pilot study on groundwater natural organics removal by low-pressure membranes, *Desalination* 102 (1995), 47-56.
- [215] M. Mänttari, H. Martin, J. Nuortila-Jokinen, M. Nyström, Using a spiral wound nanofiltration element for the filtration of paper mill effluents; pretreatment and fouling, *Advances in Environmental Research* 3 (2) (1999), 202-214.
- [216] S. Platt, M. Nyström, G. Capanelli, A. Bottino, Stability of NF membranes under extreme acid conditions, (in preparation),
- [217] M. Mänttari, A. Pihlajamäki, E. Kaipainen, M. Nyström, Effect of temperature and membrane pretreatment on the filtration properties of nanofiltration membranes, *Desalination* 145 (2002), 81-86.
- [218] C. R. Gillham, P. J. Fryer, A. P. M. Hasting, D. I. Wilson, Cleaning-in-place of whey protein fouling deposits: Mechanisms controlling cleaning, *Trans. IChemE* 77 (part C) (1999), 127-136.
- [219] M. L. Cabero, F. A. Riera, R. Alvarez, Rinsing of ultrafiltration ceramic membranes fouled with whey proteins: effects of cleaning procedures, *J. Membrane Sci.* 154 (1999), 239-250.
- [220] G. Daufin, U. Merin, J. P. Labbe, A. Quemerais, F. L. Kerherve, Cleaning of inorganic membranes after whey and milk ultrafiltration, *Biotech. Bioeng.* 38 (1) (1991), 82-89.
- [221] E. Räsänen, M. Nyström, J. Sahlstein, O. Tossavainen, Comparison of commercial membranes in nanofiltration of sweet whey, *Le Lait* 82 (2002), 343-356.
- [222] S. S. Madaeni, T. Mohamamdi, M. K. Moghadam, Chemical cleaning of reverse osmosis membranes, *Desalination* 134 (2001), 77-82.
- [223] E. Räsänen, M. Nyström, J. Sahlstein, O. Tossavainen, Purification and regeneration of diluted caustic and acidic washing solutions by membrane filtration, *Desalination* 149 (2002), 185-190.
- [224] G. Gésan-Guizoui, E. Boyaval, G. Daufin, Nanofiltration for the recovery of caustic cleaning-in-place solutions: robustness towards large variation of composition, *Desalination* 149 (2002), 127-129.
- [225] M. Forstmeier, B. Goers, G. Wozny, UF/NF treatment of rinsing waters in a liquid detergent production plant, *Desalination* 149 (2002), 175-177.

## 13 INDEX

Please add an index to your chapter, which includes keywords and page number in your chapter.

A		Atomic Force Microscopy (AFM)	75
Absorbance	353		
Acidity of Natural Organics	21, 100	B	
Activated Carbon Adsorption	81	Backflushing	82
Adsorption of Organics on Membranes	21	Background Solution	65 92
Aggregate Formation and Structure of Colloids	31	Backwashing	82
Aggregate Size	122	Bacterial Regrowth	33
Aggregate Structure	124	Bases	7
Aggregates with Organics (SPO)	117, 119	Bioavailability	8
Aggregation of Natural Organics	22, 112	Biofilms	33
Amphiphilics	110	Blocking Law Analysis	150
Aromaticity	14, 109	Break-Up of Aggregates	147
Ash Content	10	Brownian Diffusion	6

*Introduction*